DESIGN AND DEVELOPMENT OF A RESPONSIVE MAGNETO-RHEOLOGICAL (MR) EQUIPPED SEMI-ACTIVE SUSPENSION SYSTEM FOR OFF-ROAD VEHICLES

by

Gerhardus Smidt Heymans

Submitted in partial fulfilment of the requirements for the degree

Master of Engineering (Mechanical Engineering)

in the

Department of Mechanical and Aeronautical Engineering

Faculty of Engineering, Built Environment and Information Technology

UNIVERSITY OF PRETORIA

March 2017

SUMMARY

DESIGN AND DEVELOPMENT OF A RESPONSIVE MAGNETO-RHEOLOGICAL (MR) EQUIPPED SEMI-ACTIVE SUSPENSION SYSTEM FOR OFF-ROAD VEHICLES

by

Gerhardus Smidt Heymans

Student Number:	11030501
Supervisor(s):	Prof P.S. Els; T.R. Botha
Department:	Mechanical and Aeronautical Engineering
University:	University of Pretoria
Degree:	Master of Engineering (Mechanical Engineering)

The aim of this study is to design, implement and investigate the use of a Magneto-Rheological (MR) equipped Hydro-Pneumatic suspension system to solve the ride versus handling compromise of off-road vehicles. This suspension technology makes use of MR fluid viscosity changes which are induced by a varying magnetic fields and this viscosity change serves as the basis for changing the suspension system's damping as well as the stiffness characteristics.

The primary focus of the study is to improve the response time characteristics of an existing prototype system through the use of a more comprehensive design methodology. Once an optimised MR valve has been designed, the system must be manufactured and experimentally tested under known conditions. It was observed experimentally that the new prototype valve does exhibit significantly improved electrical response characteristics while also realising the working principles of the $4S_4$. Further experimental work showed that this suspension technology's response characteristics cannot be further improved by improving the magnetic responsiveness of the MR valve as the responses are inherently limited by a MR fluid chain build-up delays. This said the observed response characteristics of the system was proved, through simulation based studies in Chapter 7, to be fast enough to achieve improved vehicle dynamics through semi-active suspension control.

Once the newly designed MR valve's characteristics had been experimentally extracted in Chapter 5, a comprehensive physics based model was developed to predict the output characteristics of the full $MR4S_4$ in Chapter 6, which is defined by the non-linear and complex interrelated elements within the system. This physics based model was validated against a complete set of test data, after which it was implemented on a quarter-car based vehicle dynamics study in Chapter 7 to estimate the achievable vehicle ride comfort and handling contribution of the $MR4S_4$ suspension system under both passive and active control. This study documents the validated approach to design, model and test a MR based $MR4S_4$ system as well as details the research performed to determine whether the $MR4S_4$ can serve as a viable suspension technology.

ACKNOWLEDGEMENTS

The Author would like to thank the following person(s) in particular:

- A foremost thanks is extended to my family and friends for their patience and support during the course of this work.
- Humble gratitude is also extended to this projects' supervisor, Prof. P.S. Els, without whose guidance and leadership the completion of this project would not have been possible.
- A special thanks is extended to Dr. Botha for his help in debugging and setting up the quarter-car simulations as well his guidance and advice throughout the work conducted.
- The Sasol Laboratory Staff for their assistance with the experimental work performed in the laboratories.
- To Leshanti Rajh Gopaul who spent countless hours ensuring that the language of this report is of the expected standard.
- To my dear friends in the VDG Post Graduate Research group, in particular I would like to mention Kraig Wright and Roland Grabé, your encouragement and support went a very long way in keeping me committed and focused during this study. When the tides turned against me, you were there to help me keep swimming, thank you!

TABLE OF CONTENTS

LIST OF ABBREVIATIONS

$4S_4$	Four State Semi-Active Suspension System
MR	Magneto-Rheological
$MR4S_4$	Magneto-Rheological Equipped Semi-Active Suspension System
FEM	Finite Element Method
FEMM4.2	Finite Element Method Magnetics Package Edition 4.2
MRF	Magneto-rheological Fluid
RMS	Root Mean Square Value
WRMS	Weighted Root Mean Square Value
FLC	Fuzzy Logic Control
AFC	Active Force Control
NN	Neural Network
SANAFC	Skyhook Adaptive Neuro AFC
LQR	Linear Quadratic Regulator Control
LQG	Linear Quadratic Gaussian Control
TFD	Tuned Liquid Dampers
TMFD	Tuned Magnetic Fluid Dampers
COTS	Commercial off-the-shelf

LIST OF SYMBOLS

Symbol	Description	Unit
η	Viscosity	[Pa*s]
$\dot{\gamma}$	Fluid shear rate	[1/s]
τ_y	Magnetic Field dependant shear stress of the MR fluid	[Pa]
Φ	Volume fraction of Iron Particles in MR fluid	
H	Magnetic Field Strength	[A/m]
B	Magnetic Flux Density	[Wb/m^2]
μ_0	Permeability of Free Space	[H/m]
ΔP_η	Viscosity Dependant Pressure Drop	[Pa]
ΔP_τ	Yield Stress Dependant Pressure Drop	[Pa]
Q	Volumetric Flow rate	[m^3/s]
L	MR valve flow channel length	[m]
w	MR valve flow channel circumference	[m]
g	MR valve flow channel gap width	[m]
N	Coil Turns	
I	Coil Current	[Amps]
μ_r	Relative Permeability	[H/m]
A_w	Coil Cross Sectional Area	[m^2]
R	Universal Gas Constant	[$m^3 \cdot bar/$ K · mol]
$\mathcal{R}$	Reluctance	[$1/H$]
MMF or $\mathcal{F}$	Magneto Motive Force	[Ampere-turn]
Φ	Magnetic Flux	[Wb]
L	Inductance	[Henry]
S	Magnetic Cross Section Area	[m^2]
ρ	Electrical Resistivity	[$\Omega \cdot m$]
T	Electrical Time Constant	[Seconds]
c_{sky}	Ideal Skyhook Controller Damping Constant	

LIST OF FIGURES

LIST OF TABLES

CHAPTER 1

INTRODUCTION

1.1. BACKGROUND TO THE PROBLEM

Modern vehicles are being built with ever increasing power, load carrying capacity, driving comfort, top speed, road clearance and manoeuvrability while wheelbase width and length still remain largely restricted in dimension as more and more cars are added to the already crowded urban roads. This brings about an interesting vehicle dynamics challenge to engineers as these vehicles begin to suffer more from the compromise between vehicle comfort and vehicle handling or stability. In particular, high centre of mass off-road Sports-Utility Vehicles (SUV's) are most susceptible to the negative effects of this compromise as they are often very powerful while they are designed to ensure passenger comfort over very rough terrains. The soft passenger comfort suspensions of these SUV's often leave them vulnerable in dynamic situations in which they become unstable and difficult to control and prone to roll over.

This thesis will present a research initiative which has been launched in an attempt to solve the ride comfort versus handling compromise for off-road vehicles. The proposed technology for this solution is a semi-active hydro-pneumatic suspension system which has been equipped with continuously variable damping capabilities that also allow for the selection of discrete spring characteristics.

The initial technology, or concept upon which the proposed solution was founded, was developed and investigated by Els (2006) where he made use of a hydro-pneumatic suspension system which was able to achieve discrete damping and spring characteristics through the control of solenoid valves. This suspension system, developed by Els, was called the Four State Semi-Active Suspension System or $4S_4$. The $4S_4$ achieves control of spring and damper characteristics by switching flow on and off to two independent pneumatic accumulators thus changing the stiffness of the system by blocking the fluid through solenoids valves. Additionally, the system's damping is altered by controlling the hydraulic fluid flow through either high or low damping paths. Although Els's system successfully reduced the ride versus handling compromise of an off-road vehicle, a further step in the development of this technology was under-taken by Grobler (2015). Grobler investigated the application of continuously variable damping, instead of discrete damping states, as utilised by Els, on this system through the use of Magneto-Rheological (MR) fluid and an MR valve system. In order to do so, Grobler had to prove that the solenoid valves could be completely removed from the system and that the MR valves could provide sufficient blocking to switch flow on and off as was previously achieved through the solenoid valves. Grobler successfully applied the MR technology to the $4S_4$ and concluded that the combination of technologies showed great potential.

Grobler, however, found that his developed $MR4S_4$ (Magneto-Rheological equipped $4S_4$) contained serious response time drawbacks. He also observed that the system exhibited some undesirable low-speed damping

characteristics which were as a result of multiple contributing factors. These undesired effects will be discussed in Chapters 1 and 2.

1.2. RESEARCH OBJECTIVE

The aim of this study is to design, implement and validate a Magneto-Rheological equipped Hydro-Pneumatic suspension system which could be used to solve the ride versus handling compromise of off-road vehicles. As a focus point to this study, the developed system must exhibit response characteristics which are primarily faster than the initial MR4S$_4$ prototype developed by Grobler. Secondly, the developed system must still provide sufficient flow blocking abilities in order to realize and utilize the working principles of the 4S$_4$ while also providing the desired range of damping characteristics. It would be largely beneficial for future research initiatives if a validated design methodology can be developed along with a model of the MR4S$_4$. Thus, this study also aims to document a validated approach to designing and modelling the developed MR4S$_4$. Finally, by encompassing experimental work as well as simulation based investigations, this study aims to provide a recommendation regarding the feasibility and possible implementation of a MR4S$_4$ on an off-road vehicle and provide commentary regarding its merit for further research and development.

1.3. PROPOSED SOLUTION AND RESEARCH CONTRIBUTION

This study proposes to design an improved MR valve through the detailed analysis of the magnetic circuit within the valve, while also considering the dynamic effects introduced by the fluid properties as they change under magnetic fields. The magnetic analysis would be conducted through the use of a finite element analysis package, FEMM 4.2, which was developed to analyse complex magnetic applications in 2D. The utilization of the program as a design tool could be key in optimising the performance of the MR valve which in turn could make the MR4S$_4$ concept a validated and viable solution to solve the ride versus handling compromise on off-road vehicles. Additionally, with a validated design approach one could easily scale the technologies for both larger and smaller vehicle applications and in doing so open up various fields of research focused on low-energy consuming semi-active suspension systems based on MR technology. This study contributes to a wider research community if it proves that the concept of the MR4S$_4$ is viable through successful design and evaluation thereof, paving the way for additional research applications in vehicle dynamics and opening the door to studies that could improve the safety and dynamic capabilities of future vehicles.

1.4. OVERVIEW OF STUDY

This study will be discussed in the following chapters:

Chapter 1: Introduction.

This chapter provides background information, in order to understand the context of the study, as well as some history and background.

Chapter 2: Literature Study.

A thorough understanding of the factors which influence the MR Valve, $4S_4$ and their characteristics must be obtained. This chapter highlights key observations made by previous research initiatives on this topic as well as discuss some of the modelling theory, MR fluid properties, the material influences and required magnetics theory for the development of such a semi-active suspension system.

Chapter 3: Preliminary MR Valve Magnetic and FEMM4.2 Validation Study.

This chapter details an initial magnetics investigation which was launched to understand the response time characteristics of electro-magnets and the factors which influence this. Additionally, this chapter investigates the applicability of using a finite element magnetics package as a design tool during MR valve development as it sets out to determine if the FEMM4.2 package can be validated against experimental results.

Chapter 4: Design, Development and Testing of the Third MR valve Prototype.

A detailed design was launched in this chapter which sought to obtain a MR Valve through co-simulation and optimization studies with FEMM4.2. It considered the costs and implications of material selection while both attempting to minimize response time of the valve and maximising the MR effect obtainable through the valve. Finally, this chapter documents the manufacturing of the designed valve and the initial experimentally observed current response characteristics.

Chapter 5: Experimental Work, Obtained Measurements and Observed Results

During this chapter the experimental work conducted to set up the required test benches to characterise the designed MR valve is discussed. Details include the test setup and control inputs and highlights the measurements taken through the data acquisitioning system. The signal conditioning processes as well as electronics developed for the application is also documented. Additionally, this chapter discusses in detail the results extracted from the experimental work conducted. It highlights the observed characteristics of the MR valve and details important observations such as the system response time characteristics and force vs. velocity characteristics. Finally, it compares these figures to the expected design results.

Chapter 6: Full MR4S$_4$ Suspension Characteristics extracted from a Physics Based Model

After obtaining the characteristics of the MR valve from the experimental results in Chapter 5, a physics based modelling approach is utilised in order to extract the expected characteristics of a fully implemented MR4S$_4$ system. This chapter details not only the development of the model but also the extracted characteristics of the suspension system.

Chapter 7: MR4S$_4$ Validation through Dynamic Quarter-Car Simulations

Once the physics based model is developed it is implemented in a quarter-car model which is run over a series of road inputs to evaluate the dynamic responses of the semi-active suspension system through both passive and active control strategies.

Chapter 8: Conclusions and Recommendations

The observations made during this study regarding the performance of the developed suspension system, as well as the overall characteristics obtainable, are be discussed along with the areas of concern for which future research is recommended.

CHAPTER 2

LITERATURE STUDY

Introduction

This chapter aims to describe the fundamental concepts of the technologies implemented well as the physical attributes of the elements which must be considered during the course of this study.

2.1. Ride vs. Handling Compromise

It's a well known fact that vehicle engineers have to consider the compromise between ride and handling when designing vehicle suspension systems. The suspension characteristics required for good ride comfort in a vehicle are contradictory in many ways to the characteristics which improve a vehicle's handling and stability. This compromise is especially true of vehicles which have higher centre of mass such as on- and off-road Sports Utility Vehicles (SUV's).

The main purpose of a vehicle's suspension system is to isolate the vehicle body from road disturbances as the vehicle travels over rough terrain while maximizing tyre contact with the ground in order to better control and accelerate the vehicle (Gillespie 1992). For good ride comfort over rough terrain it is desirable to have a compliant suspension system which allows the suspension to absorb large road inputs without transmitting it to the vehicle body. This compliance becomes very undesirable in dynamic vehicle situations as it allows significant weight transfer during a manoeuvre, often resulting in a vehicle becoming unstable. Thus, to allow a vehicle to safely complete very dynamic manoeuvers a stiffer suspension and low centre of mass is usually the design focus for vehicle engineers. In doing so these engineers are all too aware that one cannot easily design a suspension system which satisfies the requirements for both good ride and handling.

In recent years' vehicle manufacturers and engineers have placed significant emphasis on developing semi-active and active suspension systems which are capable of changing their characteristics to adapt to the terrain and vehicle activity (G. Priyandoko 2009). The use of the adaptive suspension systems often involves a large degree of non-linearity and require complicated models to capture their uncertainty but Priyanadoko (2009) states that numerical and experimental results suggest satisfactory improvements in vehicle dynamics are observed for these systems, but at a large additional energy consumption. It is within same semi-active realm that Els (2006) developed a semi-active suspension system, discussed in section 2.4, to solve the ride versus handling compromise for application on a Land Rover Defender. The solution of the ride vs. handling compromise is achieved because Els's suspension system is able to switch, using low energy consuming methods, between characteristics tailored to both ride comfort and handling.

2.2. Historical oversight of Semi-Active Suspension Systems

As in many mechanical systems, it is often necessary to isolate bodies or structures from disturbances which may act on them, or at least minimize their effects to prevent damage and increase mechanical life and operational comfort. In passenger vehicles passive springs and dampers are most often used to achieve some degree of isolation from disturbances which a road may have on the vehicle and its occupants. Passive springs and dampers have been used over many decades to achieve this to a reasonable degree. However, due to their fixed characteristics passive suspension systems are limited in their ability to isolate the vehicle at certain vibrational frequencies and road inputs (R.S. Prabakar 2009). This is an area where active and semi-active suspension control surpasses passive suspensions as they allow the vehicle to adapt to changing load and input conditions. Active suspensions often have an actuator in parallel with springs and dampers which add energy to a system in order to adjust the suspension to best handle the road profile being traversed. In contrast, semi-active suspensions typically do not add energy to the system but allows for suspension characteristic stiffness and damping changes, for example through the use of a magneto-rheological (MR) dampers or other similar technologies, as controlled by some control strategy. These strategies often have very complex and non-linear models which determine the idealistic suspension characteristics on the basis of an anticipated 'preview' or input history (G. Priyandoko 2009).

Magneto-rheological (MR) and ferrofluid dampers are a particular subset of semi-active devices, based on the principle of apparent viscosity changes in the presence of an electric field (J. Yao 2016). These devices have received considerable interest due to their mechanical simplicity, highly adjustable output characteristics, low power requirements and robustness (H. Metered 2010). Over the last few decades this technology has been successfully implemented into various mechanisms over a large range of engineering fields from civil structure dampers, to railway vehicles, military automobiles and commercial vehicles and bicycles. Carlson et al. proposed a MR damper for application to on/off road vehicles that experimentally demonstrated a good ability to control its damping forces (Carlson 2005). Lee et al. (H. Lee 2011) also proved that MR dampers can be effectively used to improve the ride comfort of a motor vehicle while specifically investigating the effect tire pressures have on this ability. Lee proved through the use of quarter car model, which encompassed an actual MR damper in a hardware in the loop quarter car investigation that this suspension technology can effectively improve vehicle dynamics independently of the vehicle tire being under-, optimally or over inflated. In comparison to the above work which focused on light passenger vehicles, Gordaninejad and Kelso (F. Gordaninejad 2000) proposed a magneto-rheological fluid (MRF) shock absorber which was specifically focused on high payload off road vehicles. Although the proposed MRF was of similar shape and size to its OEM shock absorber, it still presented the vehicle with the ability to control its suspension rebound and compression characteristics over a wide continuous range beyond the OEM version's fixed characteristics. Gordaninejad and Kelso focused on maintaining similar off state characteristic curves as displayed by the OEM shock absorber so that the system can be seen as "fail-safe" and return to acceptable characteristics when the control system fails. Interestingly, these authors

made use of fluid mechanics based model during development of the system which encompassed a three-dimensional finite element electromagnetic analysis tool to optimize and predict the MRF performance. (F. Gordaninejad 2000)

2.3. Semi-Active and Active Suspension Control Models and Strategies

In recent literature, research effort has focused on proposing several active and semi-active suspension control strategies (G. Priyandoko 2009). Often these control strategies aim to achieve optimal suspension performance through incorporating high degrees of non-linearity in the computation of the system desired characteristics. Others on the other hand achieve relatively high success by simple linear approximations in studies which include both numerical and experimental results (G. Priyandoko 2009).

Intelligent and real-time control of vehicle suspension have in recent times developed at an advanced rate due to continuous advancement in computing technologies. Sapiński and Rosół employed a MPC555 single board computer in combination with rapid prototyping development environments such a Matlab/Simulink to minimize the driver seat acceleration of a 3 DOF pitch-plane suspension model through Skyhook semi-active control of MR shock absorbers. During this work a hardware in the loop test setup was utilized where independently controlled MR dampers were used as a semi-active technology to minimize driver seat vibration with good performance (Rosół 2008). Real-time computational devices embedded on vehicles are used to control their semi-active suspensions based on control strategies such as Fuzzy Logic (FLC), Skyhook, Linear Quadratic Regulator (LRQ) or Linear Quadratic Gaussian (LQG) and Neural Network (NN) control. FLC was used by D'Amato and Viassolo (G. Priyandoko 2009) to minimize vertical car body acceleration and to control the suspension travel limits. Neural network (NN) controllers were introduced by Moran and Nagai which use algorithms to train the controller with a given time history in order to obtain optimal active suspension characteristics. The cost or minimization functions of these NN controllers focused on reducing vehicle body accelerations, maximizing tyre-road contact and minimizing vehicle oscillations. (G. Priyandoko 2009) NN controllers are capable of approximating complicated multi-input/multi-output functions and can control complex non-linear suspension systems through either direct or inverse modelling techniques. (H. Metered 2010) LQR and LQG controllers are also often used to optimise a vehicles suspension performance through a specific focused cost function which attributes a weighting to several performance characteristics and against which the controller will work to minimize the assigned cost function. In order to utilise the LQR controller the dynamics of the system needs to be modelled and represented. Jahromi and Zabihollah modelled their seven degree of freedom full vehicle model in state space form and presented that changing the position of the LQR pole changes the response of the suspension system. According to these authors changing the amount of imaginary part in the pole changes the oscillation of the system while changing the amount of negative changes the overshoot and steady state response and thus it is imperative to find the optimal placement of the pole. (A. F. Jahromi 2010) A further suspension control strategy that has been widely implemented in active suspensions is Skyhook active control strategy. This strategy is relatively simple yet can be powerfully used to reduce a vehicles response to inputs close to its resonant frequencies as proven by Karnopp et al. This strategy

attempts to keep a vehicle sprung mass as steady as possible over the terrain through a fictitious damper inserted between the stationary sky and this mass. (G. Priyandoko 2009) Lee et al. also makes use of this control strategy to improve ride comfort of a vehicle using a MR damper and successfully reduces the vehicle vertical acceleration RMS and WRMS. (H. Lee 2011). Active Force control is a robust and simple implementation of suspension control proposed by Hewit (G. Priyandoko 2009). In this strategy the controller attempts to reject disturbances inputted to the suspension system by incorporating measured and estimated parameter values to optimise the suspension controller. This control technique is often preferred for its computational simplicity making real-time applications viable and affordable from COTS computational hardware. Priyandoko et al. furthered the AFC implementation by incorporating a NN and a Skyhook control scheme to estimate vehicle parameters and adapt the suspension for optimal comfort, a scheme which was termed the Skyhook Adaptive Neuro AFC (SANAFC). This controller showed significant improvement over the PID and Passive controllers used in comparison and greatly reduced the amplitudes of the sprung mass acceleration by a marked 30% and displacement by 150%, implying a much better ride quality over the PID control scheme investigated by Priyandoko. (G. Priyandoko 2009)

2.4. The 4 State Semi-Active Suspension ($4S_4$)

The 4 State Semi-Active Suspension System (Figure 2.1) is a semi-active suspension system which is able to switch between two discrete spring characteristics while also being able to switch between two discrete damping characteristics. This is achieved by controlling a series of solenoid valves which channel the flow towards two independent pneumatic accumulators and/or through two independent orifice dampers.

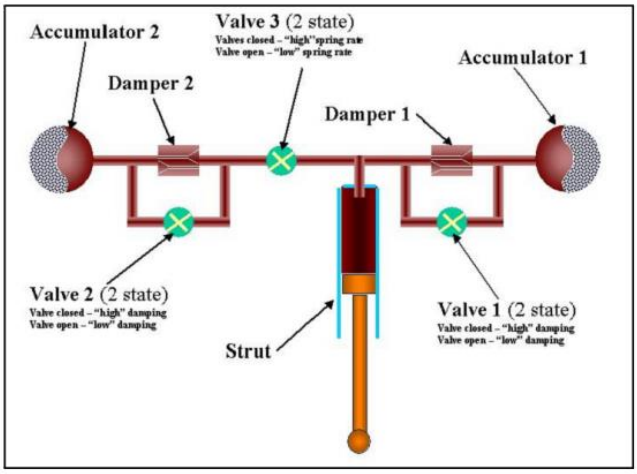

Figure 2. 1: $4S_4$ flow diagram *(Els 2006)*

Using this system above with its series of 3 valves, Els could switch the characteristics between low spring rate and a high spring rate, whilst maintaining control over a high and low damping state. In doing so he could achieve 4 discrete suspension characteristics. A prototype of the $4S_4$ developed by Els is depicted in Figure 2.2 below where it is attached to a hydraulic test bench for characterisation.

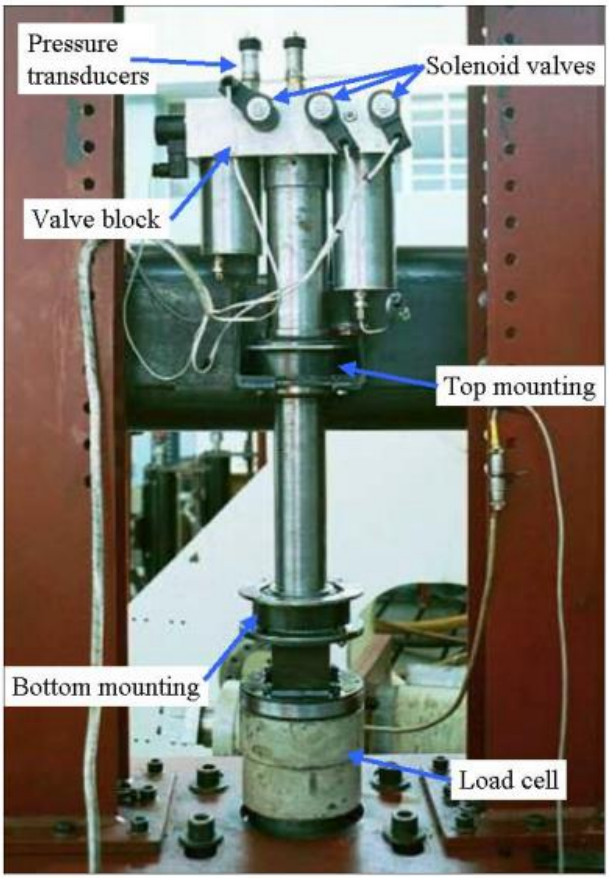

Figure 2. 2: Prototype 4S4 suspension system (Els 2006)

Els characterised the $4S_4$ on an experimental test bench and extracted the systems spring and damping characteristics in order to develop a mathematical model for the suspension system. He modelled the soft spring characteristic by isothermal gas compression with a volume of 0.5 litres. The system's effective spring rate is depicted in Figure 2.3.

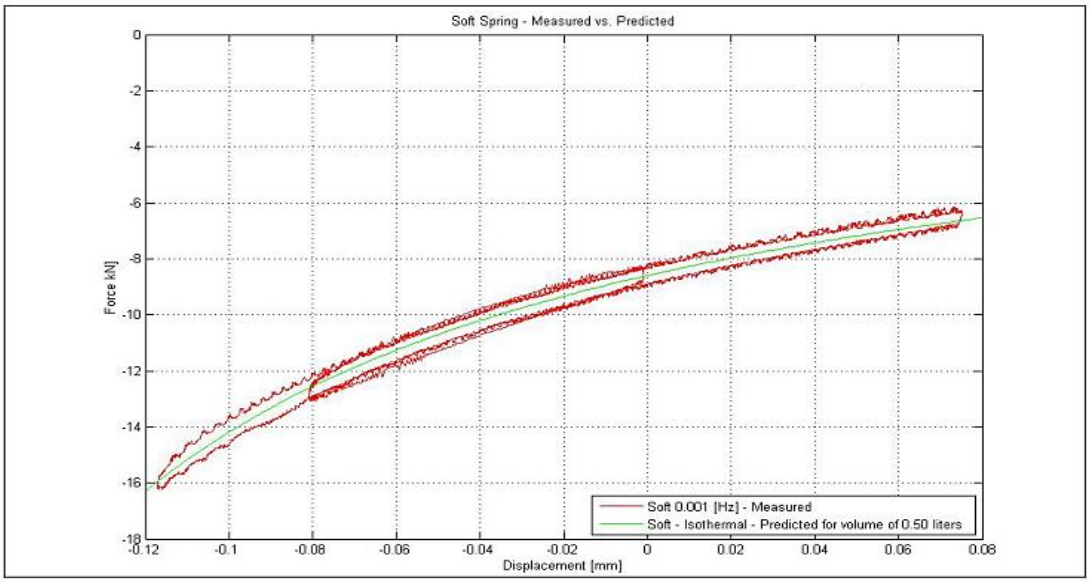

Figure 2. 3: Soft Spring Characteristic of the 4S4 (Els 2006)

Els include the effect of bulk modulus to improve stiff spring the gas model since the compressibility of the fluid is greatly influential at these system operational pressures. Els additionally incorporated heat transfer between the gas and its surroundings into a real gas modelling approach which became a

requirement to accurately capture the spring rate at the high pressures present within the system. Figure 2.4 demonstrates the correlation between the model and the experimental results.

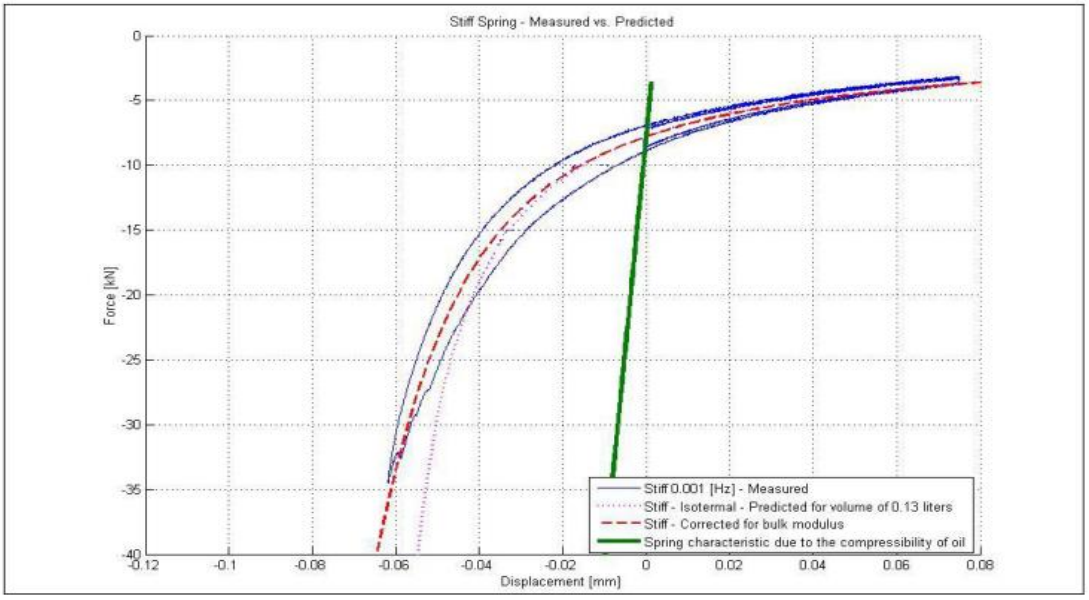

Figure 2. 4: Stiff Spring Characteristic of the 4S4 (Els 2006)

Els also characterised the $4S_4$'s damping characteristics for three of the operating states of the system. The damping force of the system was extracted as illustrated in Figure 2.5.

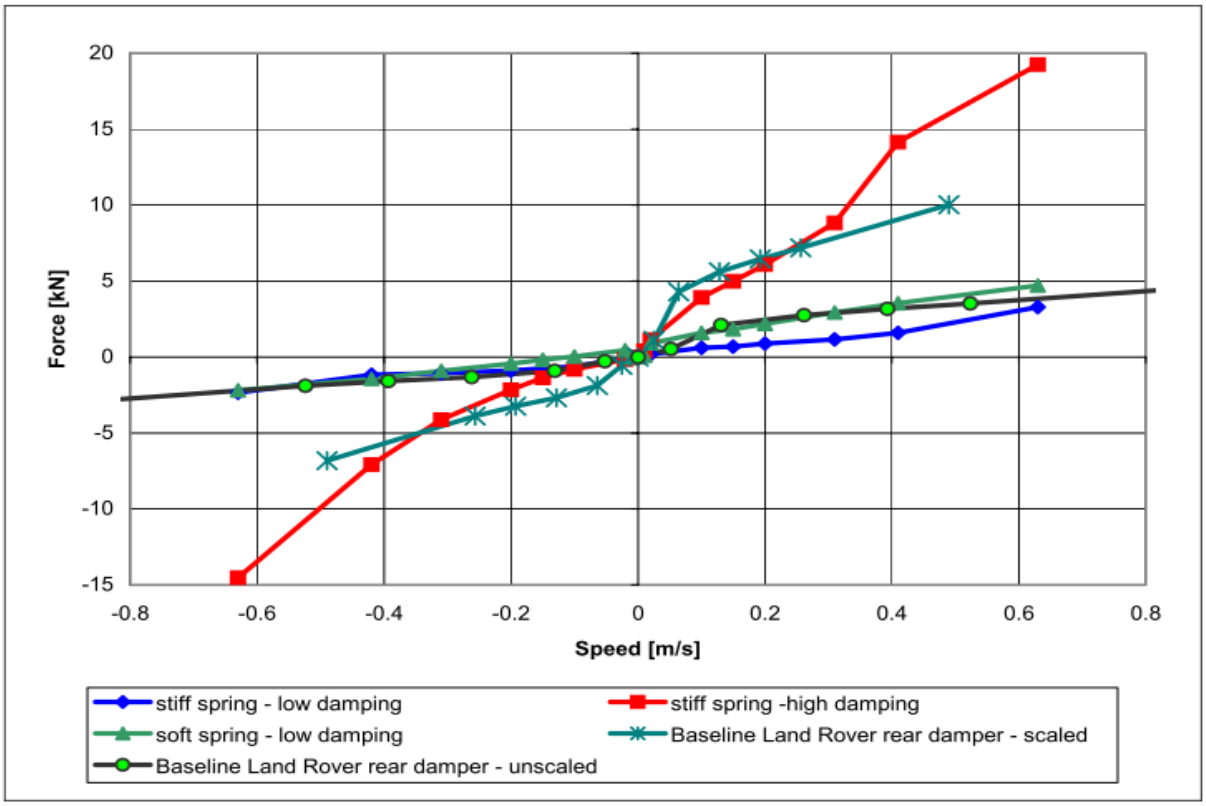

Figure 2. 5: Damping force vs. Velocity Characteristics of the 4S4 (Els 2006)

Although the $4S_4$ is able to drastically alter its characteristics it does require some time to achieve this. During severe manoeuvres stability control systems on vehicles require fast and responsive characteristics in order to effectively control the vehicle's dynamic responses. Els noted that due to the

intrinsic transient response properties of the solenoid switching valves used in the $4S_4$, the system requires between 40-90 milliseconds to switch the characteristics from 5% to 95%. This slight delay is not ideal for improving the stability of a vehicle during an unexpected manoeuvre. Els did however find that the suspension system did provide a significant improvement to the handling of the vehicle during a dynamic double change manoeuver.

2.5. The Magneto-Rheological Equipped Semi-Active Suspension System (MR$4S_4$)

In order to provide the $4S_4$ with a continuous range of damping characteristics, as an alternative to its discrete high or low damping states, Meeser (2014) developed a Magneto-Rheological valve which is capable of providing a continuous range of damping. A critical element to this work was the requirement that the developed MR valve had to block flow completely in order to allow the $4S_4$ system to still switch between discrete spring states, as was previously achieved by the solenoid valves in the $4S_4$. Meeser proved that it was possible to achieve fluid blocking through an MR Valve, or at least it provided such a high resistance to flow during dynamic manoeuvres that the flow could be considered blocked. This flow blocking was achieved by applying the magnetic field across a small annular orifice which caused the iron particles within the MR fluid to align into flow resistant structures and as such resist flow, a MR fluid characteristic which is discussed in great detail in Section 2.4. Meeser did however notice that the MR valve is not able to block flow over large periods of time as the fluid would slowly leak through the MR Valve.

Continuing on from Meeser's work, Grobler (2016) developed an MR valve which could be fitted to a prototype of the $4S_4$. His objective was to develop an MR valve which could be compact enough to install within the current $4S_4$ setup while still exhibiting the required pressure drop vs. flow characteristics. When fully energised the valve should also still be able to block flow. Grobler developed two prototype valves: one which served as an initial proof of concept (an appropriately sized valve could be developed with the required characteristics), while the second prototype was focused on real implementation of such a valve on the $4S_4$ system. His first prototype is depicted in Figure 2.6 below.

Figure 2. 6: Grobler's first prototype MR valve (Right) compared to Meeser's MR valve (Left). (Grobler 2016)

Figure 2.7 demonstrates the second prototype valve developed by Grobler as it was implemented on the original $4S_4$ system through the use of a new valve block.

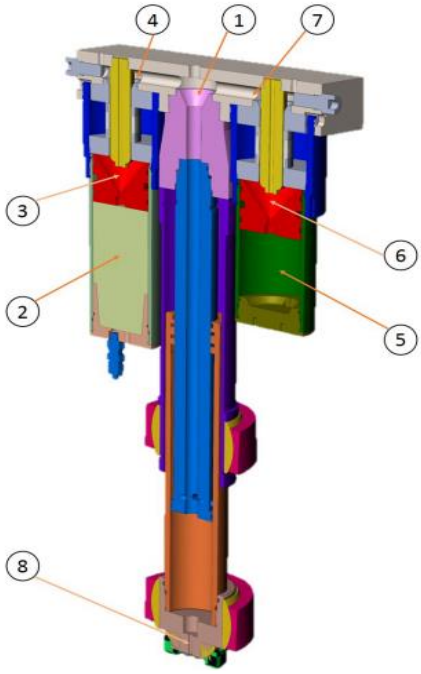

Figure 2. 7: MR4S4 with MR valves (Grobler 2016)

Grobler confirmed that the damping characteristics of the system could be appropriately controlled by the application of current to the MR valve coils. Grobler also found that the MR valves could be used to switch the system spring characteristics as was required, although there were some difficulties noted at low velocities and as a result of piston friction. Nevertheless the $MR4S_4$ system's capability of changing damping and spring characteristics was successfully proved by Grobler's work. The force velocity results experimentally obtained by Grobler are demonstrated in Figure 2.8 where it is clear that the system exhibits lower output forces than the lower bound suggested by Els. Additionally, the results also show that the system has a very high characteristic forces at low velocities while at the same time it is unable to obtain the suggested forces at high velocities of the strut. This said, Grobler proved that the force-velocity characteristics of the $MR4S_4$ can be altered through the application of current to the coils within the system and that this first iteration design initiative had been successful in developing a semi-active suspension system.

The main concerning aspect of the $MR4S_4$, as highlighted by Grobler, was that the response time characteristics of the MR valve was not yet fast enough to make this type of suspension system viable for use in commercial vehicles as actively controlled semi-active suspension systems. Although the MR valve's coil current response characteristics show that 63.2% response is obtained within 29 milliseconds and a 5-95% response is achieve in 120 milliseconds, Grobler reports that the systems output force only displays a 63.2% response in 105 milliseconds while a 5-95% is achieved in 184

milliseconds. This is significantly slower than the desired design requirement of around 40 milliseconds to observe a response on the output force of the system. The MR4S$_4$ with MR valve, designed and developed by Grobler, thus exhibited slower response characteristics than the initial 4S$_4$ system which used solenoid valves to control the characteristics.

Grobler recommends that in order to reduce the response time of the system the flow gap needs to be decreased. This will have the effect of decreasing the magnetic resistance and will increase not only magnetic response but also the physical MR fluid response as it allows for the build-up of MR fluid chains to occur more easily in the smaller gap.

Grobler reported that the developed MR4S$_4$ demonstrated the Force-Velocity characteristics depicted in Figure 2.8, as was extracted experimentally through characterisation tests. More importantly, Grobler remarked that there was some difficulty in determining the exact fluid flow conditions, or flow rate through the MR valves, present in the system during these tests as there is no way to quantify the exact amount of MR fluid flowing into either of the flow paths. As a result, Figure 2.8 highlights the overall or system force velocity characteristics of the MR4S$_4$ and not the characteristics of the individual MR valves as this is difficult to extract. The Force-Velocity plot in Figure 2.8 highlights the characteristics Grobler observed for both the "Off-State 0-Amp" tests as well as a number of other coil state combinations. It is clear that the MR4S$_4$ characteristics saturate at high activation currents while its highest damping force is still lower than the desired upper limit of the 4S$_4$ for most of the velocity range. Additionally, the MR4S$_4$ suffers from high damping forces at low velocities which is attributed to the high viscosity of the MR fluid. This is a highly undesirable effect in a vehicle suspension system as it will have a detrimental impact on ride comfort.

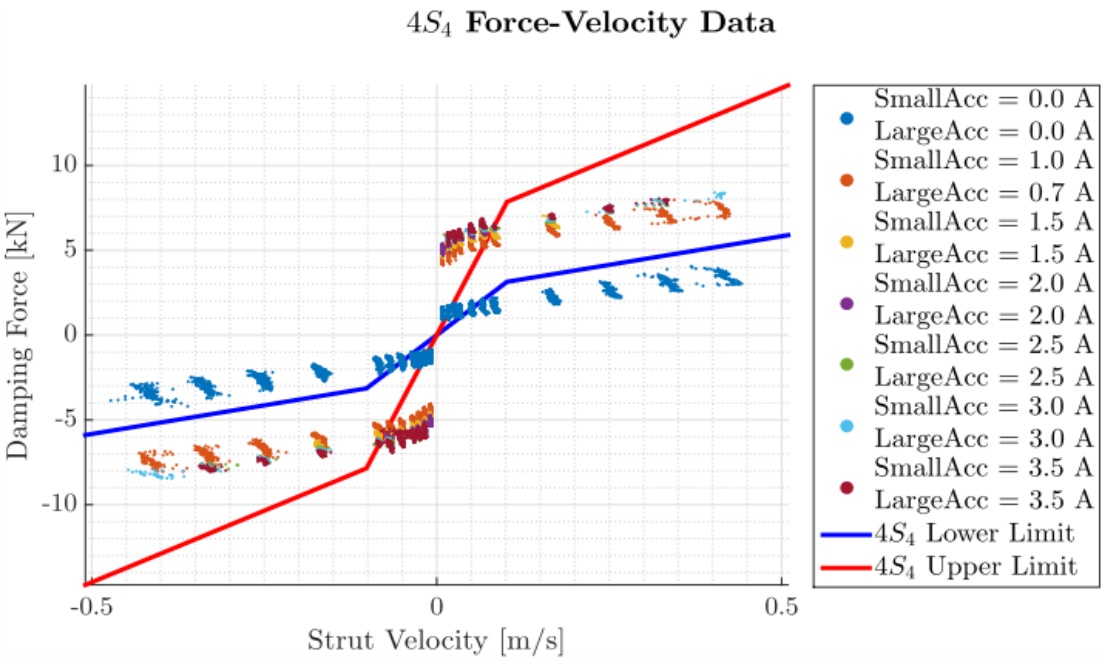

Figure 2. 8: Force vs. Velocity characteristics of the MR4S4 (Grobler 2016)

Although Grobler's implemented valves did not provide the MR4S$_4$ with the desired damping force output characteristics, Grobler was able to experimentally prove that the MR valves could be used to switch discretely between spring characteristics, as was the case with the solenoid valves in the original 4S$_4$. Grobler however noted that at some point during the stroke the MR valve would not be able to provide sufficient resistance to block flow, as the pressure drop over the MR valve would saturate, causing its blocking ability to deteriorate. This would cause the spring rate to 'soften' as flow would leak into the other flow path. This effect can be seen in Figure 2.9 whereby the second hard spring has a very stiff initial gradient but 30 mm later, during compression, the spring rate would decrease and tend toward that of the soft spring. In this figure the "Soft Spring" was the case where both MR valves were open to flow allowing compression of both accumulators resulting in a more gradual force increase. On the other hand "Hard Spring 1" is achieve through blocking flow towards the small accumulator, reducing the volume of the system from 0.6 L to 0.5 L while the "Hard Spring 2" blocks the opposite path towards the large accumulator reducing the effective volume of the system to 0.1 L and causing the observed steep compression gradient. Grobler suggests that the leakage effect could be reduced significantly by designing the MR valve with a smaller annular flow gap creating a stronger blocking ability.

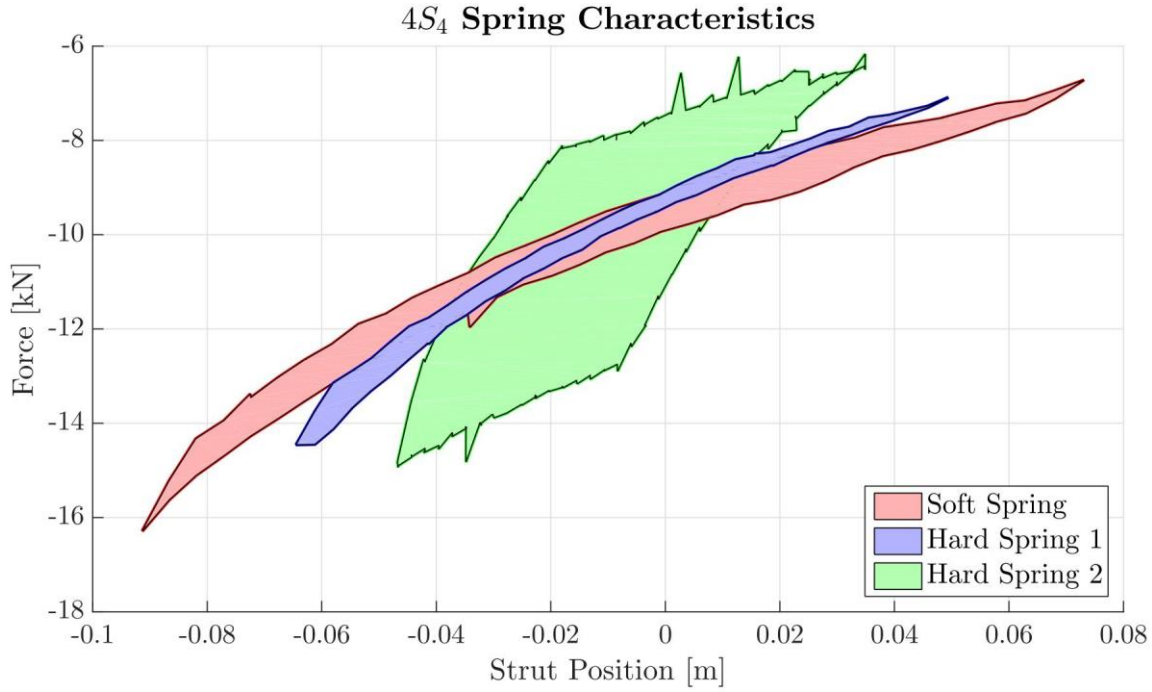

Figure 2. 9: Spring characteristic switching achieved by the MR4S4 (Grobler 2016)

During the design process of the tested MR valve Grobler estimated and predicted the magnetic field conditions within the MR valve based on an analytical approach. He developed an analogous electric circuit to represent and approximate the magnetic flow through the valve while incorporating the non-linear B-H curves of the materials which are incorporated into the calculations. Although this first principle approach provided good design insight, it was in some aspects over simplified. This study aims at extending this to a 2D or 3D magnetic FEM simulation to better understand the magnetic conditions within the valve and so doing optimising its performance.

In concluding Sections 2.1 to 2.3 as the background information to this study, it FEM based magnetic design optimisation used to develop the MR valve marks the starting point for this thesis. The objective was set to optimise the MR valve in order to obtain characteristic responses form the $MR4S_4$ which is faster and provides the desired damping forces through a thorough finite element based magnetic optimisation of the valve. In order to conduct this optimisation the following sections of technical knowledge and key concepts were required and thus detailed below for the reader's reference.

2.6. Characteristics of MR fluid and Devices

Magneto-Rheological and ferrofluid technology has received a great deal of interest in recent years due to its ability to demonstrate significant changes in apparent viscosity when exposed to magnetic fields. This change in viscosity requires only relatively small amounts of input energy, making this technology viable in a wide spectrum of engineering applications ranging from automatic transmissions and clutches, vehicle driver seat suspensions, anti-seismic applications, weapon recoil dampening and aeronautical landing gear applications. After the first invention of Magneto-Rheological fluids in the 1940's, the technology only really became of real interest to industry after the 1990's when Lord Corporation started to implement this technology in vehicle suspension, specifically the Motion Master ™ Damper. (Gravatt 2003)

MR fluids are fluids made up of a carrier oil or liquid, usually silicon-, water- or hydrocarbon-based oils which contain carbonyl iron particles which are only a few microns in size. With no magnetic field applied, MR fluid behaves in a Newtonian fashion. Under the application of a magnetic field, illustrated in Figure 2.10, the iron particles in the fluid align in magnetic dipole pairs along magnetic flux lines where they form chain like structures which resist movement or flow out of their respective flux lines to an amount proportional to the intensity of the applied magnetic field. This alignment of dipoles causes the apparent change in fluid viscosity or yield strength of the material.

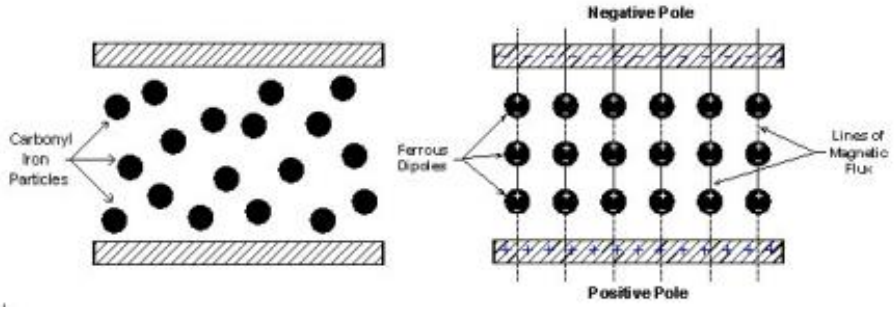

Figure 2. 10: MR fluid in inactive magnetic field (Left) MR fluid in active magnetic field (Right) (Gravatt 2003)

It is important to note that this is only an 'apparent' change in viscosity as the viscosity of the carrier liquid does not change; it is simply the thickening of the liquid due to the aligned structures of iron within the fluid. There is a point at which the ferrous dipoles within the liquid are fully aligned and any additional field strength will have little further effect on the apparent viscosity of the fluid and thus the effect saturates. Ferrofluid on the other hand is a similar to MR fluid except that the suspended iron particles are significantly smaller, 10^{-9} meter in size. The extremely small particle iron content resulted in the fluid's naming as the 'softer' fluid relative to MR fluid. Similar to MR fluid, Ferrofluid has been

proposed and investigated as the bases for dissipating energy devices such as dampers and shock absorbers by various authors in systems such as Tuned liquid dampers (TFD) and Tuned magnetic fluid dampers (TMFD) but due to the even higher cost of the Ferrofluid, MR fluid still enjoys as the most attention. (J. Yao 2016)

MR fluids do have some significant drawbacks and problems. The first of which is their inherent particle settling characteristic if not used for a long period of time. (Gravatt 2003) This is an effect which can be devastating to seals and component wear. Interestingly, Ferrofluid does not suffer this same fate. Ferrofluid particles are suspended more successfully and do not settle because they are not susceptible to settlement caused by the inherent density difference between the carrier fluid and the particles, being much smaller than MR particles. Additionally, MR fluids tend to exhibit certain viscosity related characteristic changes over time, termed by Lord Corporation as "in-use thickening (IUT)". IUT occurs when the iron particles suspended in the fluid shear into smaller particles. This has the effect of further increasing the viscosity of the fluid and can raise the force vs. velocity characteristics by as much as 250% according to the manufacturer. To combat this wear and the settling effects Lord Corporation have developed abrasion inhibitors as well as stabilizers which are added to their MR fluids to reduce settling and IUT effects throughout the fluid life (Gravatt 2003).

According to Butz & Stryk (2002) MR fluids and MR fluid devices have typical properties and characteristics as is summarised in Table 2.1. Additionally, LORD Corporation's MRF-132 (an 80% active MR fluid) properties, as was obtained from the product data sheet, are summarised for comparison.

Property	**Butz & Stryk**	**MRF-132 MR Fluid**
MR fluid Response Time	milliseconds	milliseconds
Plastic Viscosity (η) at 25 $^{\circ}C$ (Pa.s)	0.2 to 0.3	0.112 +/- 0.02
Operational Temperature Range ($^{\circ}C$)	-40 to 150	-40 to 130
Power Supply	2-25 Volts 1-2 Amps 50 watts	-
Maximum achievable Yield stresses (τ_y)	50 to 100 kPa at (150 to 250 kA/m)	48 kPa
Density (g/cm^3)	3 to 4	2.95-3.15

Table 2. 1: Typical MR fluid and MR device properties

2.7. MR Fluid Flow and Magnetic Property Models

It is critical that a thorough mathematical understanding of the behaviour of MR fluid be developed in order for one to more accurately predict the behaviour of the MR valve and $MR4S_4$ system. MR fluid could be regarded as a Newtonian fluid when it is in the absence of a magnetic field. This means that

there exists a linear relationship for the fluid shear stress as the product of the fluid shear rate and the dynamic viscosity of the fluid:

$$\tau = \eta\dot{\gamma} \qquad (2.1)$$

However, in the presence of a magnetic field MR fluids have been found to be appropriately modelled by Bingham fluid models whose shear stress can be defined by (M.R Jolly 1999):

$$\tau = \tau_y(H) + \eta\dot{\gamma} \qquad (2.2)$$

$\tau_y(H)$ in equation 2.2 is the field induced yield stress shift in the MR fluid due to the development of the particle chains which resist flow, while the second term in the summation accounts for shear stress effects of fluid flow. Before any fluid flow occurs, the MR fluid shear yield stress first needs to be overcome after which the shear stress of the fluid follows a near linear characteristic as a function of shear rate as a Newtonian fluid. These relationships are described in Figure 2.11.

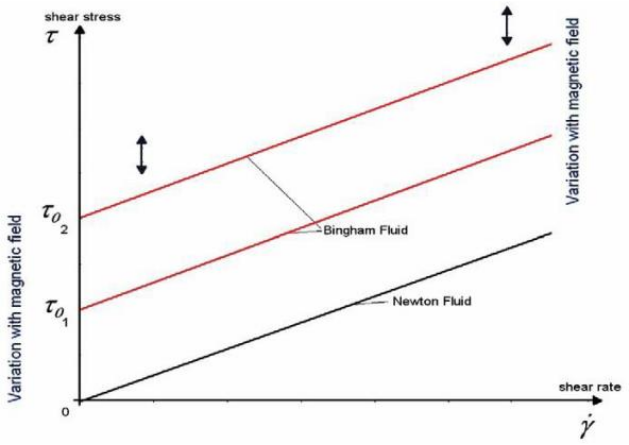

Figure 2. 11:Bingham and Newtonian model for Off and On State fluid flow shear stress (A. Grunwald, 2008)

In order to model the field induced yield stress $\tau_y(H)$ observed in the MR fluid an empirical equation was developed which estimates the yield stress as a function of magnetic field strength applied across the fluid: an equation known as "Dr. Dave's empirical equation for MR fluid shear yield stress" Carlson (2005). This equation fits the fluid shear stress relationship of several MR fluids against magnetic field strength as is discussed by Carlson. The equation appears as follows for the field dependent fluid yield strength $\tau_y(H)$:

$$\tau_y(H) = C * 27170 * \phi^{1.5239} * \tanh(6.33 * 10^{-6} * H) \qquad (2.3)$$

Where ϕ - is the volume fraction of iron particles in the fluid, H - the applied magnetic field strength in A/m while a constant C scales the equation to accommodate for various carrier fluids. C equals 1.0 for hydrocarbon oil, 1.16 for water based MR fluid or 0.95 for silicon oil.

Additionally, one requires the MR fluid's magnetic flux density (B) vs. magnetic field strength (H) relationship, known in magnetic terms as the 'B-H' curve, to predict an MR fluid's magnetic behaviour. This relationship was also modelled empirically and is called the "Dr. Dave's empirical relationship for magnetic flux density" which is described by: (Carlson 2005)

$$B(H) = 1.91 * \phi^{1.133} * (1 - \exp(-10.97 * \mu_0 * H)) + \mu_0 * H \qquad (2.4)$$

where μ_0 is the magnetic constant equal to $4\pi * 10^{-7}$, H is again magnetic field strength in A/m while the resultant magnetic flux density (B) is in tesla.

Alternatively one can use supplier data sheets if provided, such as the following curves provided by Lord Corporation of their MRF-132 fluid, to describe the yield strength and magnetic flux density curves of the MR fluid.

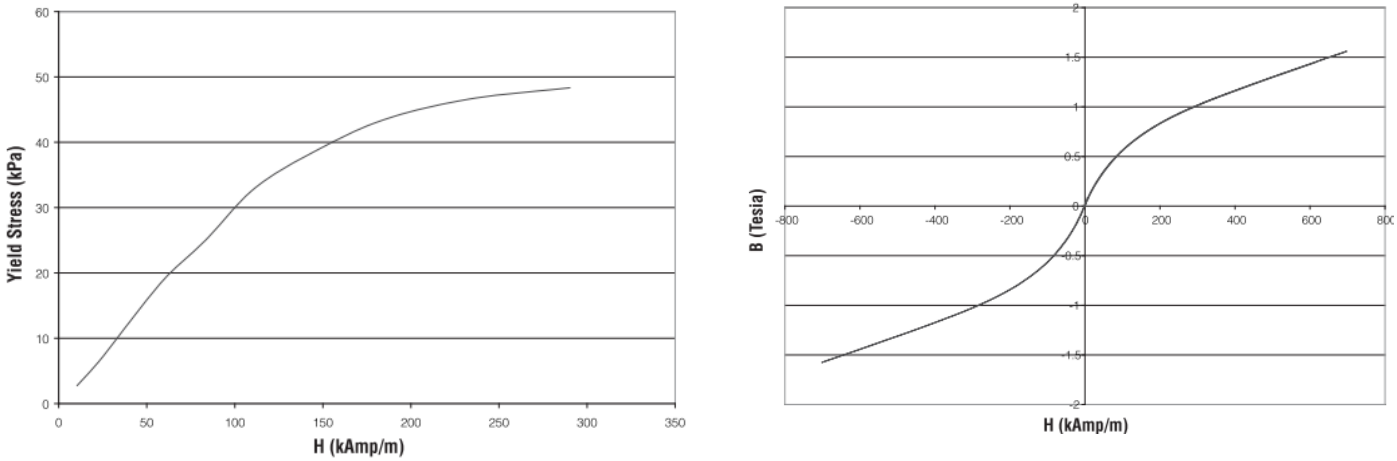

Figure 2. 12: Yield Stress vs H as well as B-H curves of MRF-132 MR fluid. (Lord Corporation 2011)

An important characteristic to take into consideration when working with MR fluid is its particular shear stress versus shear strain behaviour under the application of a magnetic field. When a magnetic field is applied, and the MR fluid has developed the flow resistant microstructure chains, there is usually a very high initial stress required to break the structure down in order to achieve flow, after which the shear stress decreases. Figure 2.13 highlights this effect where a MR fluid is subjected to a uniform magnetic field of 372 kA/m and its chain 'breaking' reduction in shear stress can be observed versus fluid shear strain. Note that Pe defines the normal stress (pressure) that the fluid is subjected to.

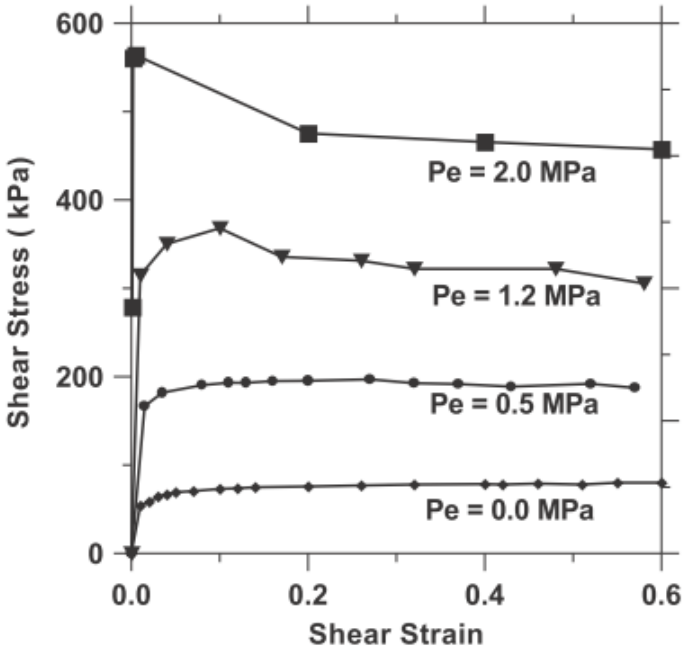

Figure 2. 13: Shear Stress vs. Shear Strain characteristics of MR fluid under magnetic fields. (Tao 2013)

This initial high shear stress at low shear strain effect is an undesired characteristic effect of MR fluid devices when the technology is used in vehicle dampers. This is because the pressure drop, or resistance across the MR device, would initially be high and then decrease somewhat after flow has been achieved and the micro structure within the fluid has been broken. This same effect was observed by Grobler during his experimental work. Grobler commented on how this effect would have an undesirable impact on a vehicle's secondary ride, or ride comfort, due to high damping forces at low velocities.

2.8. Development of the MR Valve for Suspension Damping

MR devices fulfil a range of tasks in mechanical systems. From clutches, dampers in suspension systems or MR brakes, a critical component to this system is the area upon which the MR fluid interacts with the magnetic fields known as the Magneto-Rheological Valve. In the process of designing an efficient and operational MR device it is required that one considers a wide variety of simultaneous design variables and factors. These factors include the type of MR fluid, the MR device size, shape and flow geometry, the required forces, pressures and torques (of both ON and OFF state operations), the fluid flow dynamics, the non-linear MR fluid properties under magnetic fields, the non-linear magnetic interaction of components within the devices as well as electrical constraints of the coil and the respective electrical response time influences. Additionally, one must also consider the device durability, sealing and manufacturability and operational requirements such as bearings and assembly. These are only some of the considerations which must all be considered alongside the fact that this technology is still very expensive to implement due to the very high cost of MR fluid.

Regardless, in many instances MR technology provides a mechanical platform which is a unique and effective solution to accomplish certain tasks. For this reason, research initiatives have undertaken defining the physics and mathematics behind an MR valve application. Phillips (1969), suggested that

the pressure drop (ΔP) across a device which utilizes variable yield stresses can be defined by the relationship which combines a yield stress dependent component (ΔP_τ) with a viscous (ΔP_η) component as in equation 2.5 below:

$$\Delta P = \Delta P_\eta + \Delta P_\tau = \frac{12\eta QL}{g^3 w} + \frac{c\tau_y(H)L}{g} \qquad (2.5)$$

In this relationship the pressure drop is a function of the MR device geometry where L is the length of the valve where the fluid interacts with magnetic fields and g and w are the gap and width of the flow channel respectively. Q is the volumetric flow rate through the devices, while η is the viscosity of the MR fluid in the absence of magnetic fields and c is a fitting constant. τ_y is the yield stress of the MR fluid in the presence of the magnetic field which must be obtained from the fluid data sheet or an empirical fit such as the one in equation 2.3.

Grobler (2016) developed his MR valve based on the popular pressure driven flow mode of operation wherein the MR fluid flows perpendicularly to the magnetic field in the device such that there is a build-up of MR fluid chains across the fluid gap. Grobler designed this MR valve such that the shear rate build-up across the MR gap would be sufficiently large in order to block any flow from passing through the device. Figure 2.14 shows the interaction of the magnetic field lines as they run perpendicularly to the direction of fluid flow in the pressure driven flow mode.

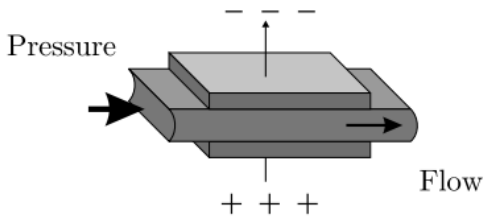

Figure 2. 14: Pressure Driven Flow mode of operation used by Grobler in his MR Valve (Butz and Stryk 2002).

What complicated the design was that Grobler had to design the valve so that it was able to achieve the flow blocking effect while the same valve had to exhibit the required low damping "off state" characteristic. To achieve this Grobler constructed a MR valve with sufficient flow area to enable the off state characteristic flow. Following on from this he then developed a magnetic circuit which was able to generate sufficient magnetic field strength to achieve flow blocking. The MR valve designed by Grobler utilised a magnetic coil which is so strong it saturates a number of the components magnetically in order to achieve sufficient shear stress in the fluid to block flow. This is an undesired design approach as it has a knock-on effect of reducing response time because of the excessively large coil which must be energised. The reduction in response time occurs because the magnetic field now takes a long time to build up to the saturated values on the (B-H) curve and thus this would have the inherent drawback of slowing all the response properties of the system down due to the magnetic circuit. The MR valve designed by Grobler can be seen in Figure 2.15.

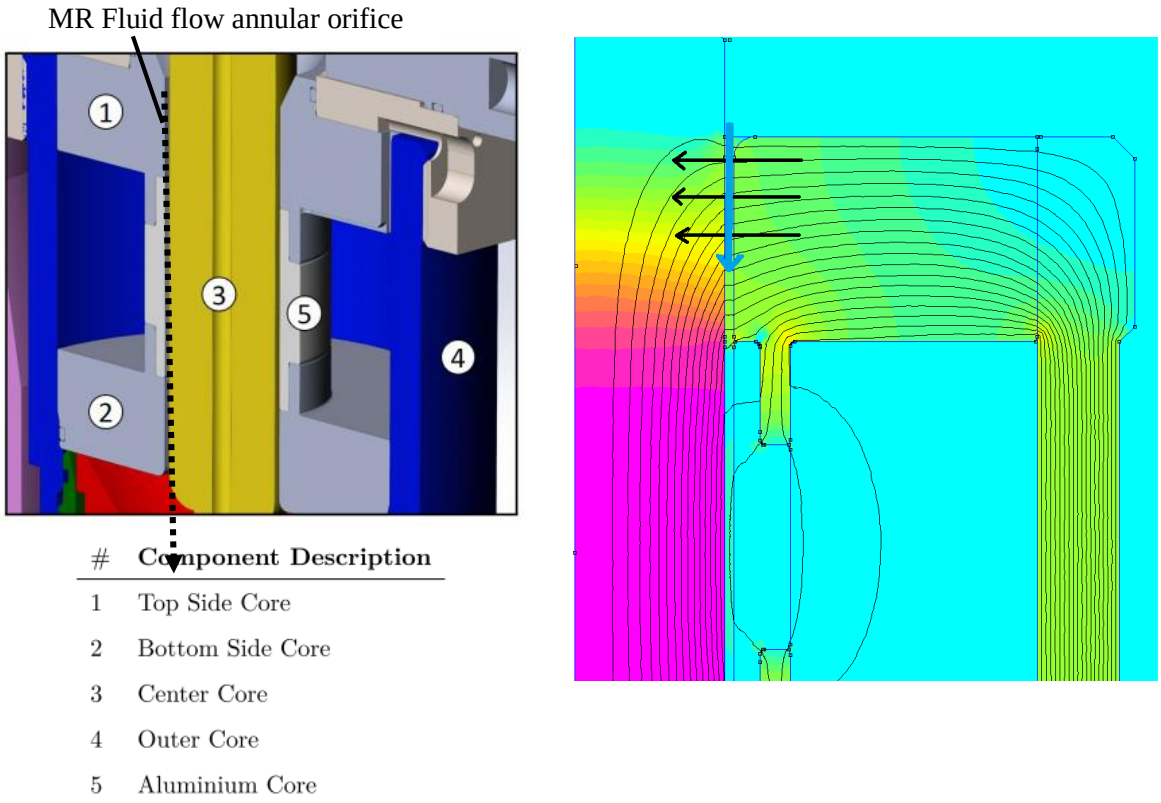

#	Component Description
1	Top Side Core
2	Bottom Side Core
3	Center Core
4	Outer Core
5	Aluminium Core

Figure 2. 15: MR valve developed by Grobler (2016)

This MR valve channels the MR fluid through the annular flow gap between the centre core (3) and the top- (1), bottom- (2) and aluminium core (5). Although not shown in Figure 2.15, the coil for this valve is situated in the gap around the aluminium core. The purpose of the aluminium core in the circuit is to act as a magnetic insulator which forces the magnetic flux through the MR liquid in the perpendicular orientation as required by the pressure driven mode. This is illustrated by the second graphic in Figure 2.15 which show the magnetic fields (black arrows) run perpendicularly to the fluid flow direction (blue arrow).

The magnetics in the MR valve was solved by Grobler from a first principle approach where he considered the following analogous electric circuit for the magnetics problem. Note that each of the components labelled in Figure 2.15 correspond to their component numbers in Figure 2.16.

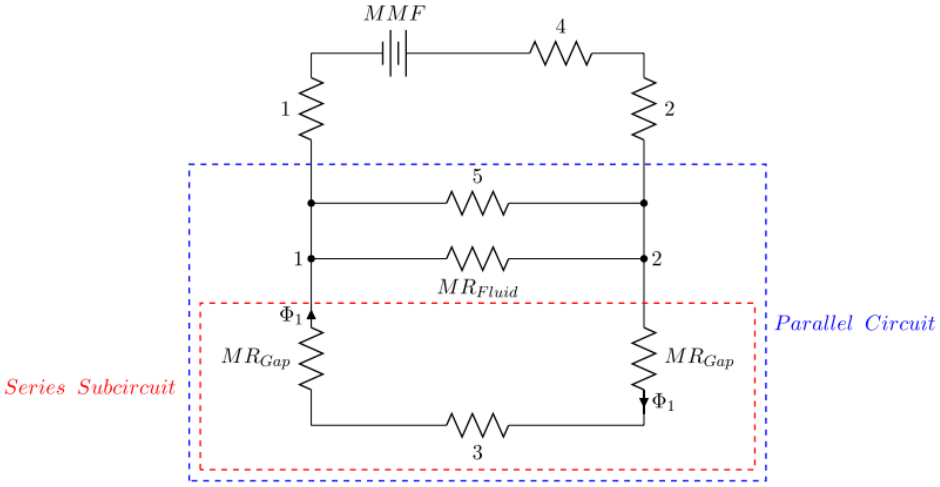

Figure 2. 16: Analogous circuit for the magnetics problem within the MR valve (Grobler 2016)

Although this analogous design methodology appears simplistic, the solution of the actual problem requires significant iterative effort as the magnetic interaction of the components in the analogous circuit are non-linear and coupled.

In order to quantify the pressure drop over the MR valve during the design Grobler used a modified version of equation 2.5 which he determined experimentally using the characterisation of his initial prototype MR valve. This modification required taking into account the shear thinning property of the MR fluid, which required adjusting the viscosity of the MR fluid as a function of shear rate, as well as adding a small modification function to reduce the yield stress dependent component of the relation also as a function of shear rate. The adjusted flow model for the MR valve pressure drop was thus defined by Grobler as:

$$\Delta P = \Delta P_{\eta} + \Delta P_{\tau} = \frac{12\eta(\dot{\gamma})QL}{g^3 w} + \frac{c\tau_y(H)L}{g} \cdot \frac{1}{2}(2 - e^{-q \cdot \dot{\gamma}}) \qquad (2.6)$$

where $\eta(\dot{\gamma}) = a(p \cdot \dot{\gamma})^{-k}$ with the constants in the scaling functions captured as $a = 1$; $p = 1.3e^{-4}$; $k = 0.51$; $q = 1e^{-3}$ and $c = 2$. Interestingly, to prove that the Phillips equation was appropriate in predicting the MR valve pressure drop, a similar design study of an MR valve conducted by Grunwald and Olabi (2008) suggested that the initial unmodified equation was appropriate to be used for designing MR valves. Their MR valve, with an almost identical layout, was able to achieve pressure drops of 1.5MPa with a much smaller coil, although these authors never commented on the correlation of their experimental characteristics with the original designed estimations.

2.9. Basic Magnetic Theory

It is important for the purposes of this study that there is a basic understanding of the magnetic elements within the MR valve as their interaction forms an integral part of defining the final response time, overall damping pressure drop and output characteristics of the MR4S$_4$.

2.9.1. The Magnetic Circuit

In the same way that electric current flows through a circuit of resistors driven by a power source, magnetic flux is driven through the magnetic materials in a magnetic circuit by a coil which acts as the power source. Behaving in a similar fashion to electricity, in order for magnetic flux to flow, a closed loop must be available for the flux to travel through and the flux will always follow the path of least resistance. Also worth noting is the fact that the magnetic flux (Φ), which travels through the materials, is a function of the magnetomotive force from the coil and the reluctance of the magnetic circuit. However, the magnetic flux density (B) changes depending on the cross sectional area (S) of the material through which the flux is travelling according to (Grobler 2016)

$$\Phi = \mathrm{B} \cdot \mathrm{S} \qquad (2.7)$$

Note that air, or the lack of a material, also conducts magnetic flux however its resistance is significantly higher.

2.9.2. The Magnetic Coil or Solenoid

The magnetic coil is a single length of insulated copper wire that is tightly wound onto a bobbin. When current is allowed to flow through this coil, a magnetic field is generated which is defined by the right hand rule. The total magnetic energy generated to drive the magnetic circuit by the coil is referred to as magneto-motive force (MMF) and is a function of the number of coil turns (N) and the current (I) flowing through the coil, while the resistance of the wire is a function of coil length and thickness of the wire. The current and thus MMF of the coil is limited by the coil cross-sectional area and its ability to carry a certain current density. It is usually suggested that a coil should be designed to carry current such that it has a current density of 4 A/mm^2. According to Ampere's law, one can calculate the output MMF of a coil as (Grobler 2016)

$$\mathcal{F} = N\,I \qquad (2.8)$$

The MMF ($\mathcal{F}$) for a magnetic circuit could also be calculated via means of Hopkinson's law as

$$\mathcal{F} = \Phi\,\mathcal{R} \qquad (2.9)$$

where $\mathcal{R}$ is the magnetic reluctance of the MR valve.

2.9.3. Calculating the Magnetic Flux Density Generated by a Coil

The magnetic flux density (B – in Tesla) in the interior of a wound coil with N number of turns may be calculated as a function of the current, length, number of turns and the permeability of the core (μ_r) as follows (Ulaby, Michielssen and Ravaioli 2010)

$$B = \frac{\mu N I}{l} \qquad (2.10)$$

where $\mu = \mu_r \mu_0$, with μ_0 being the relative permeability of free space.

2.9.4. Calculating the Inductance of a Coil

A coil's inductance is critical to its response time characteristics. The inductance (L – Henry's) of a coil is governed by (Ulaby, Michielssen and Ravaioli 2010)

$$L = \mu\left(\frac{N^2}{l}\right) * S \qquad (2.11)$$

where S is the cross sectional area of the loop/coil.

2.9.5. Electrical Resistance of a Coil

Electrical resistivity (ρ) is a property of a conductor that governs how strongly it opposes the flow of electric current and this property can be related to the resistance (R – in ohms) of a coil though Pouillet's law as (Ulaby, Michielssen and Ravaioli 2010)

$$R = \rho \frac{l}{A_w} \quad (2.12)$$

where A_w is the cross-sectional area of the wire while l defines the length of the wire. The resistivity of copper at room temperature is given as $\rho = 1.68\ x\ 10^{-8}$.

2.9.6. Inductor Time Constant and Response Characteristics

The MR valve coil has an electrical time constant which is determined by its inductance and resistance whereby the time it takes for the current to reach 63.2% of the steady state value can be calculated as follows:

$$T = \frac{L}{R} \quad (2.13)$$

In this equation T is used in seconds, L calculated in Henry and R is the total circuit resistance in ohms. This is a useful quantity in estimating the response property of the MR valve but it will exclude any other physical effects such as the compressibility of the MR fluid and mostly govern only the coil current response.

2.9.7. Magnetic Reluctance

Reluctance is the resistance of a path to allow the flow of magnetic flux. The reluctance of a magnetically uniform material can be calculated as (Ulaby, Michielssen and Ravaioli 2010)

$$\mathcal{R} = \frac{\mathrm{l}}{\mu\,\mathrm{A}} \quad (2.14)$$

where l is the length that the magnetic field has to travel through the material, A is the cross-sectional area of the element and μ is the magnetic permeability. The larger the magnetic permeability is the better a material 'conducts' magnetic fields. It is important to note that the reluctance of a magnetic field is not constant. The reluctance of a magnetic circuit increases as the elements begin to saturate at high magnetic fluxes.

2.9.8. Magnetic Permeability

The link which connects the magnetic flux density (B) within a material and the strength of the magnetic field (H) through that material is captured by the magnetic permeability of the material. Magnetic permeability is a material's ability to support the formation of magnetic fields within itself defined as

$$B = \mu\, H \quad (2.15)$$

It is often convenient to refer to a material's relative permeability where this is simply the ratio of the materials permeability to the permeability of free space (μ_0)

$$\mu_r = \frac{\mu}{\mu_0} \qquad (2.16)$$

where $\mu_0 = 4\pi\ x\ 10^{-7}$.

A magnetic material exhibits a non-linear relationship between its flux density and the magnetic field strength, even though equation 2.15, suggests otherwise. This is because the permeability of a material changes as a function of the magnetic flux density (B) passing through material. At high magnetic fluxes a magnetic material saturates, thus reducing the permeability of the material, increasing the material's reluctance and decreasing the gradient of the B-H curve. One can see this saturation clearly on a B-H plot of low carbon steel.

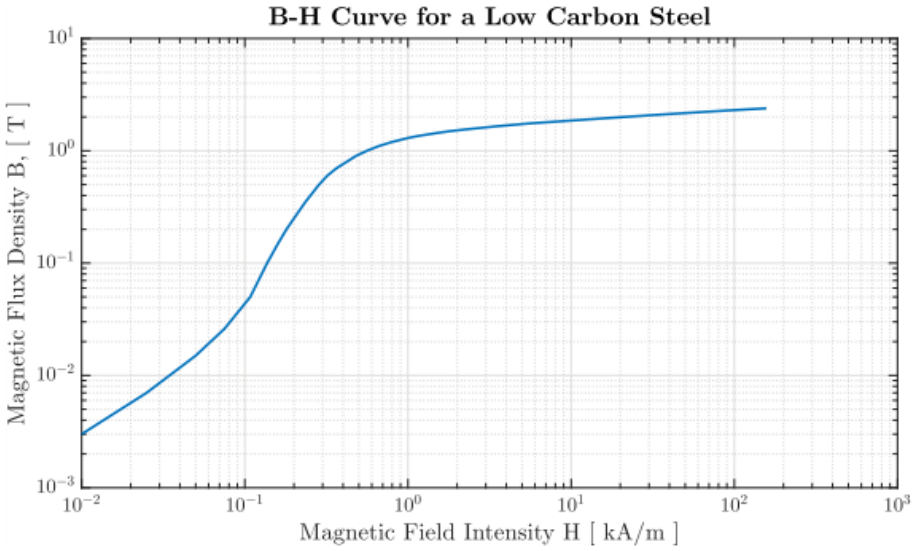

Figure 2. 17: B-H Curve of Low Carbon Steel (Grobler 2016)

To conclude, in this section it was determined that if one would need to increase the magnetic responsiveness of the valve the following must be taken into consideration: Firstly, the responsiveness of the valve is largely influenced by the degree to which its components saturate magnetically. The permeability of the materials deteriorates drastically during saturation which will cause a very slow magnetic build-up and thus saturation must be avoided as far as possible in all of the involved components. Additionally, the magnetic resistance (or reluctance) of the valve must be minimized. This can be achieved through reducing the MR flow annular gap. Then the use of better magnetic materials will also improve the responsiveness of the magnetic circuit by reducing the magnetic reluctance through an improved permeability, often by a very large factor. Lastly, a large contribution to the responsiveness of any magnetic device is its coil properties. The coil's inductance and resistance describe the amount of energy, therefore time, required to build up the magnetic field through the application of current to the coil. The larger a coils resistance is the faster its current will reach a steady condition while the time required to build its magnetic field is increased by a higher coil inductance. All of the above mentioned factors must be considered in the search for a more responsive MR valve.

2.10. Magnetic 2D Simulation with Finite Element Magnetics (FEMM4.2)

In order to account for the non-linear interaction of the magnetic circuit within the materials of the MR valve it was important to conduct a finite element based magnetic study, extending the simplified magnetic analysis conducted using the analogous approach utilised by Grobler. Initially a complex 3D ANSYS and MARC simulation were considered, however, it was soon found that a simple 2D axis-symmetric analysis of the MR valve using FEMM4.2 would be more appropriate and would provide a rapid tool to use during the design process.

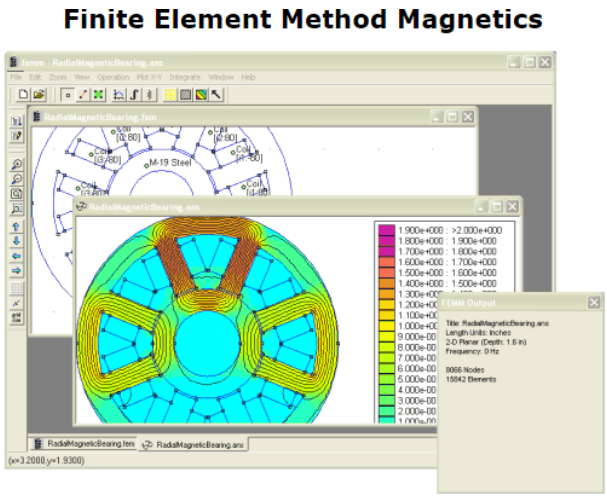

Figure 2. 18: Finite Element Method Magnetics (FEMM4.2) Package. (David Meeker 2014)

The Finite Element Method Magnetics (FEMM) package takes into account the non-linear B-H curves of the materials, the coil electric energizing current and coil dimensioning and provides detailed 2D simulation result of the magnetic conditions within the components during steady state operation. Grunwald and Olabi (2008) commented on the use and applicability of the FEMM4.2 software as they utilised it during the design and development of MR valves. These authors used the software as a design and optimization tool to anticipate the magnetic conditions across the MR gap. Figure 2.19 illustrates one of their simulation studies highlighting the magnetic conditions within the MR valve.

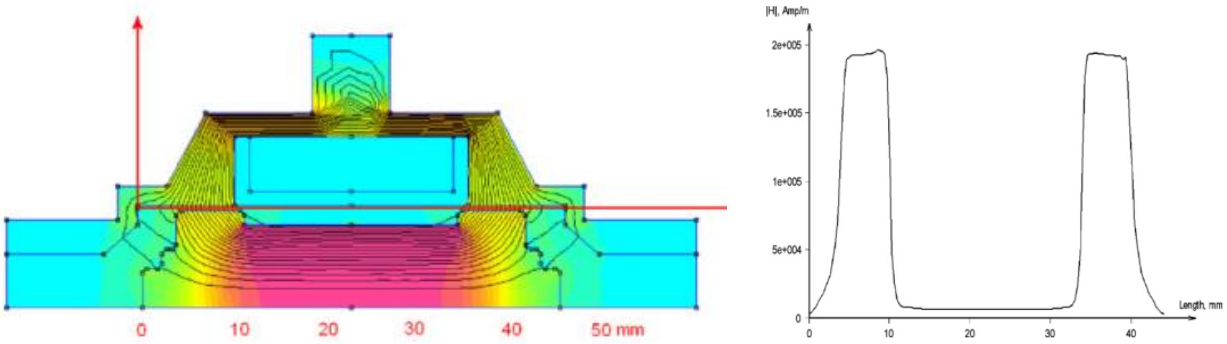

Figure 2. 19: Magnetic simulations and results obtained for MR valve using FEMM (A. Grunwald 2008)

One can see in Figure 2.19 that the magnetic conditions across the MR valve vary greatly as a function of the geometry and proximity to the axis-symmetric axis not to mention the effects of material properties. The figure proves that during design of complex magnetic components one must consider using at least a 2D or even 3D simulations to anticipate the magnetics as the use of simplified empirical models could lead the designer to false conclusions.

Conclusion

In Chapter 2, a thorough study was described in order to understand the fundamental concepts of importance in this research initiative. The overall background to the development of the MR4S$_4$ system was discussed and characteristics of the MR fluid and MR valves where highlighted along with possible modelling and analysis tools which will be used during the course of this dissertation.

CHAPTER 3

PRELIMINARY MR VALVE MAGNETIC AND FEMM4.2 VALIDATION STUDY

Introduction

In this chapter a baseline study was conducted to understand the magnetics and electrics of the MR valve. It is critical to have a good understanding of all the elements and their influences which must be considered during the design of the MR valve so that a more optimized and responsive valve may be developed.

The aim of this chapter is to determine if a more robust and effective design methodology could be employed, through FEMM simulations, to design and understand the MR valve's magnetic conditions. This would replace the analogous electric circuit method employed by Grobler as discussed in Section 2.6. To determine whether a finite element magnetic analysis could serve as the basis of the design methodology. The original MR valve developed by Grobler was examined both through FEMM simulations as well as experimental observations. Through the comparison of the experimental and simulated results it is hoped that a correlation may be observed which will validate the use of the FEMM simulation package and provide the required confidence that the software is appropriate for use as a developmental tool to evaluate the magnetics within the valve.

Finally, the influence that the MR valve material plays on the time response of the system was not well understood and quantifiable, and thus a short investigation of this was also carried out. It was important to get a sense of what the possible magnetic response time benefits would be if softer/better magnetic materials were used inside the MR valve. At the initial stages of this research project ARMCO PURE IRON was considered for use since it is a high purity soft steel with considerable magnetic advantages over conventional steel. However, replacing the steel inside the MR valve, and in so doing attempting to improve the response characteristics of the valve, comes at a significantly higher financial cost. Therefore, before this material was purchased an initial investigation was conducted in order to quantify whether the benefit of this material would be worth the cost.

3.1. Original Valve Experimental Investigation

The original MR valve, as developed by Grobler, was experimentally tested for its electric and magnetic response characteristics as well as several electric properties of the coil. This was done so that the electric and magnetic response characteristic could be compared against the simulated properties.

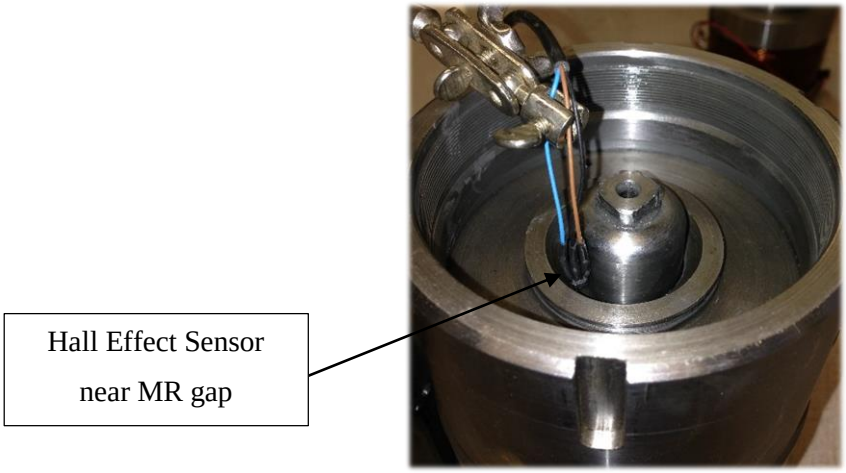

Figure 3. 1: Hall-Effect sensor measuring the magnetic field response experimentally

3.1.1. Magnetic and Electric Response Observations and Measured Coil Properties

The magnetic field generated in the MR gap by the coil was experimentally recorded through the use of a Hall Effect Sensor as shown in Figure 3.1. Additionally, the current through the coil was recorded in order to draw comparisons between the transients of the magnetic field and that of the current. Figure 3.2 shows the magnetic field measured while sampling at 2000 Hz. To examine the influence of the MR fluid, as well as the effect of the energising voltage on the response characteristics, a set of tests were conducted with and without MR fluid in the gap as well as by energizing the coil with a 6 and 12V battery respectively. Excellent repeatability was observed during these response tests since the results of three repeated tests plotted show no observable deviation. This repeatability provides a measure of confidence that the curves obtained are truly the responses of the system under the applied conditions.

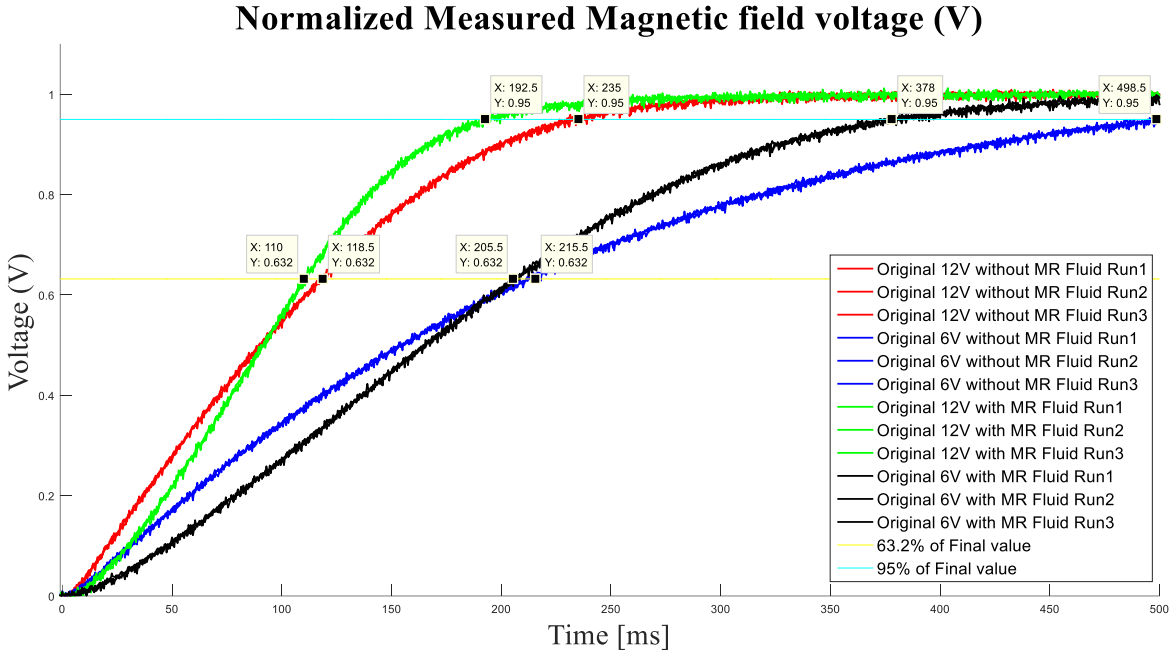

Figure 3. 2 : Measured magnetic field response

One can observe that the response of an MR valve energized by 12V is faster than that of 6V which is expected since the energy density of the supply is higher thus almost halving the response time - an effect which is visible across all the tests. Additionally, it is observed that filling the valve with MR fluid improves the transient response of the magnetics, for a 0-95% rise, when compared to a MR valve filled with air. This is expected due to the fact that air has a lower permeability compared to the MR fluid and provides higher resistance to the generation of magnetic fields, especially at high flux densities. Although the valve filled with air initially responds faster as observed during the initial stages of the ramp (0-10ms for the 12V case), the air saturates earlier leaving the MR filled valve to increase with a steeper gradient. This proves that the permeability of materials does influence the MR valve coil response characteristics.

In comparison to the magnetic field response above, the normalized current responses are illustrated in Figure 3.3.

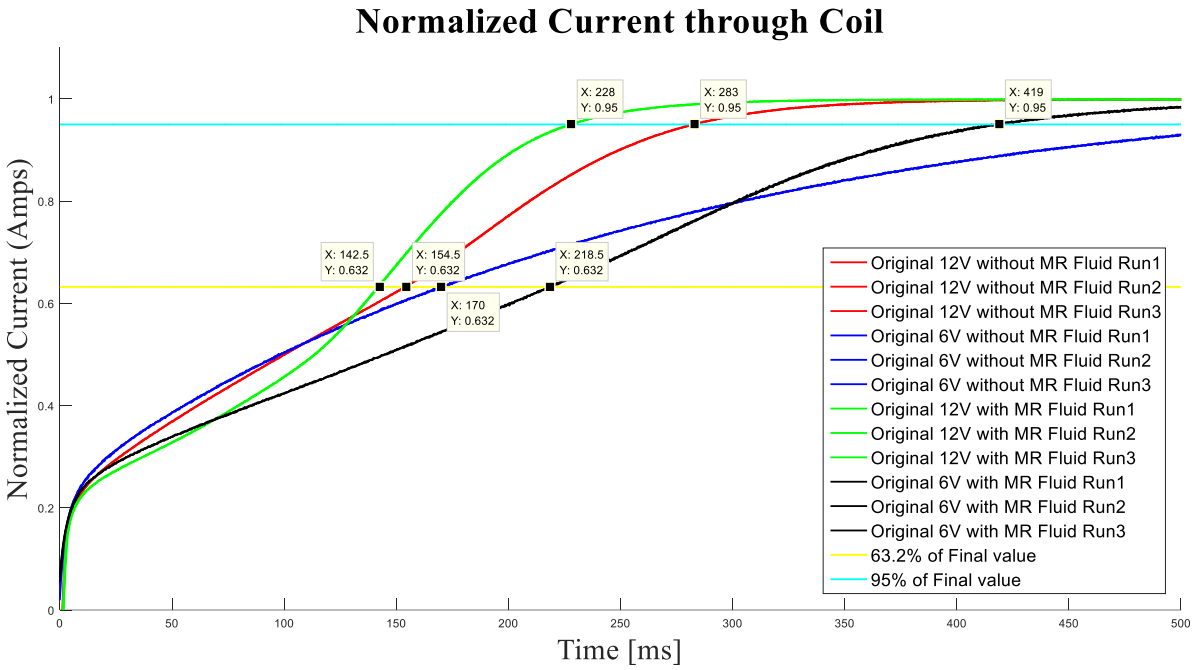

Figure 3. 3: Measured Current Response Characteristics.

Once again excellent repeatability was observed in the current measurements with similar response trends as observed in Figure 3.2. For the ease of drawing conclusions from this data the response time characteristics for both the magnetic flux density and coil current are tabulated in Table 3.1 and Table 3.2:

Table 3. 1: Experimental Time Response Investigation of the original MR valve magnetic response.

Original MR Valve Magnetic Response (ms)

	12V without MR fluid	12V with MR fluid	6V without MR fluid	6V with MR fluid
63.2%	118.5	110	215.5	205.5
95%	235	192.5	498.5	378

Table 3. 2: Experimental Time Response Investigation of the original MR valve current response.

Original MR Valve Current Response (ms)

	12V without MR fluid	12V with MR fluid	6V without MR fluid	6V with MR fluid
63.2%	154.5	142.5	170	218.5
95%	283	228	556.5	419

From Tables 3.1 and 3.2 it is easy to conclude that the MR Valve magnetic field saturates when energized by both 6V and 12V supplies. This conclusion can be drawn because the magnetic field settles to its 95% value before the coil current does in the majority of the tested cases.

3.2. Original Valve Finite Element Simulation Investigation

After the initial experimental work to obtain the electrical and magnetic response characteristics in Section 3.1, the original MR valve geometry in 2D was imported into the FEMM4.2 package for an axis-symmetric simulation demonstrated in Figure 3.4. An equal amount of coil turns were placed in the valve while it was energized using the same amount of steady state current as was experimentally measured in section 3.1 in order to draw meaningful comparisons between simulated and measured results.

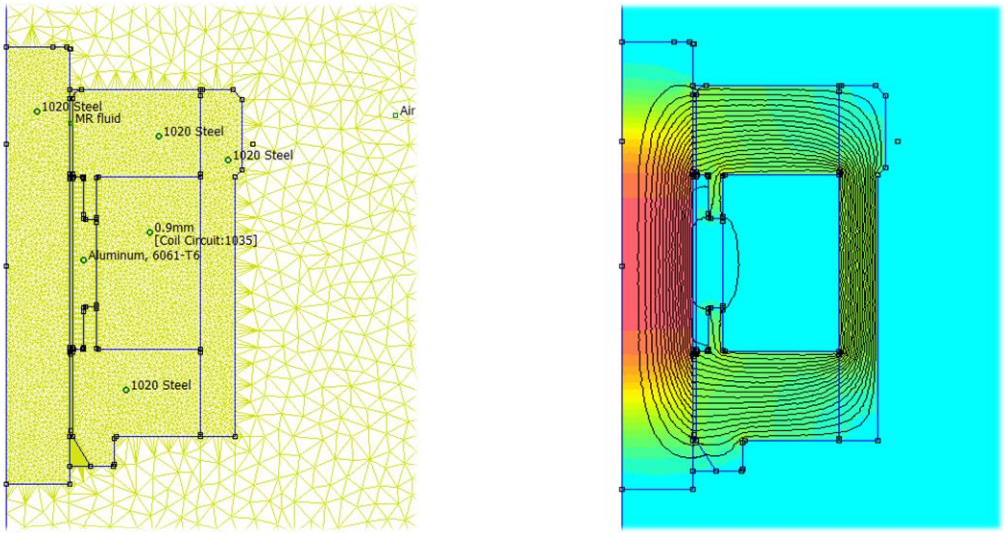

Figure 3. 4: FEMM Axis-symmetric modelling and magnetic simulation results

3.2.1. Simulation Output Response Time Observations and Coil Estimated Properties

From the simulation one can obtain an estimate for the coil resistance, its inductance, its voltage drop and power dissipation based on the coil thickness and the energizing current. Note that although reference is made to an exact 6 and 12V supply, the actual sources were 6 and 12V batteries (fully charged) and thus provided slightly larger voltages to the coils than their respective nominal values. This did not affect the applicability of the correlation since the steady state current from the experimental results were used as an input parameter to the simulation based tests, thus accounting for the slightly higher power sources. The simulation results correlated as follows with measured results:

Observed Property	**Units**	**Measured Values**	**Simulated Values**
Coil Resistance	(Ohms)	6.3	6.1334
Steady State Current 12V	(Amps)	2.213	2.213 (input)
Steady State Current 6V	(Amps)	1.095	1.095 (input)
Number of Coil Turns	-	1035	1035 (input)
Inductance at 12V	(Henry)	-	0.8261
Inductance at 6V	(Henry)	-	1.4394
Centre of MR Gap Magnetic Field at 12V	(kA/m)	-	138.15
Centre of MR Gap Magnetic Field at 6V	(kA/m)	-	126
Power Dissipated at 12V	(W)	30.85	30.03
Power Dissipated at 6V	(W)	7.553	7.367
Voltage Drop Measured at 12V	(V)	12.44	13.57
Voltage Drop Measured at 6V	(V)	6.335	6.72
Electrical Response Time at 12V (Tau)	*(ms)*	142.5	134.7
Electrical Response Time at 6V (Tau)	*(ms)*	218.5	234.68

Table 3. 3: Simulated vs. Measured Observations

Form Table 3.3 it is clear that FEMM4.2 does captures the electrical characteristics such as voltage drop, resistance and particularly the electrical response times accurately when compared to measured values. Of particular interest is the correlation in response time values where in both the 6 and 12V experiments the simulated values were within 16ms of the measured values. It was also observed that the simulated magnetic conditions were also in line with what is expected. As the simulation suggests, the magnetic field strength at the centre of the MR gap was 132 kA/m at 12V where it was designed to be around 180 kA/m by Grobler at the full 3.0 amp current. Also of importance to note is that the MR valve designed by Grobler saturates past 6V to a large degree, showing little magnetic change in response to the doubling the applied voltage - an effect which was suspected by Grobler.

Furthermore, to investigate whether the simulation's electrical response time $[\frac{L}{R}]$ is influenced by the material properties and valve geometry, the inner coil of the MR valve was changed to a pure iron material and the simulation re-run. Interestingly the inductance output changed and the response time reduced by 7.7ms to 227.2ms - an effect which is expected if the component's permeability was increased by the purer metal. This indicated that the output response time characteristic $[\frac{L}{R}]$ of the simulation is in fact an approximation of the 'effective' MR valve response time and not simply an electrical characteristic of the coil. For this reason the $[\frac{L}{R}]$ value obtained from the simulation could be used as an indication of the magnetic field response times one can expect of the valve, provided that there is not a large amount of saturation occurring within the valve.

Through the investigation in Section 3.1 and 3.2, sufficient confidence was gained that the FEMM 4.2 package could be used as a development tool of the MR valve as it would certainly provide reliable insight into the magnetic and electrical properties of a designed valve.

3.3. MR Valve Material Influence Experimental Investigation

To attempt quantifying the potential response time benefit of changing the components within the MR valve from EN24 to a more magnetically suitable material, such as ARMCO PURE IRON (< 0.01% Carbon Composition), a simple investigation was undertaken to compare the response time characteristics of EN24 (0.36-0.44% Carbon Composition) and a much softer low carbon EN3A (0.16-0.24 % Carbon Composition) material. Two identical circular cores were wound with 250 windings of 0.9 mm coil wire, where both coils had an identical resistance of 1.4 ohm. These solenoids were then energised by both a 5V switch-mode power supply as well as a 6V battery and their current and magnetic responses measured. Figure 3.5 shows the two solenoids undergoing testing.

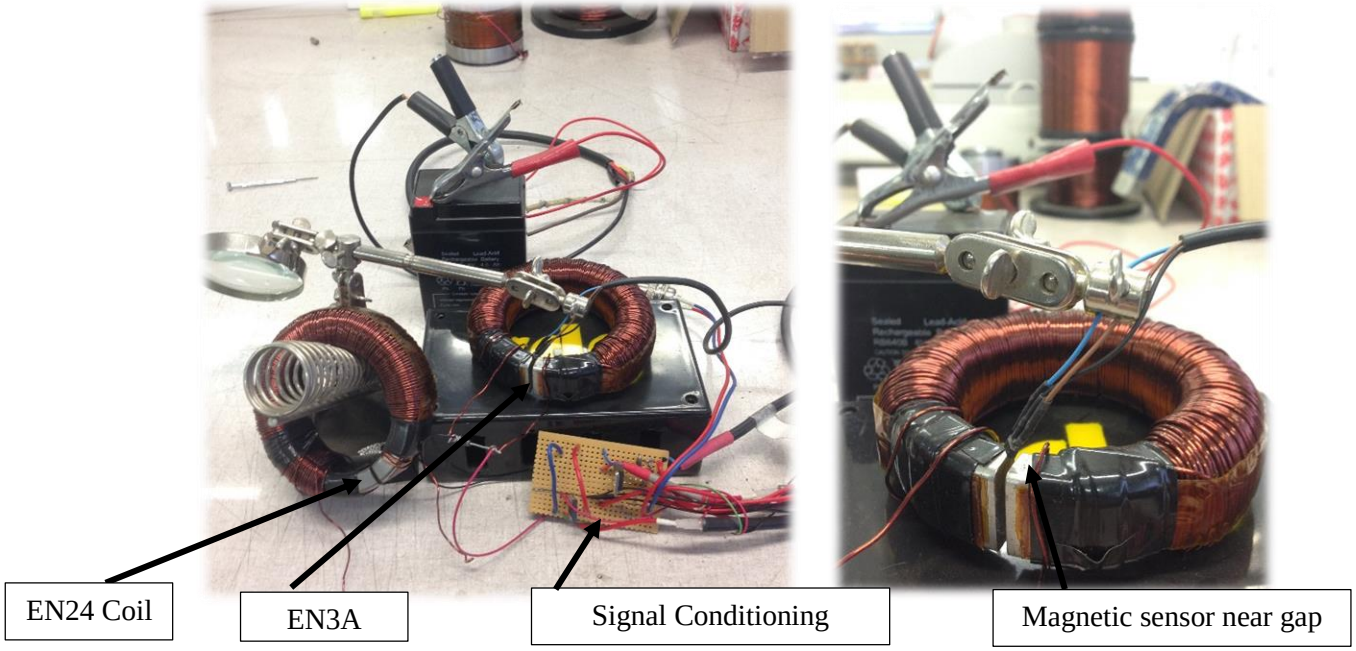

Figure 3. 5: Material influence experimental investigation

Soft irons are used in magnetic applications because of their ability to 'lose' their magnetic domain alignment when the magnetic field is removed, thus leaving a low residual magnetism when the magnetic field has been removed. Such materials also have a higher permeability which increases their ability to generate and carry a magnetic field within the material and decreases the time required for a magnetic field to build up. The purer an iron is, the higher its permeability can become, often by a significant factor. Pure Iron (such as ARMCO PURE IRON) has a relative permeability of 200 000 while electrical steel has a relative permeability of 4000. Normal carbon steel only has a relative permeability of 100-10000. This permeability does change as a function of the applied magnetic field whereby the permeability reduces as the magnetic field strength increases.

Experimentally it was noted that there is a significant benefit for using the EN3A steel over EN24. It was measured that EN3A generates both a higher magnetic flux density while it also achieves the same flux density as EN24 in a shorter period of time, thus having a better response characteristic. Figure 3.6 shows the change in magnetic flux density measured while energised by a 6V battery with each coil's 95% percentile line plotted. Note that these measured voltage values are not converted to an exact magnetic flux density for a quantitative comparison as the sensor was not placed at an identical distance from the respective coils. Rather, the sensor was placed in such a manner so as to ensure that its reading does not saturate during measurement since the output value of the sensor is extremely sensitive to the distance from the magnet. For this reason, the change in measured magnetic voltage (ΔV) is plotted and not the absolute measurement in order to remove the effect of sensor proximity. Also note that during these tests the hall effect sensor was placed perpendicular to the applied field.

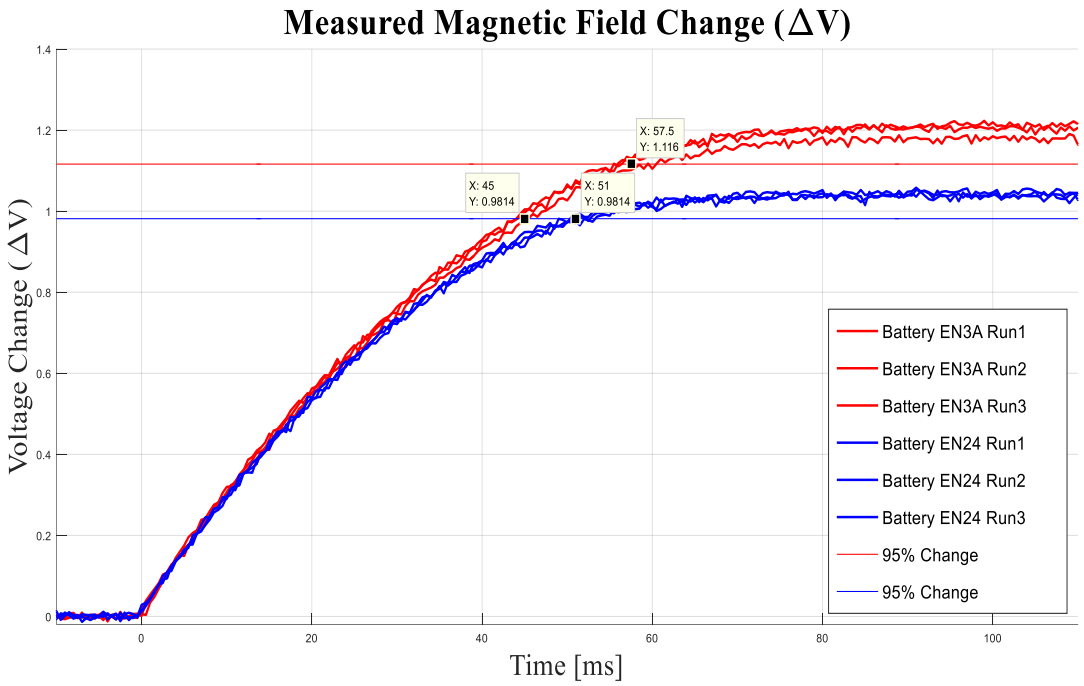

Figure 3. 6: Measured Response of the Magnetic Field

Firstly, the EN3A coil has a 15% larger change in magnetic flux density when energised in comparison with the EN24 coil. According to the conversion on the Hall Effect Sensor data sheet, this voltage difference suggests a $4.8 \cdot 10^{-3}$ Tesla higher magnetic flux density. One must note that although this seems to be a small change, it is in fact significant because the magnetic flux density measured by the Hall-Effect sensor is only for the 'leaked' magnetic fields since the sensor was placed far from the actual path of the magnetic field to avoid saturation. Therefore, one can expect a much higher increase in both magnetic field strength as well as magnetic flux inside the actual magnetic field path of the valve if the core is constructed from a lower carbon softer steel.

Secondly, it is notable that the EN3A coil reaches the equivalent 95% voltage change of the EN24 coil 7 milliseconds earlier. This confirms that a higher permeability, lower carbon soft iron will improve the response time properties of the MR valve as was suggested by the literature although the benefit was not as significant as initially hoped.

Figure 3.7 supports the theory that the magnetic field in both EN24 as well as EN3A coils have been saturated. This can be concluded because across all the cases the change in magnetic flux density reached 95% long before the current inside the coil reached its respective 95% value.

Interestingly one can also observe that the EN24 current ramp to 95% is faster than the EN3A, however, this does not suggest that EN24 provides a better magnetic response time. This phenomenon is believed to be the result of lower magnetic flux density which can be generated inside the EN24 coil, possibly significantly less, when compared to the softer iron which leads it to saturate magnetically much faster. Once the core has become magnetically saturated it provides less inductive resistance and therefore the current builds up in the EN24 coil faster and reaches its final value prior to the more magnetic EN3A.

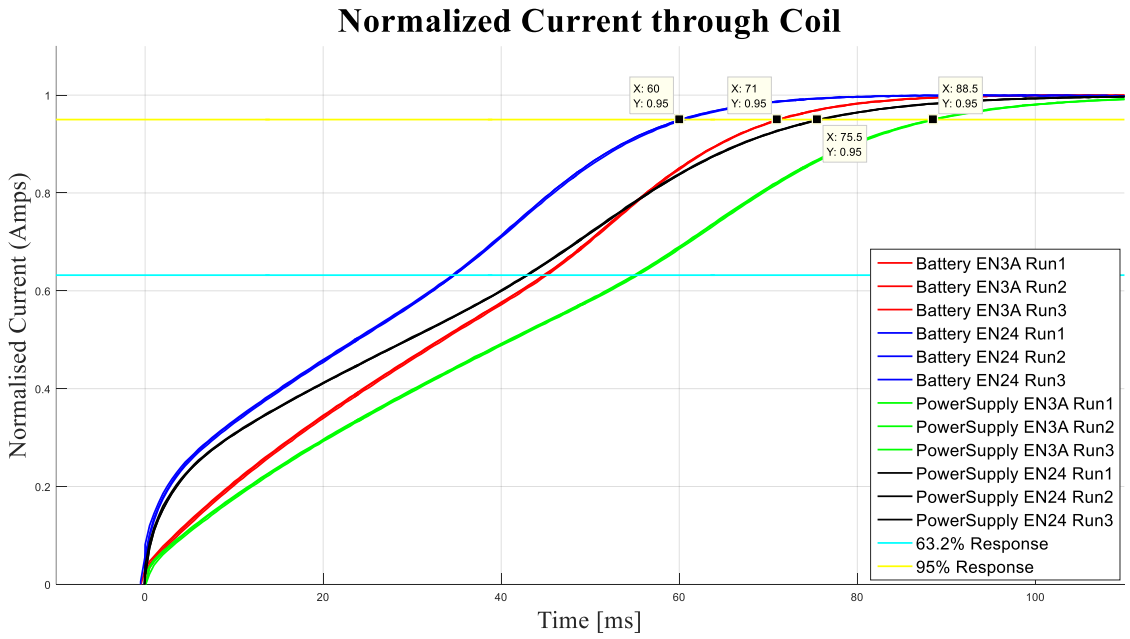

Figure 3. 7: Normalized Measured Current Responses of EN3A and EN24 Coils

Figure 3.7 shows that EN3A's current takes 71 milliseconds to build up to a 95% of its final value whereas EN24 only requires 60 milliseconds. Again it is expected that this is due to an earlier saturation of the magnetic field within the EN24 as the actual steady state current within the coils are identical.

Finally, an observation is made if one considers the switch-mode power supply's current ramp as compared to the battery. The switch mode is not able to provide the steep initial current which the battery does as it tries to adapt its output to accommodate the sudden load which has been applied. This additional delay of a switch-mode supply must be considered when designing an MR valve based system as the power supply used to energise the coils will have a significant impact on the overall characteristics of the system as is highlighted here.

Conclusion

During this preliminary study it was found that one could use the FEMM4.2 simulation package with confidence to accurately predict not only the magnetic conditions within a designed MR valve, but also to extract properties of the electric circuit and very importantly that of the expected response characteristics of the MR valve. Furthermore, it was proven that the magnetic material used within the MR valve would certainly have an influence on the overall magnetics and response characteristics of the valve. It became apparent that such influences must be carefully studied and considered during the design process, which at least could now be done using a finite element approach with good confidence. Finally, it was proven that in the design of a magnetic component where the magnetic response is of importance one should pay careful attention to the saturation condition of its components. The saturation of a component or multiple components in the magnetic valve would be detrimental to the response dynamics of the building magnetic field and this should be avoided as far as possible.

CHAPTER 4

DESIGN, DEVELOPMENT AND TESTING OF THE THIRD MR VALVE PROTOTYPE

Introduction

Once the applicability and accuracy of the finite element magnetic simulation package, FEMM4.2, was verified through the investigation in Chapter 3, it became a design tool which could be extensively used to optimise and analyse the magnetic conditions within the MR valve. The main aim of the optimisation was to decrease the response time of the valve such that the suspension system fitted with the MR valves could be more dynamically controlled. Additionally, it was important to maintain the flow blocking ability of the MR valve in the efforts to improve the pressure drop vs. flow characteristics. According to Grobler (2016), the magnetic circuit is responsible for 2/3 of the total response of the $MR4S_4$ system and if this could be improved the MR valve flow switching capability would be on par with the solenoid flow switching capabilities. This chapter will discuss the design process followed to develop and optimise the third prototype MR valve.

4.1. MR Valve Flow Annulus Optimization

In order to decrease the magnetic resistance of the MR valve's magnetic circuit, in order to increase the response characteristics of the MR valve, it was important to minimize the flow gap between the inner core and the outer cores. A smaller flow gap decreases the magnetic reluctance of the magnetic flux to 'jump' the gap and travel through a less magnetically permeable MR fluid. Decreasing the magnetic reluctances creates a stronger and more rapidly building magnetic field. However, in order to maintain a similar 'off-state' characteristic, it was imperative to keep the same annular flow area such that the valve could achieve similar flow characteristics to Grobler's second iteration of the MR valve. Therefore, to achieve the gap reduction whilst maintaining the same valve flow area as the second prototype, the annular diameter of the flow path had to be increased. This gives the inner core a larger inner diameter as illustrated in Figure 4.1. In Figure 4.1 the new design is shown alongside Grobler's second prototype MR valve. The new design was developed to fit into the assembly of the original valve, keeping the fastening mechanisms as well as the flow path lengths identical to the previous iteration of the valve.

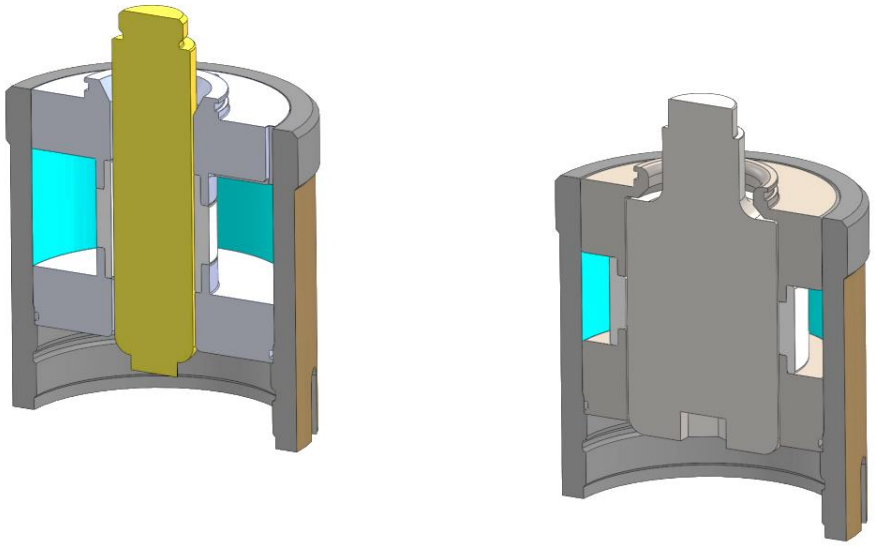

Figure 4. 1: Comparison between MR Valve Geometries.
Left MR valve was developed by Grobler (2016). Right is the new optimized MR valve design.

A clear advantage brought about by the increase in size of the inner core is that the inner core no longer saturates as much as was the case in the original valve whose inner core saturated extensively due to the small area which had to carry the magnetic flux. Figure 4.2 illustrates how the inner cores of the two comparative geometries saturate during their maximum current energising condition - an effect which reduces the maximum achievable MR effect as well as the responsiveness of the valve. The reduction in magnetic reluctance as well as the decrease in the magnetic saturation of the inner core therefore allows the newly designed MR valve to generate much higher field strengths and do so at a faster rate.

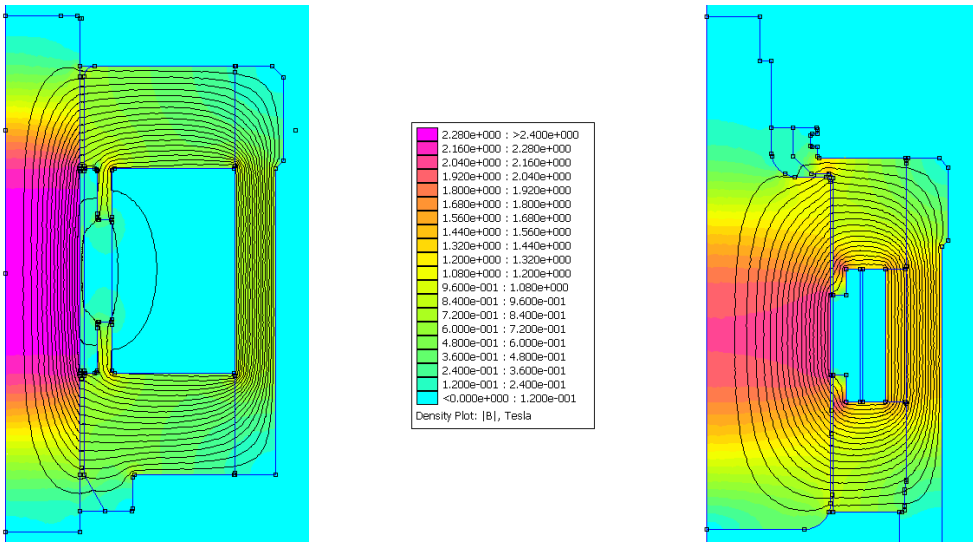

Figure 4. 2: Comparison of Magnetic Saturation Condition during full energising

However, since the MR effect of interest only requires a magnetic field strength of 200 kA/m, as higher field strengths saturate the MR fluid yield stress abilities as shown in Figure 2.12, the new design now requires a significantly smaller coil to produce the same magnetic conditions. The utilisation of a smaller coil will further improve response time characteristics. The new design MR annular flow gap was decreased from the original 0.9mm to 0.51 mm by increasing the annular diameter proportionally in order to ensure the same flow area as the original MR valve.

After finalising the MR valve geometry in Section 4.1, which defined the off-state characteristics, an iterative simulation based design approach was used in order to design/select the magnetic coil which would energise the valve most effectively. This iterative design optimisation effort is discussed in the following section.

4.2. MR Valve Magnetic Field Optimization

The MR valve's magnetic circuit was analysed and optimised extensively through the use of a co-simulation between Matlab © and the FEMM4.2 © software. The FEMM package has the capability of being executed from a Matlab based script such that one can change input parameters, geometries and coil conditions. The results can also be extracted into Matlab for analysis once the simulation has been performed. This capability was used in the search for an optimised MR valve.

4.2.1. Single Energising Coil

In the search to find the optimised coil for the MR valve, a design investigation was conducted based on a single coil approach. The new valve geometry, as depicted in Figure 4.3, was imported into the FEMM software. During the investigation the coil diameter and number of turns were iteratively changed and the response time and magnetic field strength observed. A series of simulations were performed to extract the average magnetic field characteristics from within the MR gap as well as the response times of the coil from the simulations. Coil geometrical size and shape was taken into account during the process to ensure that the coil solution obtained would be able to fit within available geometry.

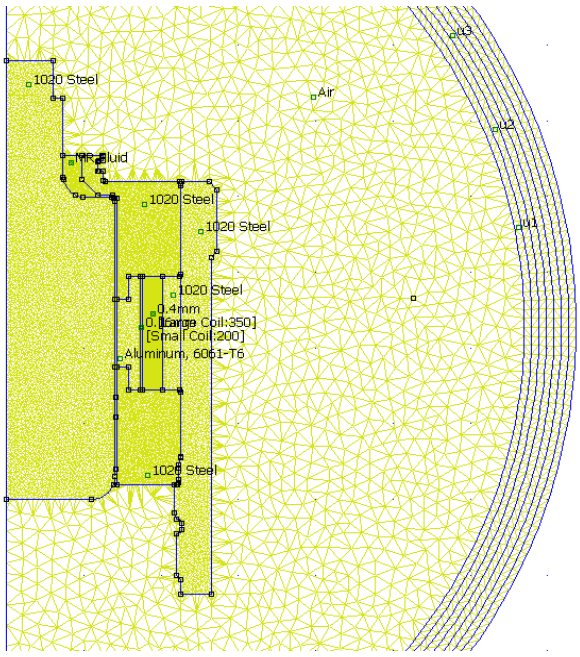

Figure 4. 3: New Geometry FEMM Setup

To compare the effect of reducing both the MR gap size and saturation of the inner core on the magnetic field conditions within each respective MR valves are plotted in Figure 4.4. Figure 4.4 shows the magnetic field strength as a function of coil wire diameter and coil turns for each of the valves. From this comparison one can see that under the same input conditions the magnetic field strength in the new MR valve was almost 2.8 times larger in the MR gap. The original valve shows very little magnetic field increase when its coil turns and coil diameter is increased compared to the new valve which highlights its magnetic saturation.

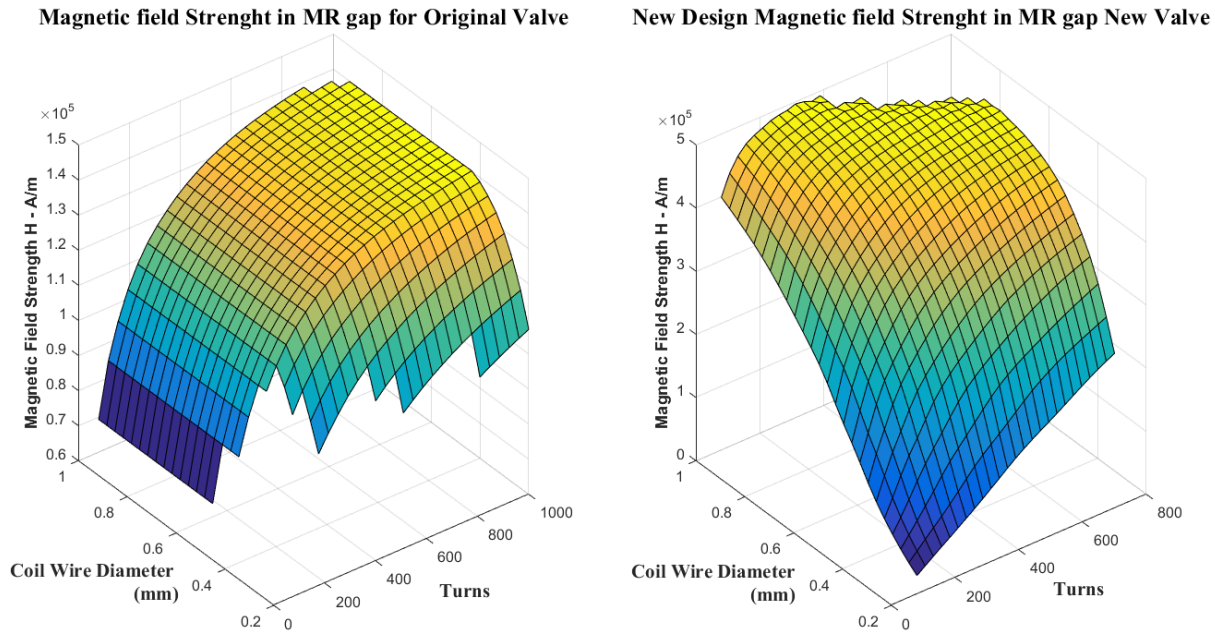

Figure 4. 4: Comparison of Magnetic Field Strength of New and Original MR Valve

In order to find the best combination of wire diameter and number of turns to maximizes the magnetic field strength while minimizing the response time, a non-linear optimiser within the Matlab platform was used in an optimisation study of the MR valve coil. It was, however, soon realized that no possible single coil configuration would be capable of achieving response time characteristics of less than 30ms while generating sufficient magnetic field strength to achieve flow blocking. Since both of these criteria were of great importance to the study it was decided that the implementation of a duel coil configuration would be investigated.

4.2.2. Double Energising Coil Approach

Since one could not achieve both the flow blocking requirement as well as the required time response characteristics with a single coil, a double coil approach is configured in order that a smaller coil may be used to achieve rapid responses and control in the MR valve characteristics while a second larger coil would then be able to generate sufficient magnetic fields to achieve the required flow blocking within the valve.

Equation 2.6 suggests that in order to achieve sufficient flow blocking the magnetic field strength required within the MR gap must be around 220 kA/m. The magnetics analysis suggested for a range of coil diameters the field strengths depicted in Figure 4.5 can be obtained in the new MR valve with 364 turns. Figure 4.5 therefore suggests that when a coil with a diameter of 0.3 mm is energised at its maximum current rating using 364 turns sufficient magnetic field strength will be generated to achieve the required flow blocking condition.

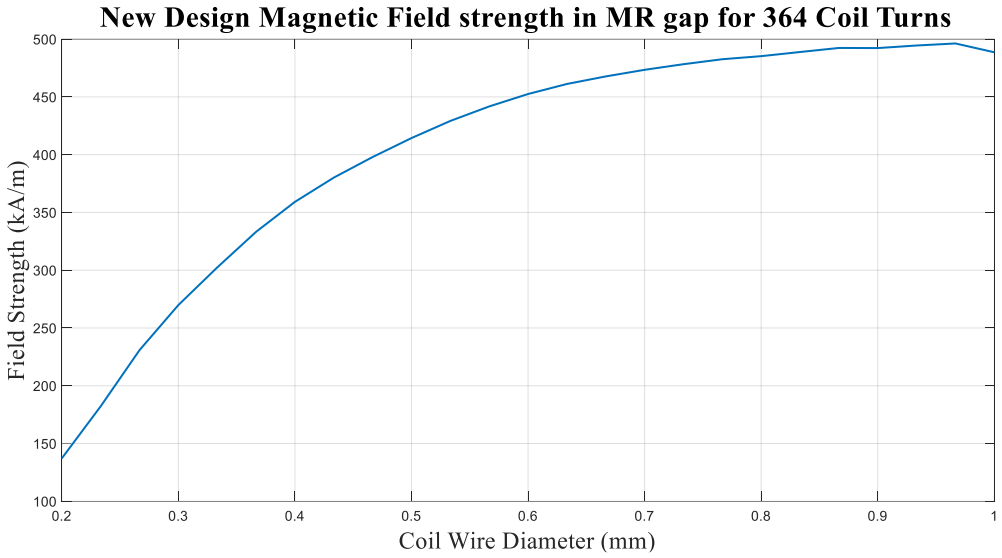

Figure 4. 5: Achievable Magnetic Field Strength in the MR gap vs. Coil Diameter at maximum current

Since a 0.4 mm diameter coil wire could be sourced from a local supplier and it provided some additional magnetic field strength, the decision was made to use this in the valve with 350 windings as the flow blocking (large) coil.

In designing the smaller response coil, the primary focus was placed on ensuring that it would respond within 30 milliseconds thus providing a faster characteristic than that of the baseline $4S_4$ system. Again the number of coil turns and coil diameters where investigated. It was decided that 200 turns of a 0.2 mm diameter wire would be a suitable compromise between strength and speed. Such a coil would provide 43% of the locking magnetic field with 87 kA/m within the MR gap, and in less than 26 milliseconds.

Figure 4.6 illustrates the simulation results when both coils are fully active, generating a total magnetic field strength within the MR gap of 360 kA/m. Note that Figure 4.7 shows the magnetic field strength condition obtained within the bottom half of the MR gap. This is a considerably higher magnetic field strength than what is required according to the Phillips equation and it would certainly saturate the MR fluid shear stress effect under these conditions. However, it was decided that because the new MR valve coils were already considerably smaller than the previous prototype and responded much faster, some over-design in terms of the magnetic field would serve as a safety factor.

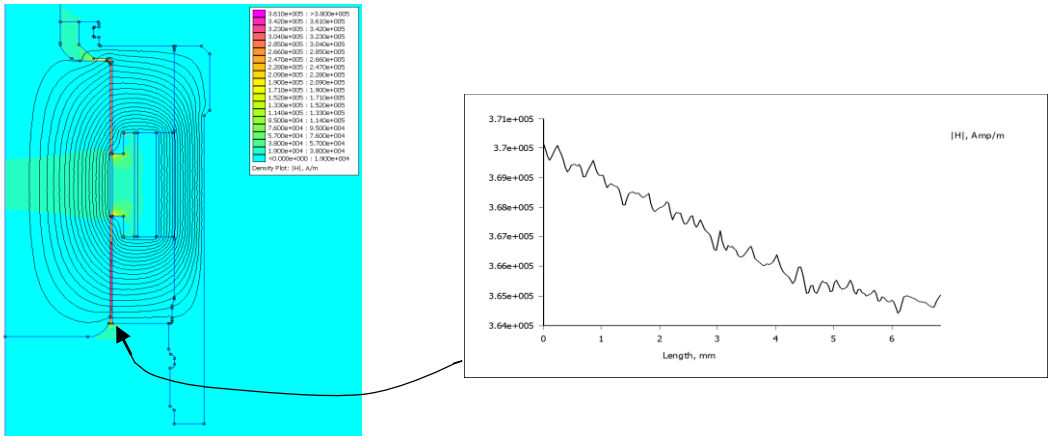

Figure 4. 6: Final design MR valve magnetic simulation at maximum energisation

The resultant magnetic field strength and response time characteristics observed during the simulation based analysis of the new designed MR valve are plotted in Figure 4.7. Note that these are the average magnetic field conditions within the MR gap. We can notice that the achievable magnetic field strength is mostly linear for the small coil suggesting little saturation of the valve. Contrary to this the large coil starts to saturate the MR valve components to some degree thus explaining its slightly more non-linear nature. As is expected the MR valves respond much quicker when higher currents are applied to the coils, simply due to the larger voltage which would need to be applied in turn with its higher energy density energising the coils.

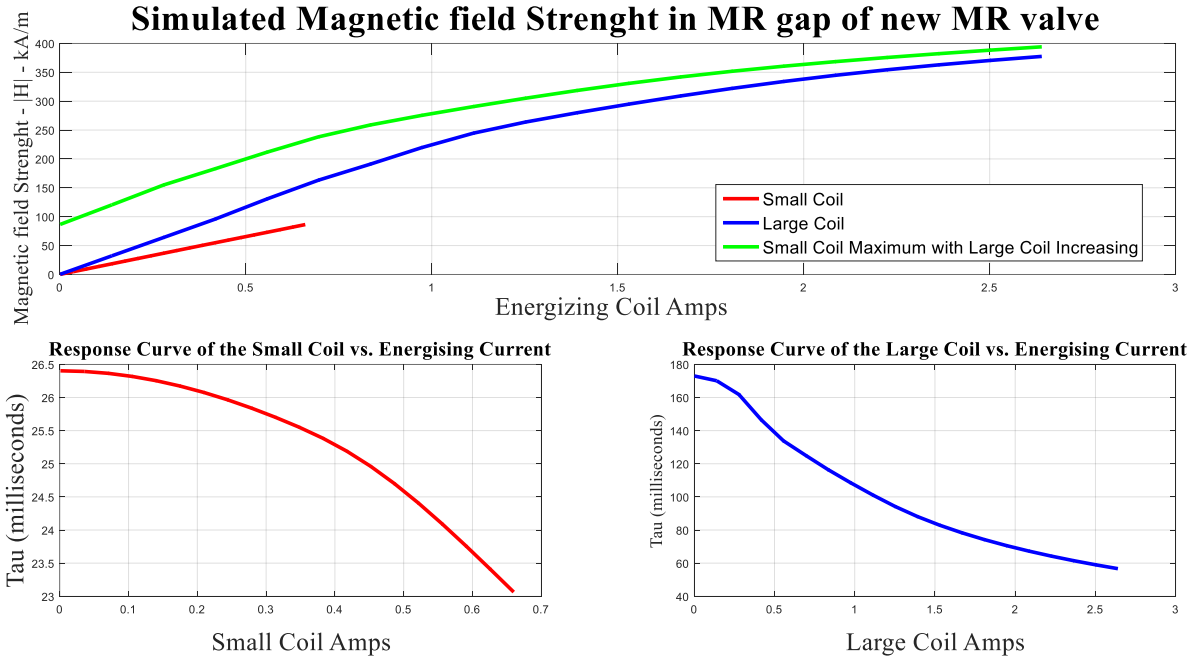

Figure 4. 7: Magnetic field strength and response characteristics of the new MR valve.

Figure 4.7 shows the magnetic field strengths one could theoretically generate using the combination of the two coils. Particularly the green magnetic field strength line above indicates the maximum achievable magnetic conditions with the small coil running at fits maximum current while the large coil is increased. Additionally, the figure also indicates that the theoretical time response characteristic $\left[\frac{L}{R}\right]$ value of the coils where the small coil will reach this point in less than 26ms while the large coil shows a higher sensitivity to applied current but that it could potentially reach the same value in less than 60ms. It is expected that the applied current could have such an influential effect on the response time of the large coil because it is bigger requiring more charge to energise its magnetic field. These results proved that one could now control the magnetic field conditions within the MR valve using characteristics which satisfy both the flow blocking and response time requirements through the double coil approach, providing control responses within 30 ms and blocking in under 100 ms. However, the effect of fluid dynamic during flow through the MR valve and its resultant effect on the spring characteristic responses is still unknown at this point and must be experimentally investigated.

4.3. Reduced Saturation during MR Valve Operation

The newly designed MR valve is expected to display a significant improvement in response time characteristics, as discussed in section 4.2, not only due to the reduced coil size, which now requires less energy to energise, but also because the magnetic conditions within the MR valve materials are not as intensely saturated. A FEMM simulation was conducted on the original valve to determine the level of saturation of the material used in the valve. The results are depicted on the B-H curve of the material as shown in Figure 4.8. This figure indicates that the material is close to saturation with the inner core being completely saturated which will have a drastic effect on the response time of the system. In comparison, the new design with its much larger inner core was simulated, while operating at maximum current on both of its coils, and the results also indicated on Figure 4.8 where it is clear that the level of saturation of the inner coil has been drastically reduced.

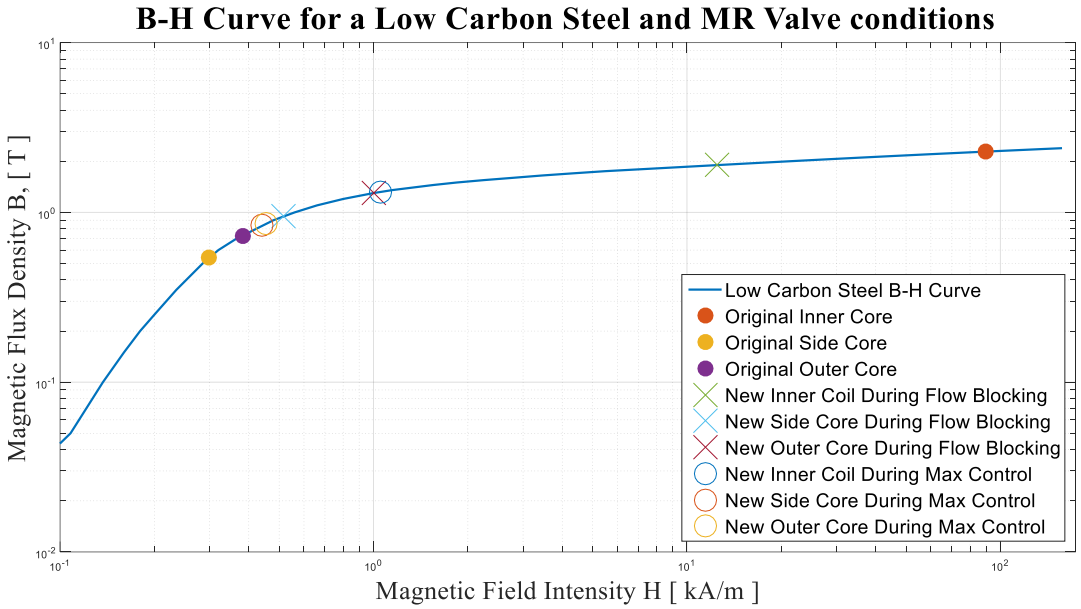

Figure 4. 8: B-H curve and simulated MR valve conditions.

Since the new valve's coils now have to spend less time building up the magnetic conditions against a very slow saturated gradient curve, the new MR valve should now be able to generate a magnetic field much faster than Grobler's prototype valve whose blocking ability relied on very saturated conditions. Notably, only the inner core is highly susceptible to saturation in both designs, thus making it a critical component to consider during the design process.

4.4. MR Valve Material Selection

As an extension to the design work conducted, an investigation was launched which attempted to quantify the possible magnetic and response time gain if the components of the MR valve are manufactured from Armco Pure Iron which has considerably better magnetic properties as illustrated by the obtainable magnetic field strength in Figure 4.9.

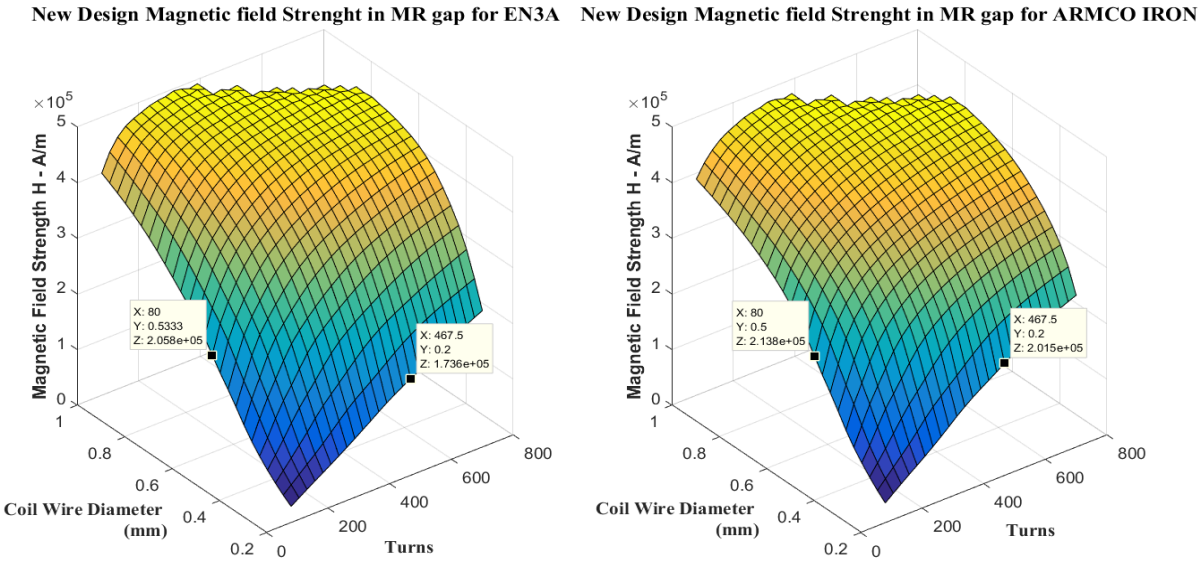

Figure 4. 9: Magnetic Field Strength generated in MR valve with various inner core materials

Through this investigation it was observed that the ARMCO Pure Iron does improve the magnetic field strength inside the MR valve, although not by a large amount as is indicated by the respective points indicated on the figure. The magnetic field strength generated by the better magnetic material was about 10-15% higher and as a result one can also improve the response time of the valve because it calls for the use of an even smaller coil. However, after obtaining a quote from the supplier for replacing the inner core with this material it was decided that the slight magnetic benefit was not sufficient to justify the order of magnitude increase in cost. Additionally, considering that the MR fluid shear stress characteristics are already mostly saturated by the magnetic strength generated using normal soft EN3A steel, the benefit of using ARMCO Pure Iron was anticipated to only marginally improve response time which does not justify the material cost.

4.5. Manufacturing the MR valve

Following the careful CNC manufacturing of the required components the prototype was assembled and a coil turner used to control the application of the coils equally and accurately. Figure 4.10 shows the coil application process which followed after component manufacturing.

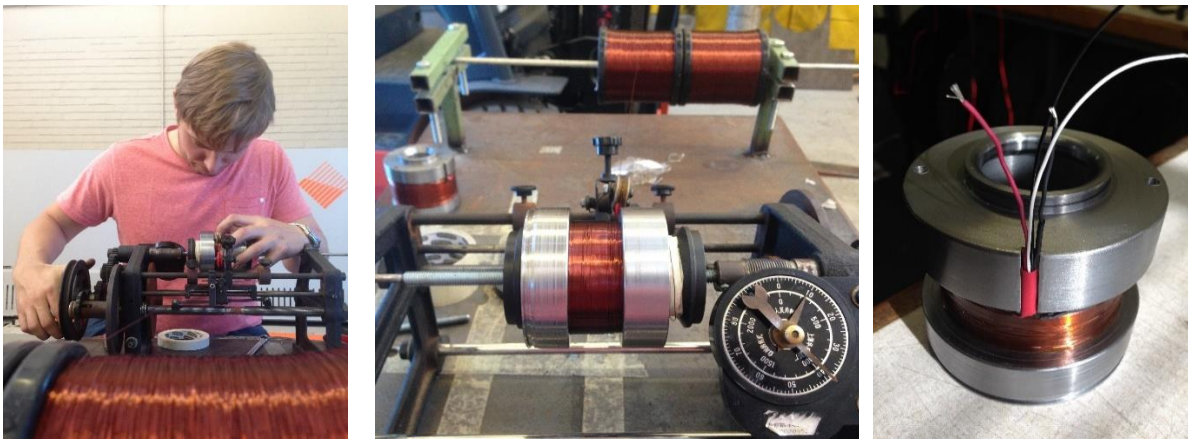

Figure 4. 10: Application of the coils to the MR valve

4.6. New Prototype Experimental Characterisation

After fitting the manufactured MR valve with the design coils and inserting the valve into the MR4S$_4$ valve block, its actual response time characteristics were investigated experimentally so as to compare it to what was anticipated during the design simulations. This testing process is illustrated in Figure 4.11.

Figure 4. 11: Experimental characterisation of the assembled MR valve

A magnetic field measurement was attempted through the use of a Hall-Effect sensor. This could not successfully be conducted because the sensor could not fit inside the MR gap and the magnetic field leakage from the valve was too small thus making the magnetic measurement impossible from the outside the gap. Even so, the two coil current responses were measured for both a 6V and 12V battery energising as shown in Figure 4.12.

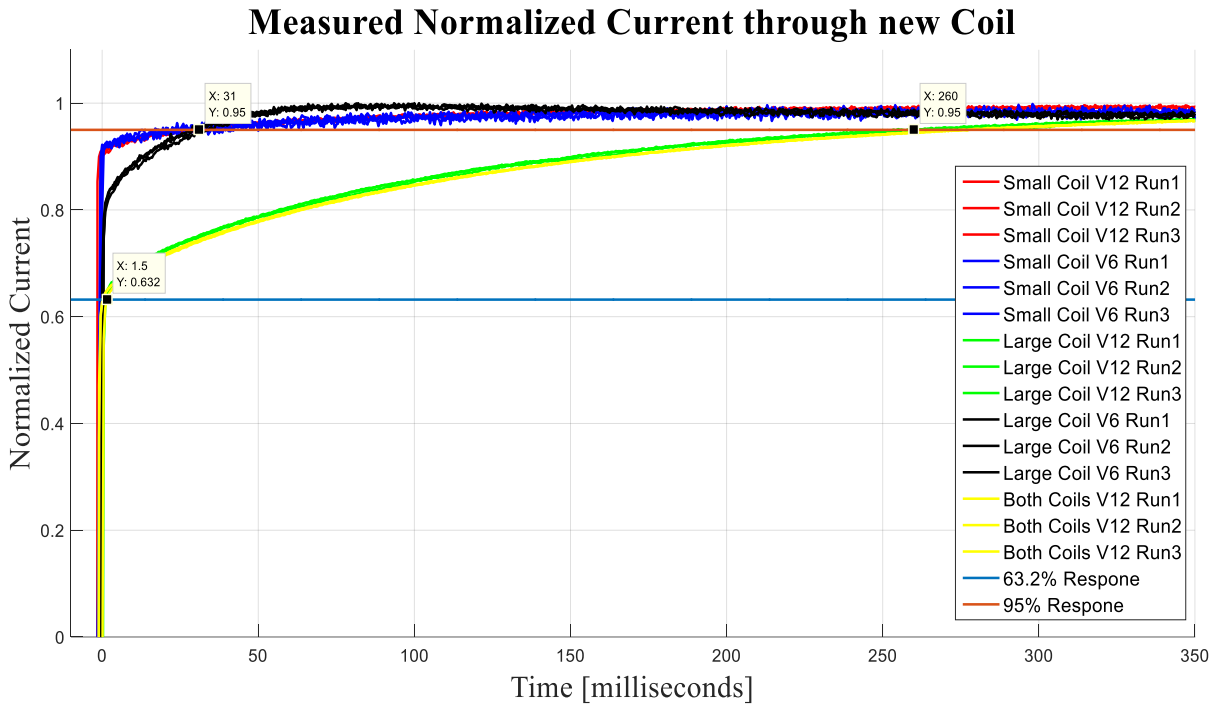

Figure 4. 12: Coil current responses measured

It is easy to observe that the current in both the large and small coil now ramp rapidly, having an almost negligible delay on the 63% response line. From there the large coil, when energized by 6V reached its 95% value in 31 milliseconds while the same coil, when energized by 12V, reached the 95% point in a much larger 260 milliseconds. The significant time difference between the large coil's 95% responses for 6V and 12V suggests that the large coil still saturates the MR valve to a large degree when energised by the full 12V. Consulting the FEMM simulation it was observed that if the large coil was energized by 6V a magnetic field of 250 kH/m is generated in the MR gap which theoretically is already sufficient

to achieve flow blocking. One could thus anticipate the MR valve to settles to a near flow blocking condition in under 40ms.

Finally, also offering great promise, the small coil settles in cases of both the 6V and 12V to 95% of its final current value in under 31 milliseconds, which is exactly what the small coil was designed to achieve.

Conclusion

Following the successful design and evaluation in this chapter of a double coil MR valve which exhibits the desired coil response characteristics while still providing sufficient theoretical magnetic strength to achieve flow blocking, it became important to validate the new prototype valve during dynamic flow conditions. It was experimentally proven that the new MR valve is significantly faster than its predecessor in its rapid current responses observed in the small coil. At this point it is still unknown what other effects will play a role on the overall response of the $MR4S_4$ valves, effects which could include the MR fluid bulk modulus or compressibility, the MR fluid shear stress build-up delay and system deflection. These effects cannot be estimated in any way meaning that they must be experimentally observed. To achieve this the next chapter will discuss the experimental setup followed and highlight some of the electronics developed to test the new MR valve.

CHAPTER 5

EXPERIMENTAL CHARACTERISATION OF MR VALVE UNDER DYNAMIC CONDITIONS

Introduction

After the theoretical optimisation and design of the MR valve it became important to validate its pressure drop characteristics during actual fluid flow conditions. To achieve this a test setup was constructed which can actuate the $MR4S_4$ system and recreate the required dynamic inputs. Of particular importance during this chapter was the decision to characterise the MR valve under known flow conditions by forcing a single flow path configuration onto the $MR4S_4$. This chapter will discuss the electronic circuitry and control signals developed to dynamically test and characterise the $MR4S_4$'s MR valve for both damping pressure drop vs. flow rate characteristics as well as time response properties. This chapter will also focus on the analysis of the raw data which was extracted from the experimental work. It will also discuss the observed response characteristics of the MR valves under dynamic operation in both a time and spatial domain. Finally, some of the difficulties and uncertainties with regard to the experimental results will be mentioned.

5.1. Valve Block Setup

With the main focus revolving around the characterisation of the MR valve during dynamic fluid flow operation, it was of great importance that the fluid flowrate through the valve is accurately known. This condition is not directly measurable during the operation of the $MR4S_4$ in its normal setup with two flow paths, since it requires the estimation of the flow conditions based on measured pressure conditions. Thus, in order to remove any uncertainties during the characterisation of the MR valve it was decided that a single flow path setup would be tested to obtain the flow condition through the MR valve with a direct relationship to the input. To achieve this the second flow path towards the smaller accumulator was blocked by a plug as depicted in Figure 5.1.

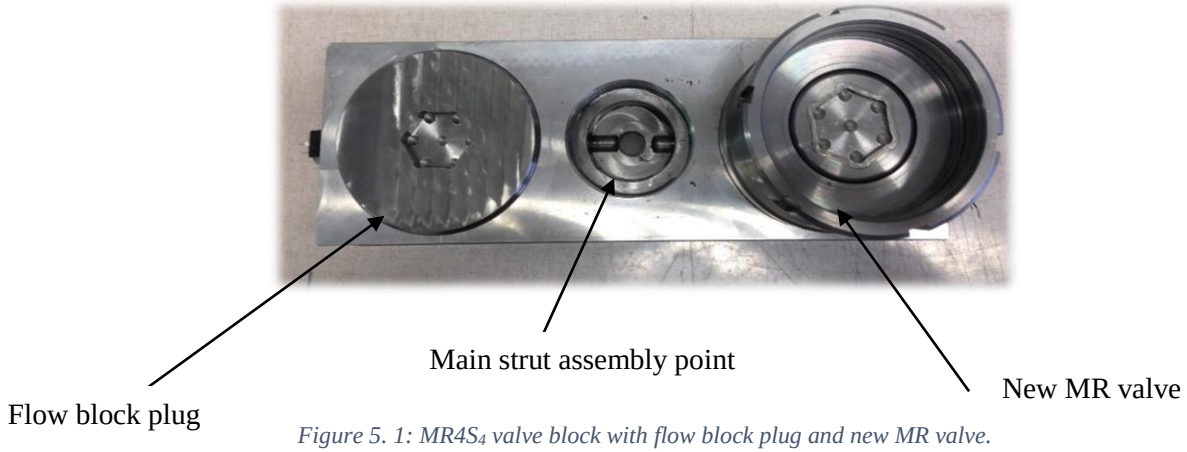

Figure 5. 1: $MR4S_4$ valve block with flow block plug and new MR valve.

5.2. Test Rig Setup

The MR4S$_4$ was assembled and fitted to test bench constructed in the Test Laboratories at the University of Pretoria. It was placed on top of a 25kN hydraulic actuator with a load-cell. Additionally, three pressure transducers were installed - two of which measured the main strut pressure before the MR valve while the third measured the large accumulator internal pressure. Furthermore, the displacement of the actuator was recorded in addition to the relative displacement within the MR4S$_4$ with a linear potentiometer displacement transducer. A displacement laser was also introduced to quantify the deflection of the test rig.

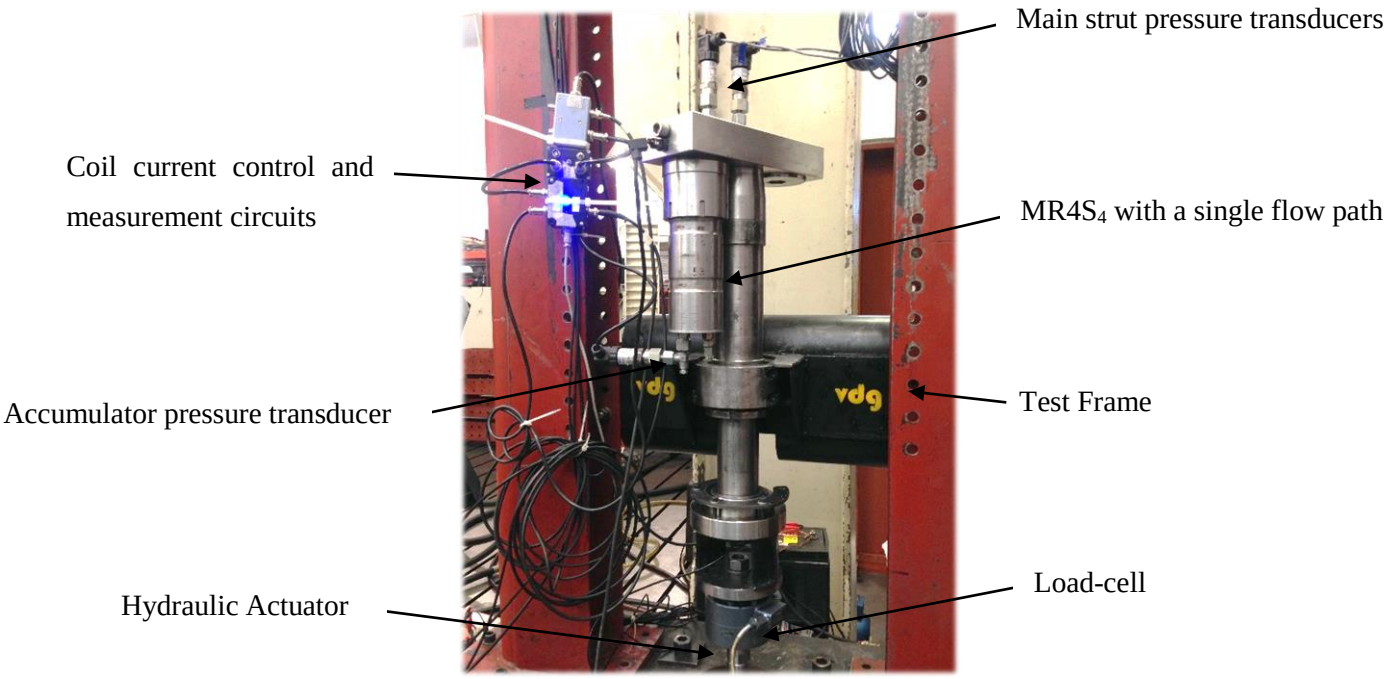

Figure 5. 2: MR4S$_4$ fixed onto test bench

Following a lengthy bleeding procedure to minimise the amount of air trapped within the MR fluid of the system, the accumulator was inflated to 10 bar. The suspension strut was slowly compressed until the load-cell registered a force at which point the air in the accumulator is being compressed, i.e. the accumulator volume starts to decrease. Once this point was observed, the suspension strut was compressed a further 15mm to form a static load on the pneumatic spring. This translated to an initial load on the suspension of around 200kg.

5.3. MR Valve Coil Control and Coil Current Measurement Boxes

Although the end goal would be to control the MR valve coils continuously, for the purpose of characterising the response time and pressure drop characteristics of the MR valve, a simple ON or OFF control of the coil current was incorporated. The coil switching was achieved through the use of a MOSFET which was controlled by a second analogue channel described in Section 5.4.

The applied coil current was measured by amplifying the voltage drop across a 0.01 Ohm resistor placed in series with the coil through the use of an instrumentational amplifier and appropriately scaled. This current measuring resistor was selected to be as small as possible so as to not affect the coil current

dynamics negatively. One could also easily switch, using a manual selector switch, between energising the small, large coil or both coils within the MR valve with the 12V battery source. Additionally, fly back diodes were installed in order to protect the amplification circuit in the current measurement box from reverse voltage spikes during coil discharge. All of the discussed electronics, including some LED's which provided visual feedback about the energisation condition of the coils, were connected up and housed in measurement boxes as is demonstrated in Figure 5.2.

5.4. Experimental Displacement and Coil Control Signals

Since the characteristics of the MR valve (or damper) were of greatest interest, it was imperative to capture the characteristics of the valve as it operates during constant flowrate conditions. For this reason, the actuator displacements were triangular in order to generate a constant flowrate through the valve which would make the flowrate dependent properties easier to extract.

The coil currents in the MR valve was discretely controlled as either fully ON or OFF. The MR valve coils were energised by a 12V battery during the ON state.

The actuator input displacement and coil current control signals were generated as an analogue output by the National Instruments Signal Generating PC. A Cubus controller was used to control the actuator based on the displacement signal while a MOSFET was used switch the respective coil states ON or OFF based on the analogue control signal from the PC.

During the experimental work, three main types of tests were conducted:

5.4.1. ON-OFF Response Tests

Because one of the main performance metrics is the response characteristics of the MR valve during dynamic flow conditions, a set of ON-OFF tests were developed which would activate the MR valve coil when there is a steady state flow condition within the valve. This activation would thus result in a change in the pressure drop condition across the MR valve allowing one to extract the response time of the dynamic system. The control input signals are sequenced such that an initial period is given for the actuator controller to achieve a constant velocity after which the coil is switched on. After 55mm displacement the coil is switched off before there is a change in direction. Figure 5.4 illustrates the control signals for a 10mm/s actuation test.

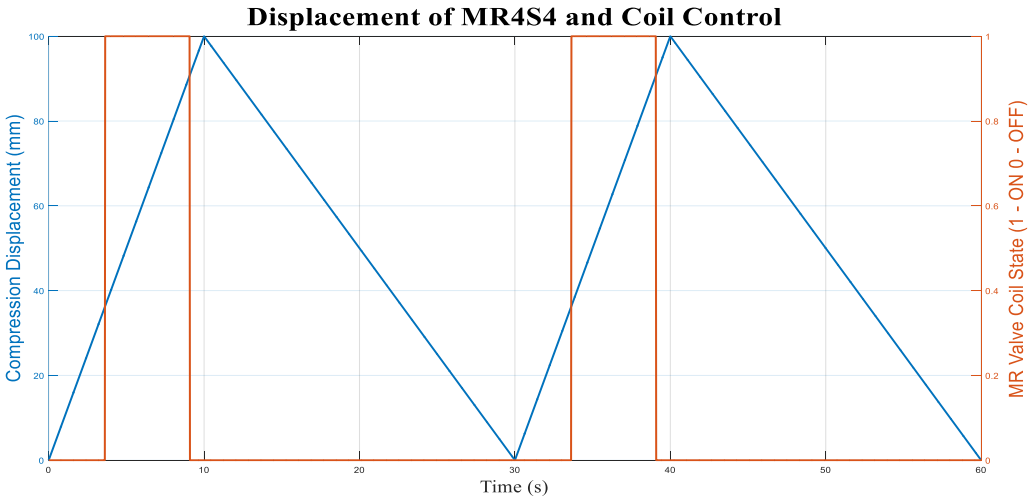

Figure 5. 3: ON-OFF Test at 10mm/s compression

It was important to ensure that, during extension, the MR4S$_4$ strut pressure does not create a vacuum and as a result the extension velocity was set to never exceeded 5mm/s while the coil was kept inactive during this period. Tested strut compression velocities include 1, 5, 10, 20, 50, 100, 150, 200, 250, 300, 400 and 500 mm/s. The response time of the small and large coil was determined independently, a test was also conducted using both coils in combination.

5.4.2. ON Characteristic Tests

To extract the expected 'steady' state damping pressure drop versus flowrate characteristics of the MR valve, a set of tests were conducted whereby the coil was active for the entire duration of the compression cycle. The tested strut compression velocities were the same as the ON-OFF tests while the extension velocity was again controlled.

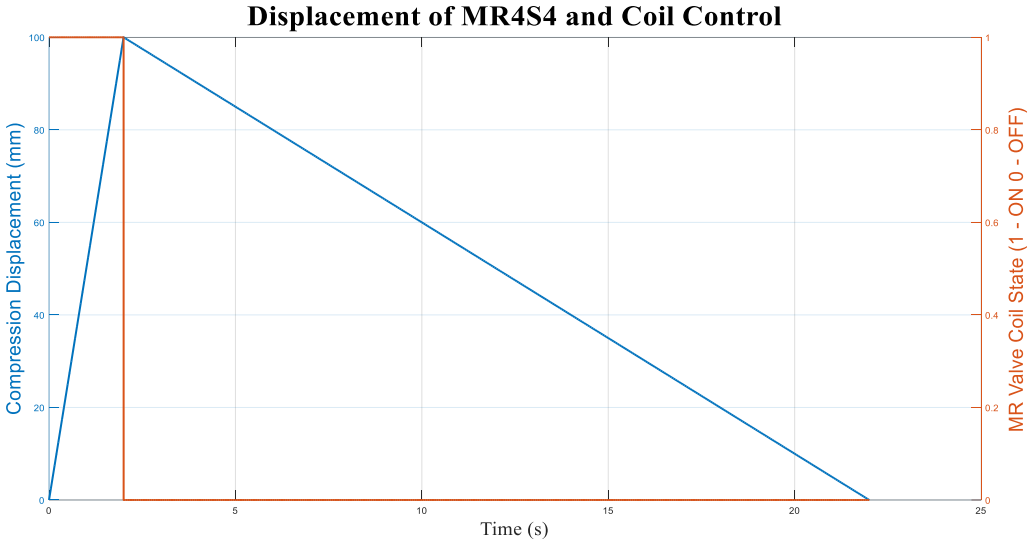

Figure 5. 4: ON Test at 50 mm/s compression

5.4.3. Step Input Tests

Finally, to assess the hydraulic actuator's response characteristics a series of step input tests were conducted across a set of 1, 2, 5, 30 and 50mm step sizes. This was done in order to assess whether the

response characteristics observed during the ON-OFF tests were not affected by the actuator response characteristics as the actuator adapts to the change in force conditions.

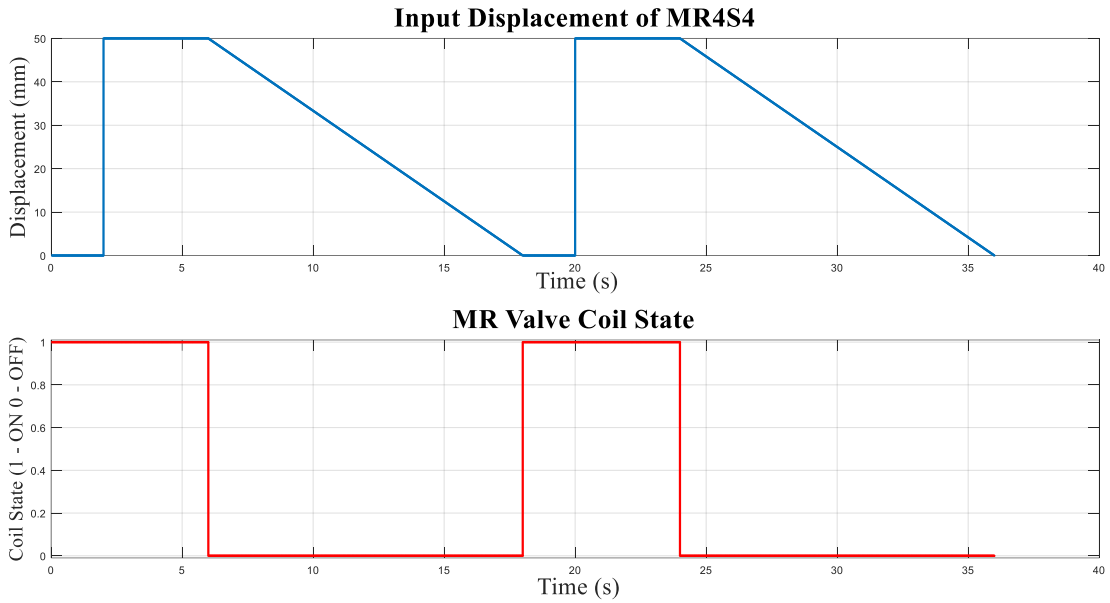

Figure 5. 5: 50 mm step input test

During these step tests the coil would be switched on and given 2 seconds to settle after which the step occurs. Once the step has occurred, the system is given more time to again settle after which it is slowly retracted while the coil is deactivated in order to avoid the creation of a vacuum in the system.

5.5. Data Acquisition and Signal Conditioning

During the experimental work a total of 10 analogue channels were recorded at a sampling frequency of 1 kHz using an in-house developed Helios-PC104 Data Acquisitioning System which is able to record an analogue range of -10V to 10V. The recorded channels where:

1) Actuator Displacement Command Signal
2) Actuator Displacement Signal
3) Actuator Load-Cell Signal
4) Coil State Signal
5) Coil Current Signal
6) Main Strut Pressure Signal
7) MR Valve Pressure Signal
8) Accumulator Pressure Signal
9) $MR4S_4$ Relative Displacement (POT) Signal
10) Deflection Displacement Laser Signal

Although most of the recorded data was relatively noise free, some of the channels did require some filtering. In these cases a zero-phase shift low pass filter was implemented where applicable in post-processing. Filtering was not applied to the response time tests to avoid the time shift effects of filtering on the extracted characteristics. Finally, the measurement values were calibrated appropriately such that the operational conditions of the $MR4S_4$ could be extracted.

5.6. Damping Pressure Drop vs. Flowrate Characteristics of the Designed MR Valve

The MR valve off-state damping versus flowrate characteristics were obtained by calculating the pressure drop across the MR valve from measured pressure conditions. This damping pressure drop across the valve, plotted in Figure 5.6, is predictably a function of flowrate.

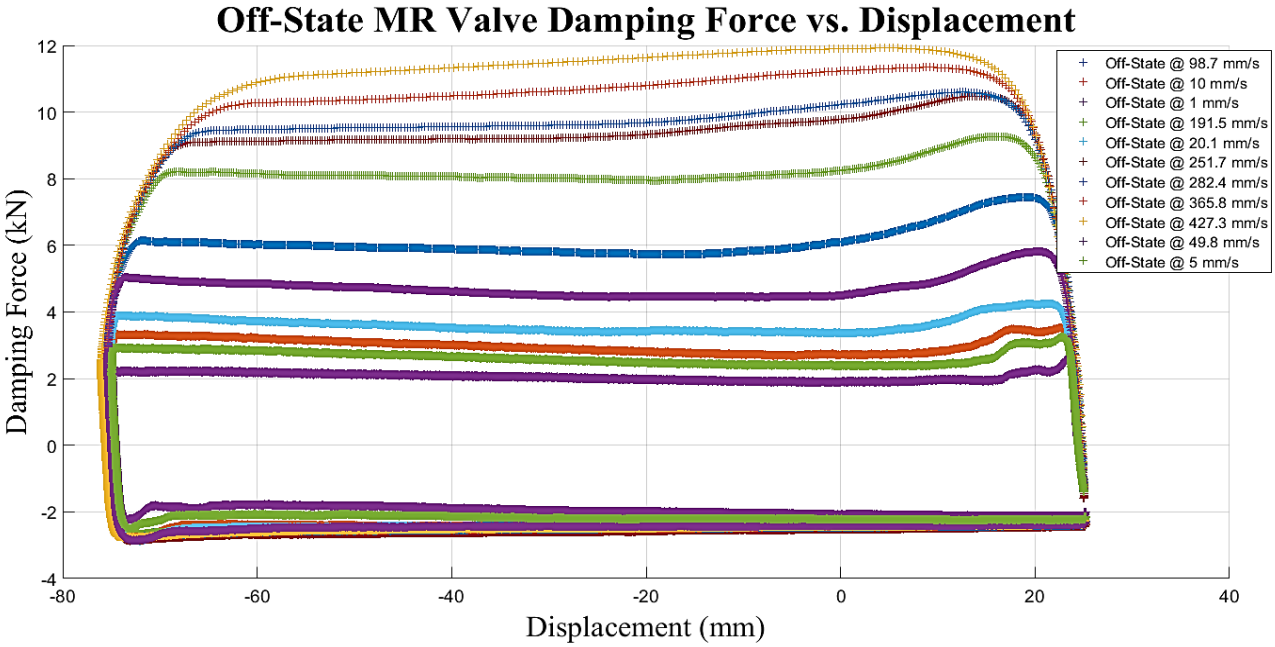

Figure 5. 6: Off-State Damping Force vs. Displacement Characteristic of the MR valve

The above measured results prove that the MR valve produces a constant force during the constant flow condition as is expected of an orifice based damper. As the velocity of the strut increases and thus the flowrate through the valve also increases which also leads to an increases in the damping force.

The damping force versus displacement measurement for the MR valve during the ON-OFF tests on the small coil are plotted in Figure 5.7 to demonstrate how the damping force changes when the small

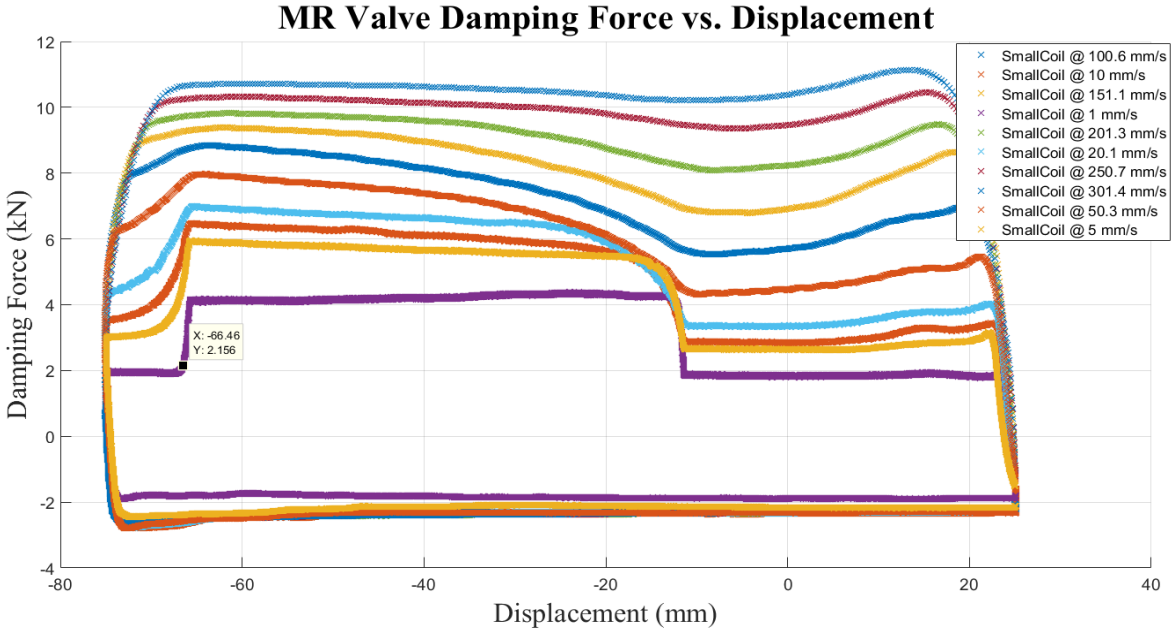

Figure 5. 7: Small Coil Controlled Damping Force vs. Displacement Characteristic of the MR valve

coil is activated. On this figure one can clearly see that when the coil is activated there is a rapid increase in damping force which again drops away once the coil is switched off at displacements of -11mm and -66mm respectively. One can also see that the magnetic field induced damping effect appears to reduce at higher flowrates, which is an expected characteristic since the MR fluid is prevented from building up the flow blocking structures or chains due to the velocity of the flow.

Extracting the damping force as an average value between -40mm and -60mm displacement, the overall observed damping force versus the respective fluid flowrate was captured as highlighted by Figure 5.8. The same figure also shows how the MR valve's characteristics compare to the minimum and maximum damping curves of the original $4S_4$ system (Els 2006) who developed these characteristics based on ride comfort and handling requirements.

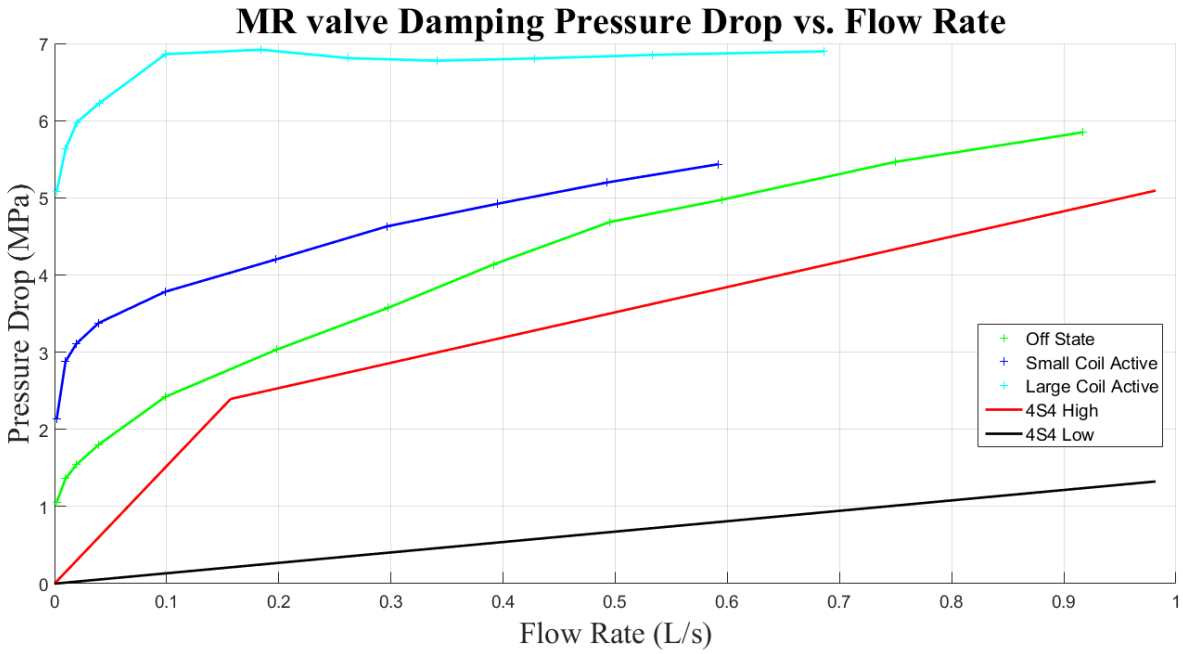

Figure 5. 8: MR valve damping vs. flow rate characteristics

The figure shows that the damping characteristics of the new MR valve design is significantly higher than desired, even for the off state characteristics. Even without the application of any current to the MR valve it was found that the damping pressure drop of the valve was higher than the characteristic of the $4S_4$ on its high damping setting as is illustrated by the figure. This suggested that the decrease in annular flow gap, even with a constant flow area, drastically lifted the pressure drop characteristics of the MR valve. This increase in the pressure drop characteristic could be attributed to the high viscosity of the MR fluid which now creates a high frictional resistance during flow through the thinned annular orifice. It could also be argued that the flow path through the MR Valve, is no longer a simple straight annular channel but incorporates a sharp bend around the inner core, which could also be generating additional pressure drop effects.

The obtained characteristics in Figure 5.8 are unacceptably high and as a result it was decided that the inner coil diameter should be reduced which would both enlarge the flow area and the flow gap width.

5.7. Damping Pressure Drop vs. Flowrate Characteristics of the Modified MR valve

The inner coil was turned down by 0.7 mm on the radius, making the annular gap 1.2 mm wide. This modification reduced the pressure drop characteristics of the valve and brought it within the desired ranges. This reduction in the pressure drop characteristic is plotted in Figure 5.9.

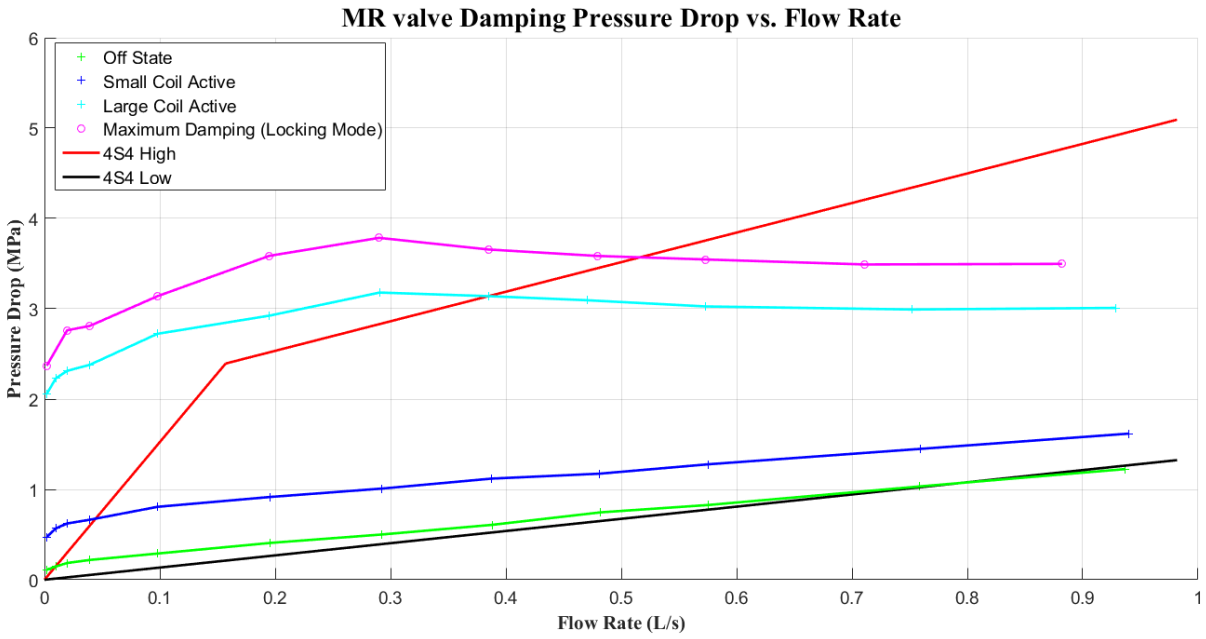

Figure 5. 9: MR valve damping vs. flow rate characteristics for the increased annular gap valve

With this modified MR valve one can now obtain a very similar off state characteristic as was initially specified by Els for the $4S_4$ system. The newly designed MR valve provides very promising characteristics in comparison with the previous prototype, in particular it has relieved the 'low-flow high-damping' problem, largely reducing the damping forces at low flowrates illustrated by the Off-state result in Figure 5.9. This can be attributed to the significant increase in annular flow area due to the increased annular gap increase which reduced the impact of the viscosity effects of the fluid on the damping force. Grobler also reported that his valve's characteristics suffered from a similar overstated low velocity damping force, as the valve tested in Section 6.1. Grobler's valve had an identical flow area to the valve tested in the previous section thus also yielding similar results which were now improved for better ride comfort with the new valve.

This improvement in ride comfort by reducing the off state low damping characteristic was not at the expense of the high damping characteristic. Looking at the maximum damping (locking) curve, obtained by energising both the small and large coils simultaneously, one can reach most of the desired $4S_4$ high damping characteristics. Thus, with appropriate coil current control in both the MR valve coils one can now obtain any damping characteristic within the 'locking' and 'off' state bounds illustrated above. The above obtained range of damping characteristics through coil current control promises to open vast opportunities for semi-active suspension control to improve the ride comfort and handling of a vehicle.

Interestingly, a slight decrease in damping characteristics of the MR valve can be observed when the flowrate increases to above 0.3 L/s which can be explained by the MR fluid's inability to form sufficient

flow resisting structures or chains due to the high flow pressures. Thus, one can observe that MR based dampers have damping characteristics which saturate with both current and flow rate when the MR effect is unable to build up any additional resistance to flow.

5.8. MR Valve Response Characteristics

Once it had been proven that the newly designed MR valve was capable of exhibiting suitable continuous damping characteristics, it still had to prove its ability to achieve this within an acceptable response time. To investigate this the ON-OFF tests were processed and the response characteristics of the coil current as well as the damping pressure drop across the MR valve analysed.

5.8.1. Coil Current Response

During these tests it was observed that the settling time for the MR coils remained constant across the various tests. The respective 63.2% and 95% response times have been illustrated in Figure 5.10. Note that the period for which the large coil is 'active' during the activation signal actually becomes shorter than its 95% response time at velocities larger than 100 mm/s, and thus these data points are not recorded because the large coil never reached its steady state current during the test.

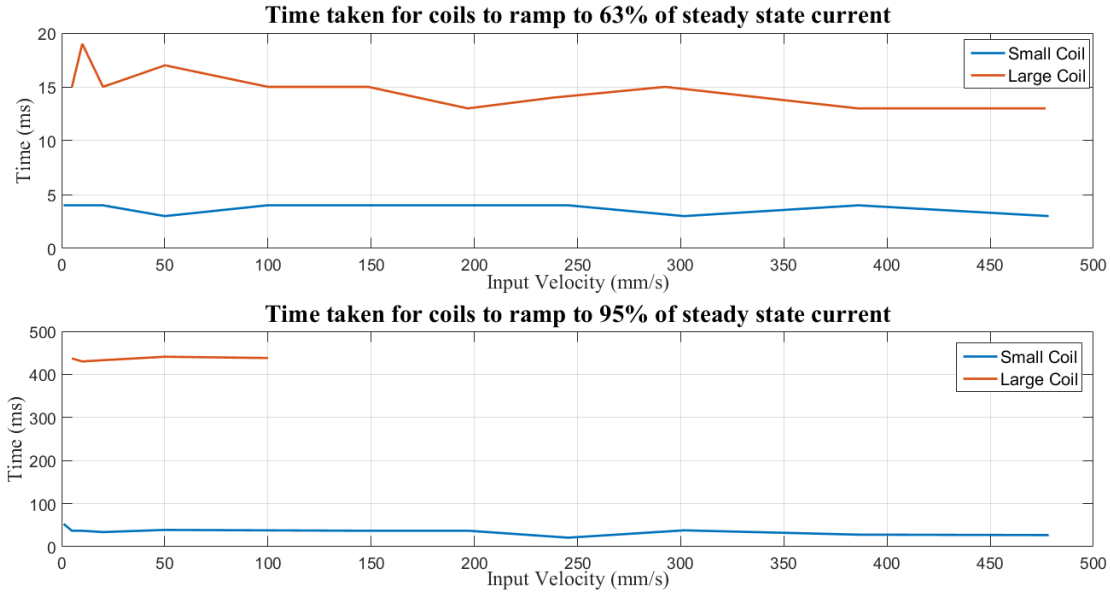

Figure 5. 10: Coil Response Characteristics

It is clear that the small coil achieves its 63.2% mark in 4 milliseconds while the large coil achieves the same at approximately 17 milliseconds. Both coils thus satisfy the control requirement of being less than 30 milliseconds as was designed for in Chapter 4. Comparatively, the small and large coil settles much faster than the simulation's predicted time response $\left[\frac{L}{R}\right]$ value as was obtained in Chapter 4. The design simulations suggested that the small coil will take 23ms to reach the 63% value while the large coil will reach this value in 60ms which is significantly larger than the actual measured values. The reason for the difference is possibly explained by a sight error in the inductance and resistance estimated by the FEMM package. Looking at the experimental measurements it can be seen that the small coil settles to 95% of its final value in 28-35ms which is a very promising observation for semi-active control

as most of the small coil magnetic effect can thus be achieved within the control response time bracket. On the contrary, one notes that the large coil requires a much larger time to settle to 95% of its final value, requiring around 420 milliseconds. The prolonged settling time for the large coil still suggests that a fair amount of magnetic saturation is present within the valve causing the very lengthy build-up difference between the 63% and the 95% response time for the large coil.

5.8.2. Damping Pressure Drop Response

Of greater significance than the coil current response time is the overall system damping force response characteristics of the MR4S$_4$ system. These characteristics were extracted from the ON-OFF tests by calculating the time required for the damping force to build to 63% and 95% of its final steady state value, as is demonstrated by Figure 5.11. In this analysis the coil was switched on during constant flowrate through the valve, illustrated by the period of constant damping pressure drop from 10-38 seconds in the figure, after which the build-up of damping pressure drop was monitored. The figure below illustrates the 63% and 95% lines of the final steady state damping pressure value from which their respective response times could be calculated.

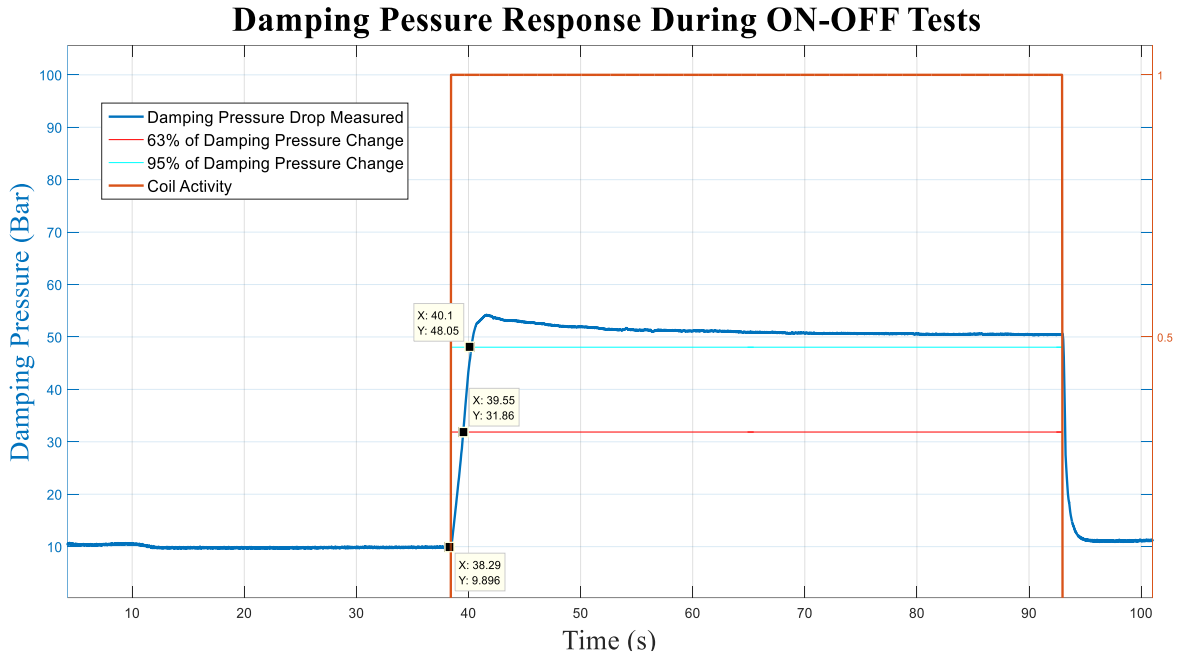

Figure 5. 11: Damping Pressure Response Extraction

It was noted that the response characteristics of the MR valves are affected by the input velocity of the strut. This is somewhat expected if bulk modulus effects are present since these effects cause slower responses at low velocities. The obtained time response results across several velocity tests for the 63% and 95% damping force changes are noted in Figure 5.12.

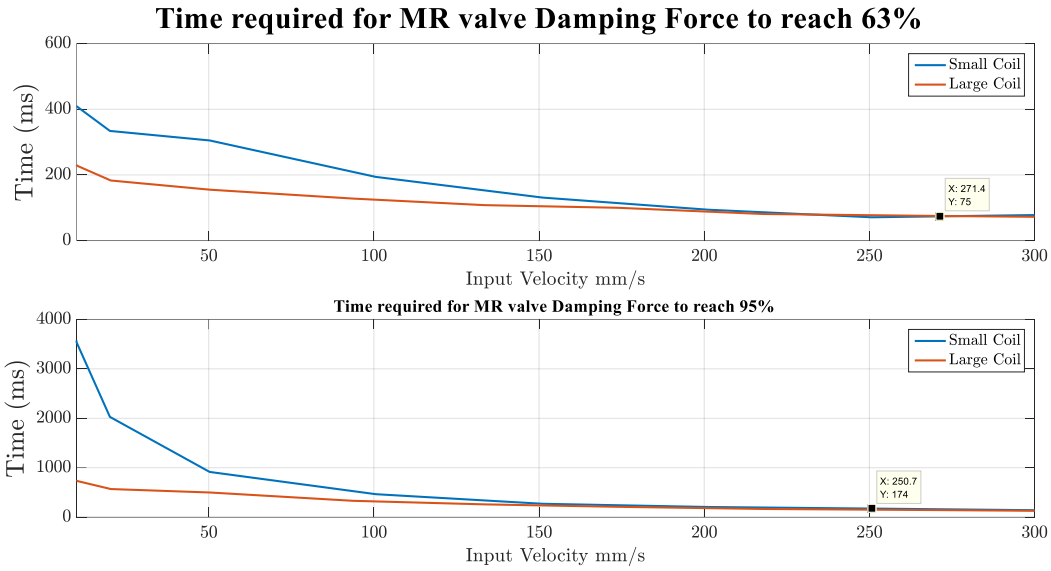

Figure 5. 12: Damping force response time after coil activation

To reach 63% of the change in damping force at actuation velocities over 200mm/s one would require around 75 to 100 milliseconds, while a full 95% characteristic change is achieved in 175 milliseconds for velocities higher than 250 mm/s. Similar characteristics were observed by Grobler who concluded that a 63.2% damping force response was observed in 105 milliseconds while a 95% response was observed in 184 milliseconds for his MR valve.

As is illustrated by Figure 5.12 the response time of the system is influenced significantly by the velocity of the actuator. At lower velocities the response characteristics of the valve is significantly slower. The increase in response time required at low velocities suggests that the MR valve requires a certain amount of displacement or compression in order to build up the necessary damping force across the valve. This effect could possibly be a phenomenon explained by a combination of test rig deflection and bulk modulus of the MR fluid. Additionally, this effect could be due to leakage through the MR valve at low flowrates. In order to remove the velocity dependence of the responses, the damping responses were investigated in a spatial domain and was extracted in Section 5.8.3.

5.8.3. Damping Pressure Drop Displacement Response

To observe whether a more consistent response characteristic of the system, which is less dependent on input velocity, could be extracted, the relative strut displacement required to build the damping force to 63% and 95% was extracted. This would give an indication of the spatial response of the system required to generate the damping force across the valve.

Figure 5.13 highlights a more intuitive result suggesting that the MR valve requires the suspension strut to be displaced around 20mm to achieve a 63.2% change in damping force while a 95% characteristic change would require under 40mm for both the large and small coils. Note that the indicated strut displacement on the figure is the relative displacement of the $MR4S_4$ strut so as to remove the test rig deflection effects.

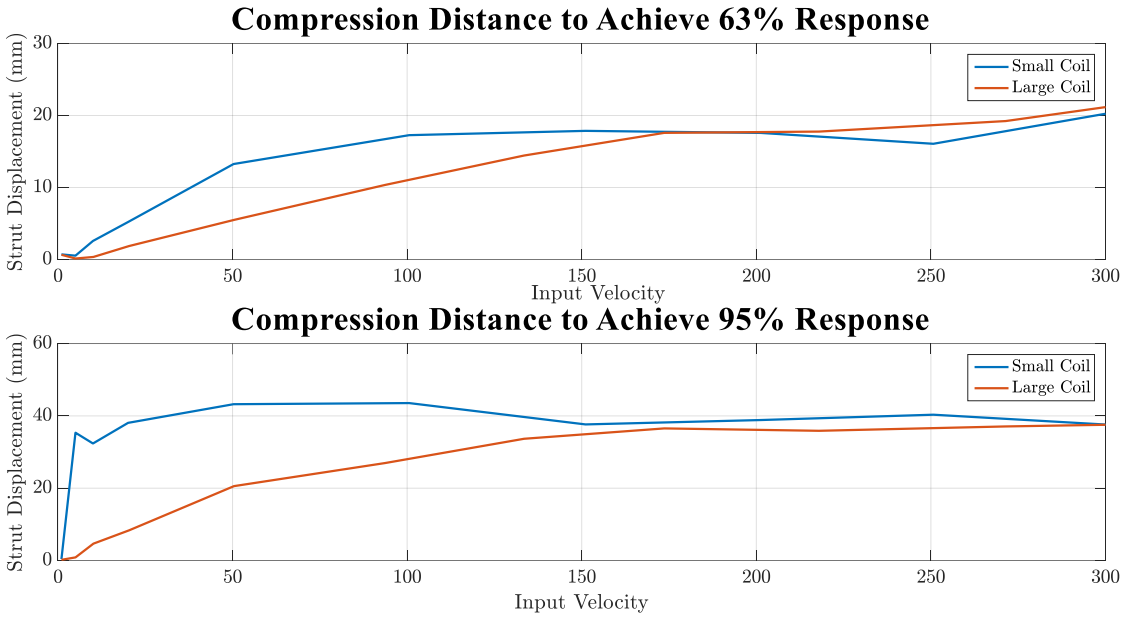

Figure 5. 13: Damping force spatial response of the MR valve

From Figure 5.13 an interesting observation can be made. Although the current response characteristic of the small coil and its magnetic field settles much faster than the large coil, due to the fluid and/or system effects one still observes that some displacement is required for the damping forces to build. Initially, this was attributed to bulk modulus effects of the fluid, explained by trapped air within the system. However, on closer inspection it was noted that the characteristic changes at very slow compression rates (1mm/s and 5 mm/s) reached 63% in under a millimetre's displacement for the both large and small coils. This suggested that there was in fact no trapped air within the system as the damping force would not build as rapidly requiring a larger displacement even at low velocities if that were case.

Thus, one is left to conclude that there are in fact fluid dynamic effects at play slowing down the response characteristics of the MR valve and that the response of the system cannot be attributed only to the magnetic response of the valves. It is expected that the MR fluid is less successful in building up resistive chains when fluid is forced through the MR valve. The MR valve's ability to build rapid MR fluid magnetic chains will decrease as the flowrate increases because the faster the fluid flow, the more they break down the formation of chains. Thus, the faster the fluid flowrate through the MR valves the longer it takes the MR valve to build its resistance making it less responsive simply due to its inherent dependence on flowrate or strut velocity. This could explain why there is an increase in the spatial responsiveness of the MR valve as the velocity increases while very slow flowrates have an almost instantaneous response. This response delay is therefore an inherent characteristic of the MR technology and not necessarily only a function of the magnetic responsiveness of the valve. One is thus left to conclude that the MR fluid's ability to generate damping forces are also effected by the fluid's flowrate, which is a characteristic that cannot be avoided through more responsive MR valve magnetic designs.

Furthermore, the fact that the small coil requires more displacement than the large coil to build its responses, particularly for velocities between 10 and 150mm/s, was somewhat contradictory to expectation and thus a closer look at these responses is plotted in Figure 5.14.

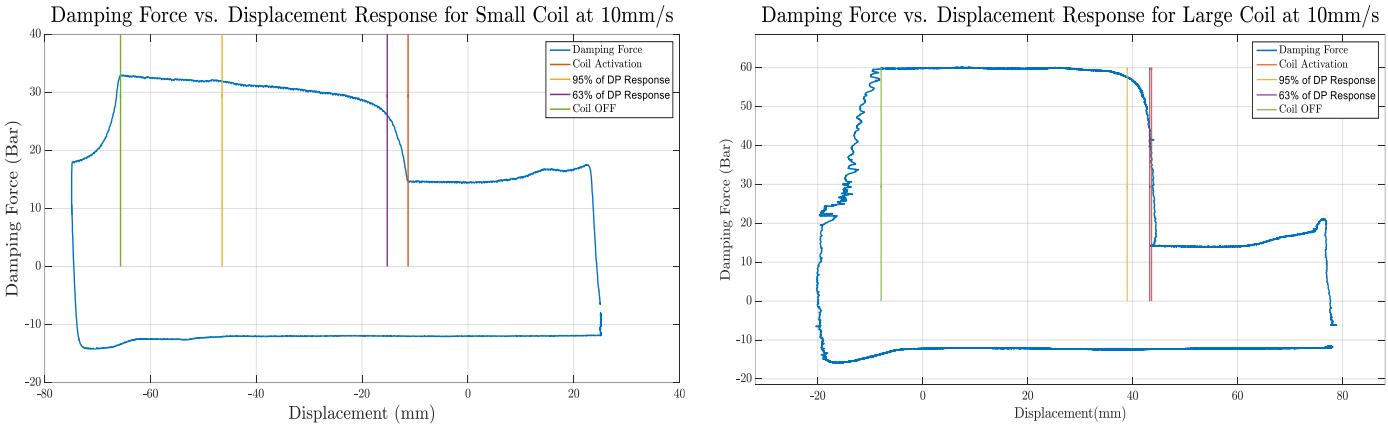

Figure 5. 14: Comparison of low velocity damping force response extraction

These figures make it quite clear that the larger coil's spatial response is in fact faster as it provides a more rapid ramp in damping force. This is probably explained by the large coil's much stronger magnetic field which is able to create a more rapid build-up of the resistive chains and thus ramping the flow resistance significantly faster than the small coil as illustrated in Figure 5.14. Even though the large coil's current response is considerably slower, its stronger magnetic field creates a much bigger 'step' in damping force making it more displacement responsive as was observed in Figure 5.13.

These figures suggest the conclusion that during small road inputs, which do not have very high input velocities, one can expect the MR valve to react within 10mm creating significant changes in damping characteristics as Figure 5.14 demonstrates, especially if the large coil is used to switch the characteristics. Alternatively, when the road is very rough with larger input velocities, one can expect that full characteristic changes to be slightly slower as the fluid struggles to build up the resistive chains and as such requiring 20-40 mm of displacement to build to a 95% change.

Even though the MR4S$_4$ will inherently display both time and displacement based delays as observed experimentally in section 5.6 and 5.7, the technology still creates a semi-active suspension system which is capable of significant and continuous output characteristic control, achievable within a maximum of 40mm of suspension travel. This ability to control its output forces may still be useful in improving the handling and stability of a vehicle during dynamic manoeuvres, even though inherent delays cannot be avoided as they are governed by the physics of the system.

5.9. Actuator Response Analysis

Priyandoko et al. comments that test bench actuators can often introduce highly non-linear adverse effects on the test results, effects which cannot simply be ignored. (G. Priyandoko 2009) Actuators through their non-linear valve dynamics and control systems can create back-pressure and delay effects between the actuator and the test object. The extent to which these effects are present in the dynamic

results obtained must be investigated. In order to quantify the actuator possible influence on the response time results obtained in Section 5.8.2 and 5.8.3, a series of step input tests were conducted to determine the response characteristics. Step input tests were conducted for 1, 5, 10, 30 and 50mm steps, while the MR valve was locked with combinations of the small and large coil, to observe the response time effects this would bring. The results from a set of step input tests while the small coil was active has been displayed in Figure 5.15. Important to note here is that the measured displacement plotted below is the value measured by the actuator's displacement transducer and is not the relative measurement obtained from the suspension struts' internal linear potentiometer, used in previous sections. Additionally, the apparent noise in the command signal for the 10mm step test is indirectly amplified by the normalisation process due to the inherent smaller amplitude range of the signal being normalised and thus the noise was not more apparent in these smaller step tests as the figure portrays.

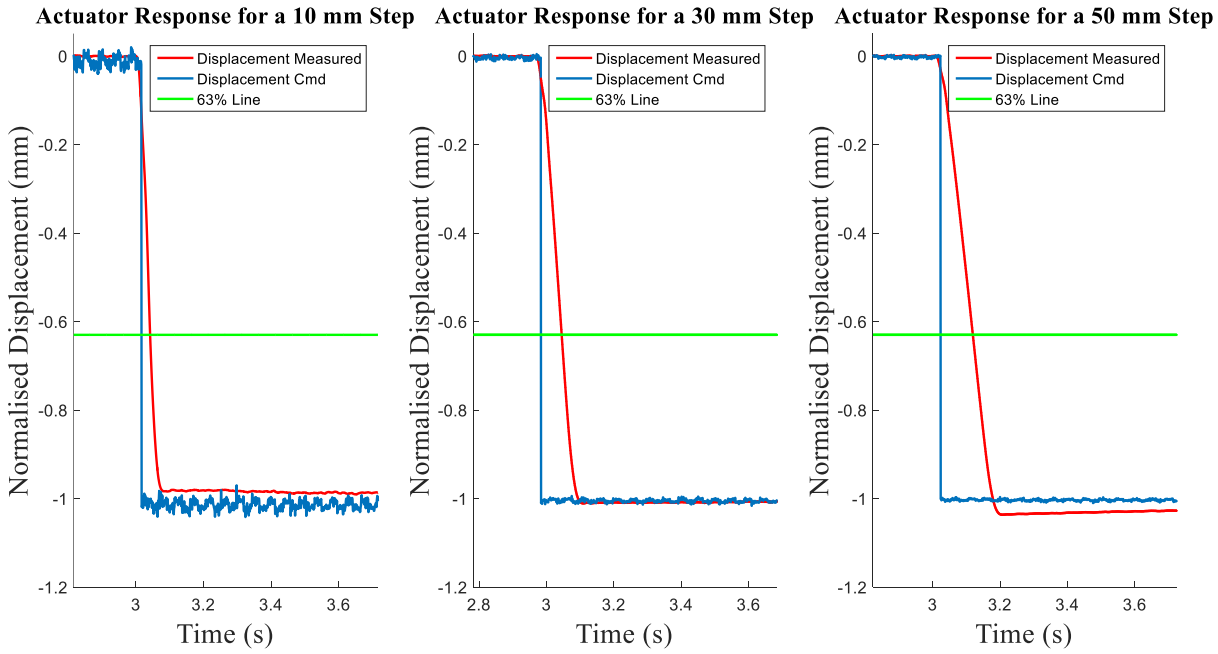

Figure 5. 15: Step Input Responses of the actuator while the small coil is active

From these figures one can see that the response delay of the actuator become significant when displacing the strut. The Figure 5.15 show that in the case of the 50mm step test, the actuator took around 180 milliseconds to reach its steady state position while the time required for smaller input steps of 10mm to reach steady state was around 70 milliseconds. The characteristic of 63% response time was however respectively measured as 25, 65 and 102 milliseconds for the above 10, 30 and 50mm step inputs above. These values correlated to the responses characteristics observed by both Grobler (2016) and Els (2006) although they also highlight that the actuator's performance is not necessarily constant as Figure 5.16 shows more clearly. Larger displacements require higher forces and energy, due to the spring within the strut and the higher damping present, and thus the actuator requires more time to provide this. The measured displacement's gradient (strut velocity) in Figure 5.15 illustrate however that the actuator achieves an almost constant velocity during its motion of around 0.2 to 0.26 m/s. One could argue that this constant velocity gradient indicate that the actuator has reached its maximum

achievable extension rate under the applied loads which is limited by the available hydraulic pressure and flowrate area of the actuator.

Although the actuator can arguably still be made more responsive by the further 'stiffening' of the PID controller so that it starts to overshoot more during these tests, this was not achievable as the further stiffening resulted in an unstable control (constant humming and vibration) of the strut and thus the conclusion was drawn that response time was inherently limited by the hydraulic flow rate available through the valve to actuate the strut.

In an attempt to improve the response characteristics of the actuator an additional MOOG valve was added to the experimental setup so that the controller would be able to achieve larger hydraulic flowrates. The controller PID settings were also tuned to maximize the ramp speed of the strut with this additional valve now added on. However, with the additional valve the actuator became even more unstable and thus the PID settings had to account for this. During this setup process trained and qualified laboratory personal were consulted to ensure an optimal setup. A second iteration of step experiments were then conducted. As Figure 5.16 suggests, the additional MOOG valve did not improve the response characteristics of the actuator and rather worsened the actuator's responses. It is also clear that as the resistance of the MR4S$_4$ strut increased, i.e. as more MR damping effect is applied by the MR valve, the slower the actuator response becomes in reaching its response value of 63% while increasing the step size had the same effect.

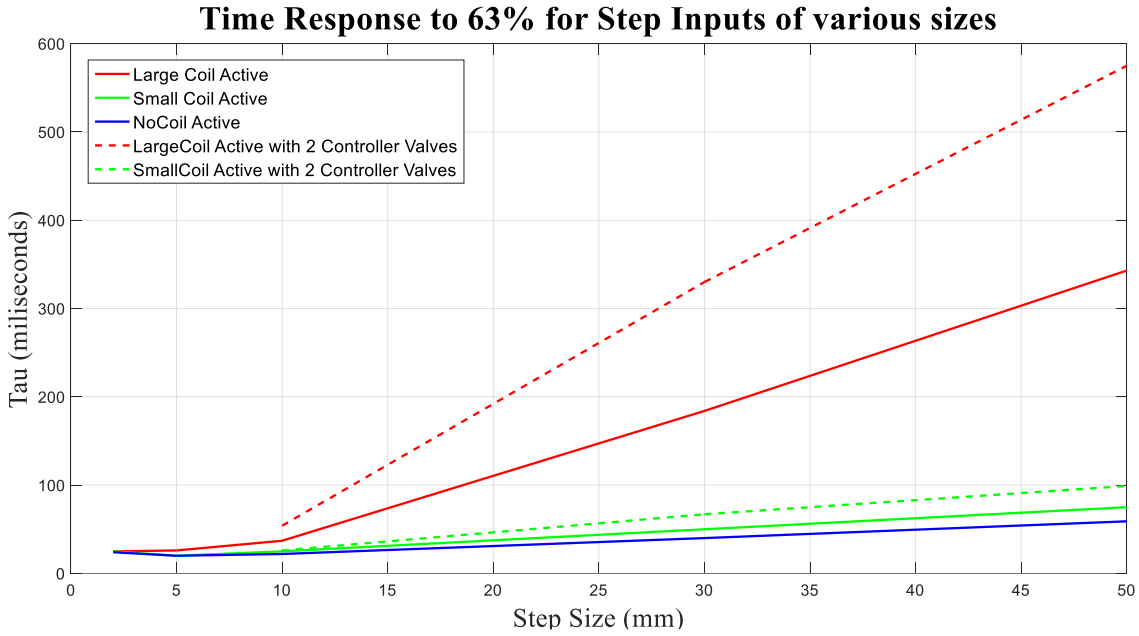

Figure 5. 16: Response characteristics of the actuator

Looking at the general trend in these results, it is noticeable that the actuator alone could be responsible for a delay of at least a 30 milliseconds but the same effect could be as great as 100-200 milliseconds where the amplitude of its influence is determined by the loading and conditions within the MR4S$_4$. This brings one to question whether the time response characteristics of the MR valve discussed in Section 5.8.2 is not largely due to the inherent actuator control delays used in the test setup. For this reason, a more trustworthy interpretation of the MR valve response characteristic is the discussion in

Section 5.8.3 were the response of the MR valve is discussed in the displacement domain as to remove the effects of the actuator as well as any test rig deflections. Still, it could be debated that the spatial domain interpretation of Section 5.8.3 does not remove the inherent actuator response time delay fully because displacement is directly proportional to time and velocity. Thus, the conclusions drawn from these sections still only provide us with an upper value of the response characteristics. It is theoretically possible to expect that the system in fact could demonstrate characteristics which are faster than what has been experimentally verified. This is debatable because the magnetic conditions settle much faster than the measured physical conditions and that the obtained force responses are largely influenced by the actuator's ability to respond to the rapid change force conditions.

It is difficult to develop an experimental setup which is able to investigate the response times of less than 30 milliseconds while dealing with such high displacements and forces, typical of the $MR4S_4$ suspension. It is therefore arguable that the testing facilities available could be obscuring the measurable response characteristics as the requirements on the test equipment is very high in order to observe the response properties of interest. In the tests conducted during Chapter 5 the most responsive actuator available was selected where additional flow valves and large accumulators were installed to help minimise the actuator effects while the PID control system was also stiffened as far as possible.

The aim of the experimental work in Section 5.9 was to quantify the degree to which the experimental setup and tests could be influencing and obscuring the previously determined response characteristics. Unfortunately, a large range of influence was noted which depended on the conditions the actuator was exposed to. Representative values of the responses as was observed by Els (2006) and Grobler (2016) were noted in these setup conditions as well as values that where both faster and slower. Thus in conclusion to Sections 5.6, 5.7 and 5.8, the observed response characteristics in these sections can only be safely regarded as the $MR4S_4$'s proven upper limit which could be experimentally observed with certainty. Arguably, the potential exists for the system to present a faster response time since its magnetic characteristics are significantly faster, a potential which is overshadowed by the physical ability to test at these conditions. At the very least, from the experimental observations one can safely start to argue that the response characteristics are already appropriately fast to successfully enable semi-active suspension control implementation, which is the overall aim of the research initiative.

5.10. MR Valve Flow Blocking

The MR valve's flow blocking ability is described by the maximum pressure drop achieved across the valve when various coils are fully active. This has been depicted in Figure 5.17. As one can expect of an orifice based valve, which never physically closes of the flow channel, its ability to block flow is dependent on its ability to slow the flow of fluid through it. It is expected that the MR valve will never be able to fully block the flow for an extended period of time, as one would be able to do with a mechanical valve, since the flow area is never mechanically closed. Although resistance will be supplied

by the viscosity shear effects, at very slow flowrates the MR fluid will still leak through the valve and as such one cannot expect to achieve quasi-static flow switching with such a valve.

That said, at the very slow strut velocity of 5mm/s the MR valve provided 28.7 bar of resistance (or blocking force) across the valve with both coils active, but as suggested by Figure 5.17, one can expect the resistance to reduce as the velocity reduces from this point downwards where the graph shows a decrease in blocking ability going from 100 to 5 mm/s (right to left) on the plots below.

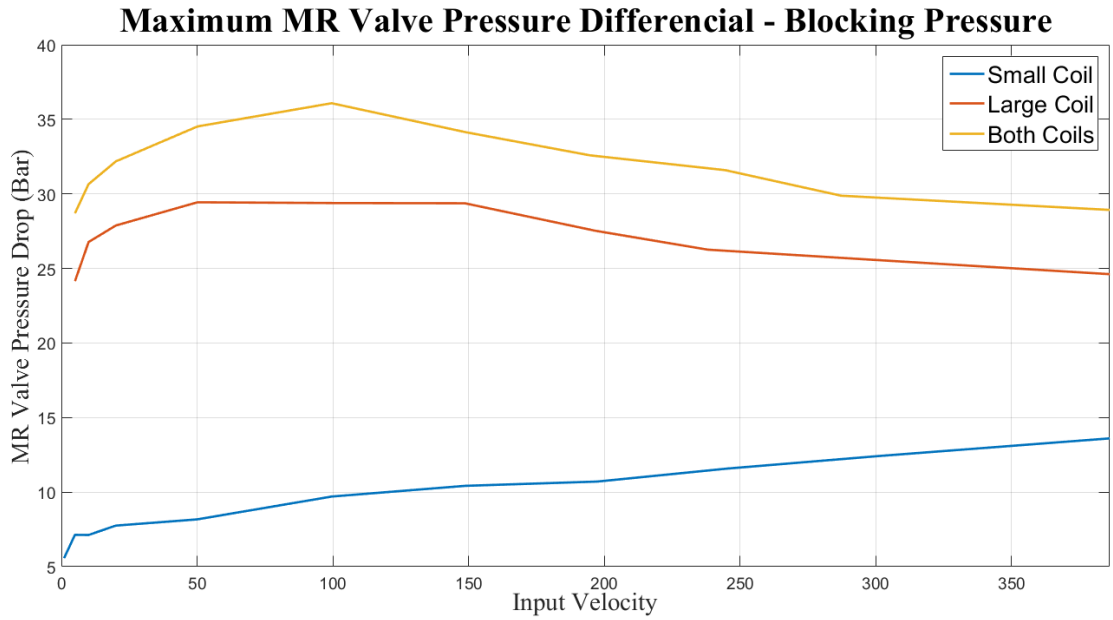

Figure 5. 17: MR valve blocking pressure drops achievable

As expected, the new MR valve, before having increased the annular gap, was able to achieve significantly higher blocking pressure drops where activating the large coil was observed to achieve a blocking pressure drop of 70 bar by itself. Although this blocking ability would enable more controlled and definite suspension stiffness switching, its effect on the ride comfort of a vehicle would be detrimental as the overall damping characteristics of such a powerfully blocking valve are also much too high.

Although there is some flow blocking dependence on input velocity, the MR valve should still be able to provide dynamic suspension "stiffness" switching when utilised within the MR4S$_4$ context. It will however only be able to do so effectively during a manoeuvre. This 'dynamic control' of the suspension stiffness is ultimately the main objective of the 4S$_4$ system: to avoid the vehicle rolling over during sudden and very dynamic manoeuvres. With this in mind it is arguable that the MR valve will provide the MR4S$_4$ with sufficient blocking capabilities.

Conclusion

This chapter's experimental work was conducted through the use of the facilities made available by the University of Pretoria. A great number of experimental tests were conducted with the purpose of

extracting the characteristics of the MR valve. Specific focus was applied to understanding and determining the time response and damping pressure drop characteristics of the MR valve under constant flowrate operation. The blocking of the second flow path removed any obscurity about the flow conditions within the valve and in doing so allowed for accurate characterisation.

After experimentally proving that the designed MR valve developed in Chapter 4 provides the desired pressure drop versus flow characteristics in Section 5.7, the response characteristics of both the valve and the actuator was investigated. It was found that due to various effects, such as the bulk modulus, actuator controller delay and rig deflection, the MR valve response time characteristic were somewhat obscured. If, however, one had looked at these responses in a spatial domain it is observable that the MR valve responds with a 95% characteristic change within 40mm of strut displacement while 63% requires 20mm of suspension displacement. Nevertheless, the MR4S$_4$ system based on the new MR valve may provide a sufficiently responsive characteristic as to be of great use in improving the dynamic stability and control of a vehicle. This will require a control system to be implemented which will identify whether a stiffer or higher damped suspension is required during dynamic manoeuvres, a characteristic change which could then be obtained within 40mm of suspension displacement. Importantly, this control system should be able to accommodate the non-linearity and complex interaction between the damping and stiffness elements of the MR4S$_4$, a process which in itself could be a considerable feat.

Furthermore, the MR valve flow blocking capability was investigated in this chapter and it was determined that sufficient blocking is provided by the MR valve to achieve the desired 'stiffness' switching, although this would only be achievable in dynamic operation of the suspension system.

The experimental work in Chapter 5 has proven that one could obtain continuous damping control within the desired ranges by utilising the new MR valve as designed in Chapter 4. Even though the valve requires some spatial displacement to change its damping characteristics, its potential could arguably be instrumental in stabilizing a vehicle body during dynamic manoeuvres such as a double lane change. Therefore, it can now be argued that this technology can provide a large heavy off-road vehicle with the ability to both improve its ride comfort, when operating on the low 'off-state setting', or achieve better handling and control by drastically stiffening the system through the MR valve's blocking capabilities.

However, since the working principle of the MR4S$_4$ is based on a twin path network of two accumulators and two dampers, the installation of two of these new MR valves into the complete MR4S$_4$ suspension system could still provide unexpected resultant characteristics. For this reason, additional research was performed to provide some insight into the expected overall characteristics of a complete MR4S$_4$ with the new MR valves installed. It was decided that this additional insight could be achieved through either an experimental or simulation based study. Since additional experimental work was out of the scope of this thesis, Chapter 6 will describe the simulation based investigation conducted to obtain the required characteristics.

CHAPTER 6

FULL MR4S$_4$ SUSPENSION CHARACTERSTICS EXTRACTED FROM A PHYSICS BASED MODEL

Introduction

This chapter aims to provide the expected characteristics of a full MR4S$_4$ suspension system, with the application of the newly designed MR valve to both its flow paths. The characteristics will be extracted by 'actuating' a physics based model of the system through a series of characterisation tests in simulation. The physics based model is computationally expensive as the model accounts for the complex physical interaction between the two air springs and two dampers within the system and their respective fluid flowrates and pressure conditions. This simulation based approach in obtaining the characteristics of the full suspension system is utilised as the physical experimental characterisation of the system was not possible. During this chapter the development of the physics based model will be discussed as well as the spring and damper element sub-models used within the model. Finally, the simulated overall characteristics extracted from a range of simulation based tests will be displayed and discussed.

6.1. Physics Based Modelling Approach to define MR4S$_4$ characteristics

The MR4S$_4$'s output characteristics are complex in nature because it is defined by the collaboration and interaction of four extremely non-linear sub-models. The sub models consist of two pneumatic springs and two MR valve based dampers with two independent flow paths. The physics based modelling approach to determine full system characteristics was also conducted and validated by Theron and Els (2007) on the original 4S$_4$ system.

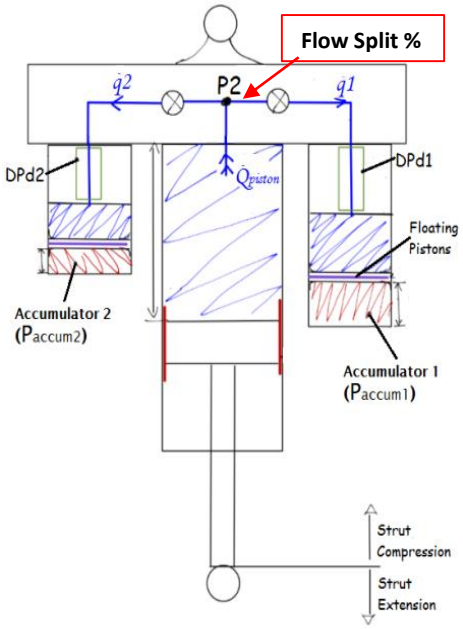

Figure 6. 1: Physics Based Model of the MR4S4

Theron and Els (2007) utilised experimental observations to develop look up tables to capture the damping characteristics used within his model of the $4S_4$. This contrasts to the application of the new MR valve which is much more complex due to its non-linearity and continues damping capability, requiring the use of a more complex methodology to capture an appropriate model. During the Matlab based simulation of the physics based model, the velocity of the suspension strut it obtained as an input. The model needs to determine how the fluid, pushed by the strut, is split into the two independent flow paths and respective accumulators. Since the accumulators have different volumes and the damping across the MR valves may be different, this flow split needs to be determined at each time step. The fluid split is defined by the following equations: (Theron and Els 2007)

$$Area_{piston} * Velocity_{piston} = Q_{piston} = q_1 + q_2 \quad (\frac{m^3}{s})$$
$$Q_{piston} = [(1 - \%) * Q_{piston}] + [\% * Q_{piston}] \qquad (17)$$

(%) – Fluid Split Estimate

The model starts with an initial estimate of the flow split percentage. Using the estimated split and total flow rate, the respective damping pressure drop across the MR valves are determined. The model integrates these flowrates in order to obtain the respective change in volumes of the accumulators and calculates the internal pressures of the accumulator using an ideal gas model. From this point the model evaluates whether the flow paths are in equilibrium with each other; that is, the centre of the system (P_2), as shown in Figure 6.1, is obtained from the sum of the pressures along both flow paths, as is defined by the following equation:

$$P_{accum1} + \Delta P_{Damper1} = P_2 = P_{accum2} + \Delta P_{Damper2} \qquad (18)$$

If this condition is not met, the model iteratively changes the assumed split condition percentage (%), using a gradient based solver and recalculates all the MR valve and accumulator components until it has obtained a suitable solution and an equilibrium pressure. Once equilibrium has been obtained, the output force is the equilibrium pressure multiplied by the area of strut piston.

6.2. Detailed Development of the MR Valve Damping Sub-Model

According to the Philips equation, the MR damper pressure drop is a function of a flowrate dependent viscous shearing term (ΔP_η) which is summed with a magnetic field induced yield stress (ΔP_τ) term. The magnetic field induced yield stress is the fluid's initial resistance to fluid motion due to the development of particle chains which resist flow in the presence of magnetic fields. Whereas the viscous shearing term is simply the viscosity of the MR fluid acting in resist to fluid flow which is a velocity dependent characteristic. To model the MR valve pressure drop, the Phillips equation was modified by replacing the viscous term suggested by Phillips with a more simplified modelling equation for viscous flow pressure drop in a pipe. The resulting equation used to model the MR damper looks as follows:

$$\Delta P = \Delta P_\eta + \Delta P_\tau = \frac{C \cdot 4 \cdot L \cdot \tau_\eta}{D} + \frac{c \cdot \tau_y(H) \cdot L}{g} \quad (19)$$

where τ_η is the shear stress due to viscous flow defined by

$$\tau_\eta = \eta(\dot{\gamma}) \cdot \dot{\gamma} \quad (20)$$

Equation 19 requires the magnetic field dependent yield strength $\tau_y(H)$ of the fluid as well as the shear rate dependent viscosity of the MR fluid $\eta(\dot{\gamma})$ which had to be modelled as a function of shear rate. Additionally, the annular gap width (g), annular gap length (L), annular circumference (w) and volume flowrate (Q) of the fluid must be known. There are also two scaling factors, C and c, which must be determined.

The first step in modelling the damper pressure drop is obtaining the magnetic conditions within the MR valve under an applied coil current condition. The average magnetic strength $\tau_y(H)$ across the gap was obtained by simulating the MR valve in the FEMM4.2 package for the applicable coil current condition. From the simulation the MR gap magnetic conditions could be extracted in two dimensions as depicted in Figure 6.2. It was then decided that $\tau_y(H)$ would be best described by an average value along the MR Valve's flow channel at the centre of the annular gap. Note that the apparent dip in the magnetic field strength is the area alongside the aluminium which forces the magnetic fields to move around that section, refer to Figure 4.2 and 4.3 to observe these fields in the MR valve.

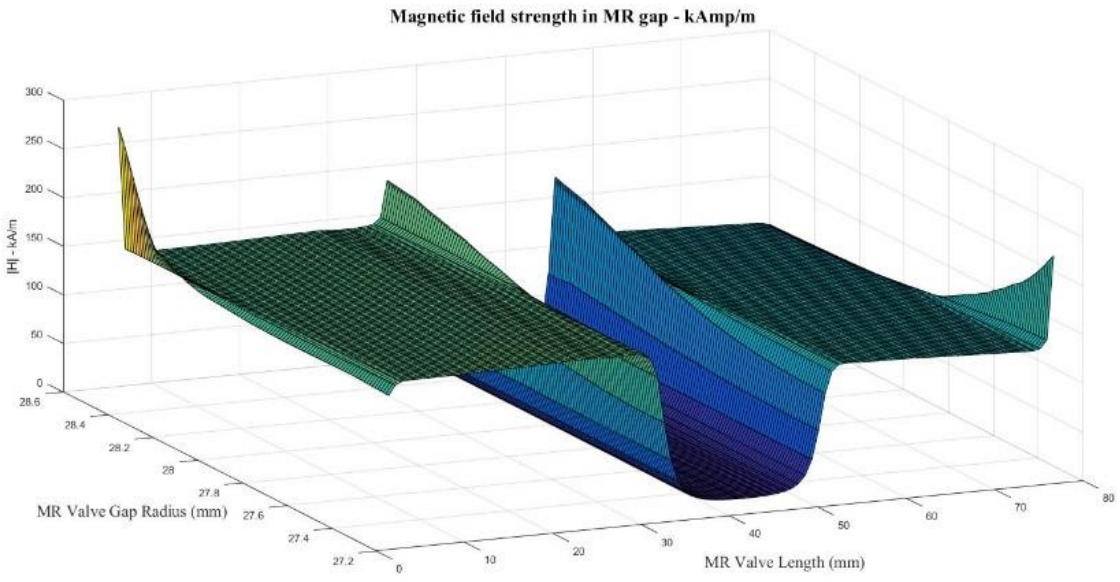

Figure 6. 2: Extracted magnetic conditions in the MR gap extracted from FEMM

Once the average magnetic field strength for a particular coil condition has been extracted from simulation, the expected MR fluid yield strength is obtained from a characteristic curve of fluid yield stress (τ_y) versus magnetic field strength (H). It was later noticed during comparison with experimental results that correlation was improved if the fluid yield stress characteristic curve was slightly reduced, an effect which is possible since the characteristic curve for the fluid used in the experimental testing

was not made available by the manufacturer. The characteristic curve used in the modelling process was obtained from LORD Corporations' MRF 132 fluid data sheet, which is a similar fluid to the one used during testing. Figure 2.12 shows the LORD's MR fluid characteristic which was scaled by trial and error until the experimental data aligned with the simulated data more appropriately. The MR fluid used during the experimental tests was Liquids Research MRHCCS4-B (80% Active) MR fluid which is commercially available. From the adjusted characteristic curve, shown in Figure 6.3, it can be seen that the achievable yield stress of the actual fluid saturates at a stress value of 40kPa. Using the obtained magnetic conditions from FEMM, the MR valve geometry, along with a fitted scaling factor (c) of 0.7, the magnetic field induced yield stress (ΔP_τ) was modelled and is plotted in Figure 6.4.

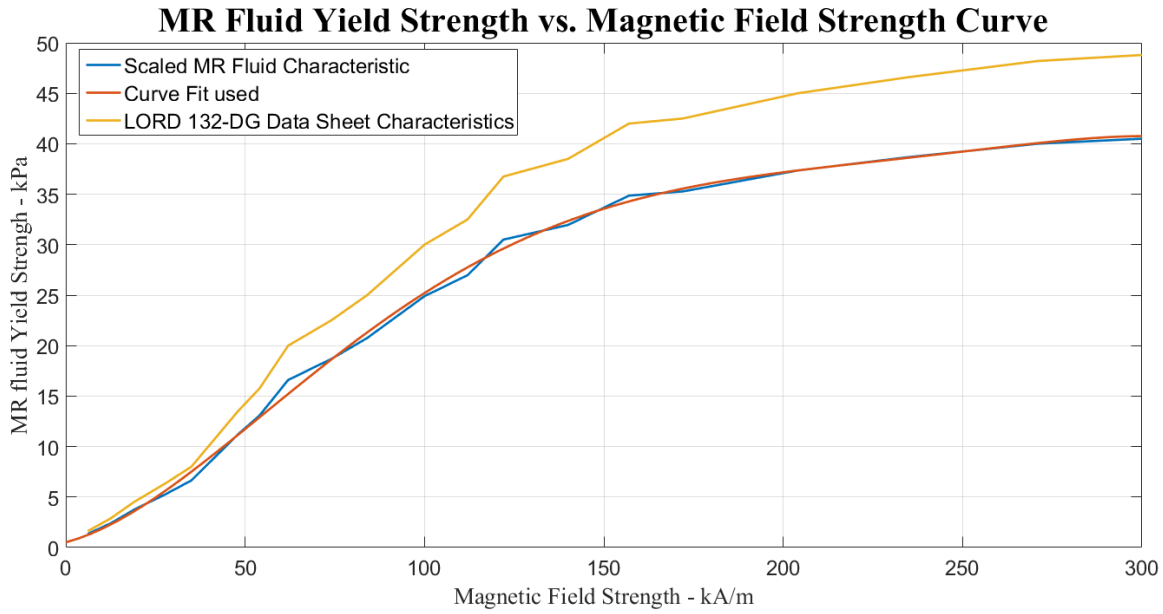

Figure 6. 3: Adjusted MR fluid Characteristic Curve

From experimentally observed damping force characteristics, illustrated in Figure 6.4, it was observed that the MR fluid undergoes significant shear thinning which causes saturation of the damping force at higher flowrates. This was taken into account by modelling the shear thinning of the viscosity into the viscous shearing term (ΔP_η) of equation 19.

The shear thinning was modelled with the following shear rate dependent equation:

$$\eta(\dot{\gamma}) = \left(\dot{\gamma} * 1.1e^{-4}\right)^{-0.3} \qquad (21)$$

Where $\dot{\gamma}(Q) = \frac{6Q}{wg^2}$

The resulting viscosity thinning model and damper pressure drop curve, as described by the shear rate term in the equations 19, 20 and 21, is seen in Figure 6.4.

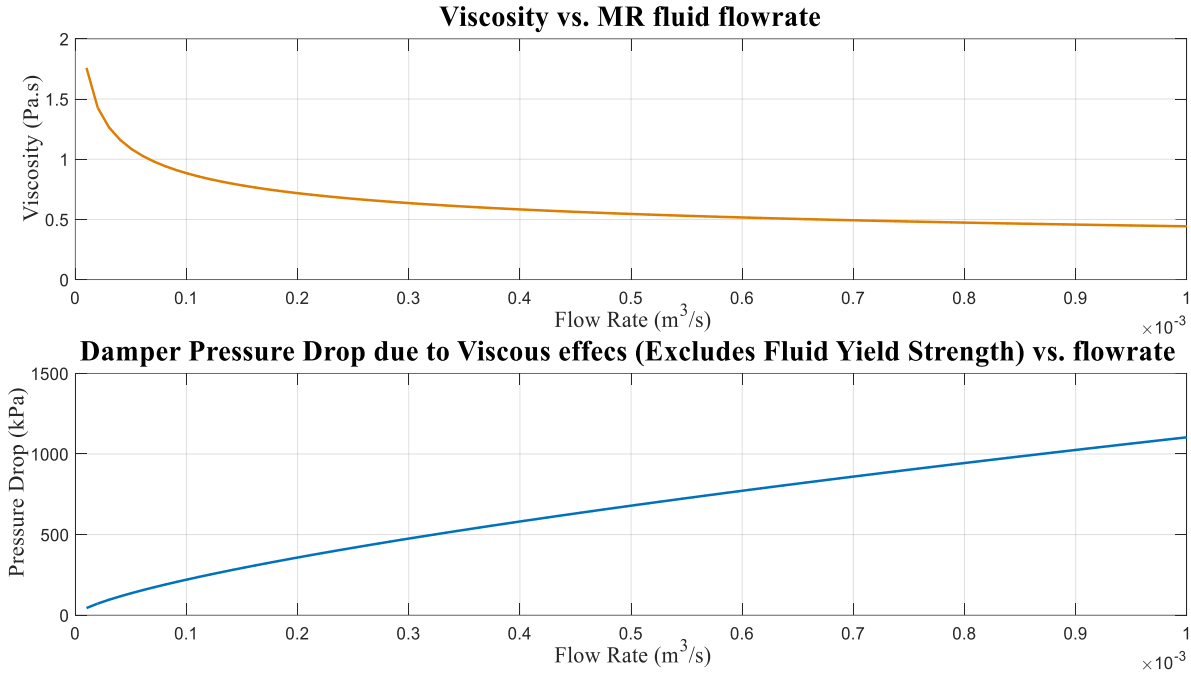

Figure 6. 4: Viscosity Shear Thinning model and resultant MR damper pressure drop curve

To validate the developed damper model which incorporates the simulation of the magnetic fields under each case, the experimentally tested conditions were repeated in simulations and a comparison drawn across all cases tested. Figure 6.5 illustrates that the model is able to appropriately capture the pressure drop characteristics of the measured MR valve prototype. Particularly for the off-state and for the small coil curves.

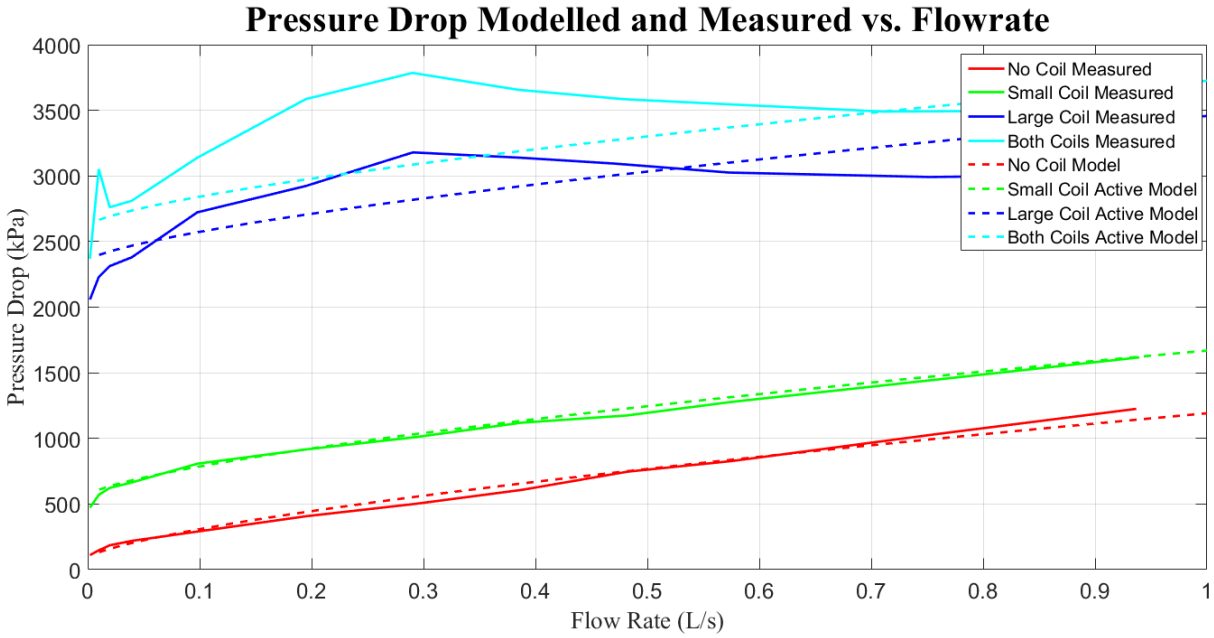

Figure 6. 5: MR Valve damping model validation

After the damper model had been validated across the off-state, small coil, large coil and both coil energising conditions depicted in Figure 6.5 it was implemented into the MR4S$_4$ physics based model. It was soon observed that due to the large discontinuities within the model, a numerical solution could not be found accurately and speedily. To ensure that a numerical solution of the physics based model

system could be obtained, the MR valve's damping characteristics were scaled at very small flow rates so that the model will not be discontinuous and will pass through zero.

The resulting modelled MR valve damping output force, across a range of flowrates, is displayed in Figure 6.6. The dashed lines represent the small coil damping curves whereas the solid lines represent the damping curves when the large coil is proportionally added. The sharp gradient change at low flowrates, smaller than 0.005 L/s, in the model was added in order to force the model through zero and to remove the discontinuity of the damping model and ensure that a numerical solution of the system could be obtained, further discussed in Chapter 7.

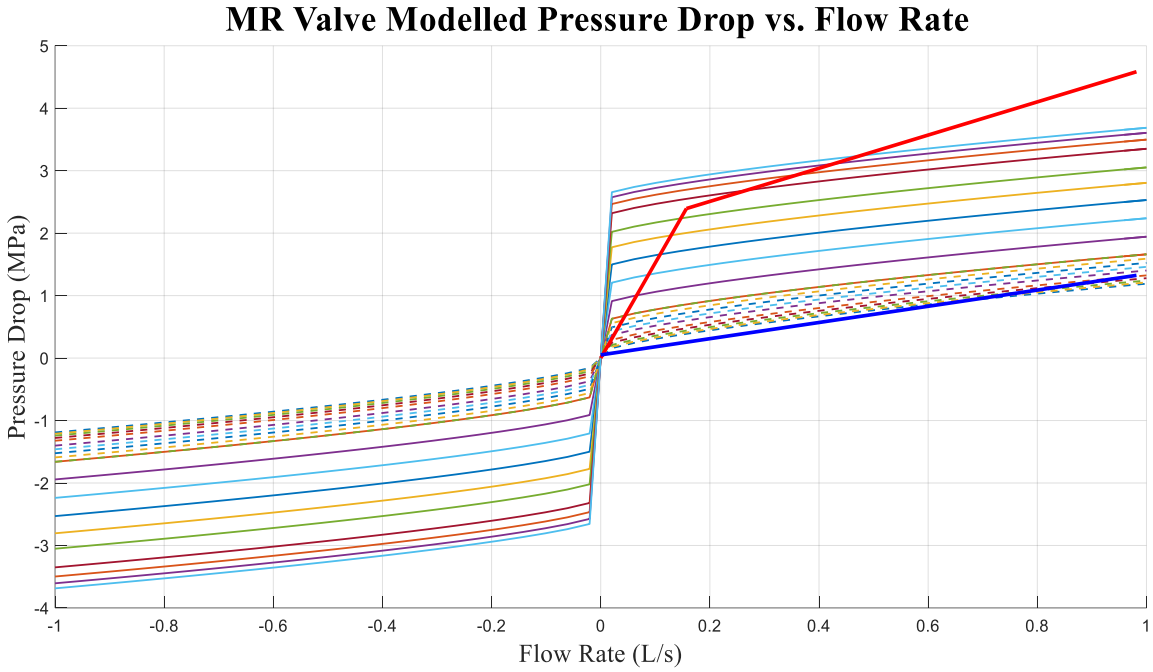

Figure 6. 6: MR valve damping force model results

In order to speed-up the simulation model the FEMM simulation was run for various coil currents and a lookup table generated for the magnetic field strength generated in the valve. The MR valve model uses the lookup table and performs a 2D interpolation in order to obtain a suitable magnetic field strength for any coil current combination across the small and large coil without requiring the FEMM simulation to be re-run.

6.3. Physics Based Model Validation

Unlike the many 'curve' fit or characterisation based models, the developed physics based suspension model captures the fluid and thermodynamic properties as they interact with the forces and displacements of the system to create the output characteristics. In order to validate the developed model's ability to predict the full MR4S$_4$ suspension system characteristics, the modelling methodology was tested against available measured data. This measured data was obtained from a full system set of characterisation tests of the MR4S$_4$ as was conducted by Grobler (2016). The model was run given the measured displacement input recorder by Grobler during his physical experimental tests of the MR4S$_4$. During the process the model was set up with the same initial conditions as the physical system. The

same measured initial accumulator pressures and volumes where used in order for the output force measured during the experimental work to be directly compared with the simulated results. This validation process was conducted across a range of input velocities, as well as, MR valve current states and the observed forces compared. A series of these results are displayed in Figure 6.7 that shows several input velocities with the MR valve current being controlled (Coil 1 and Coil 2).

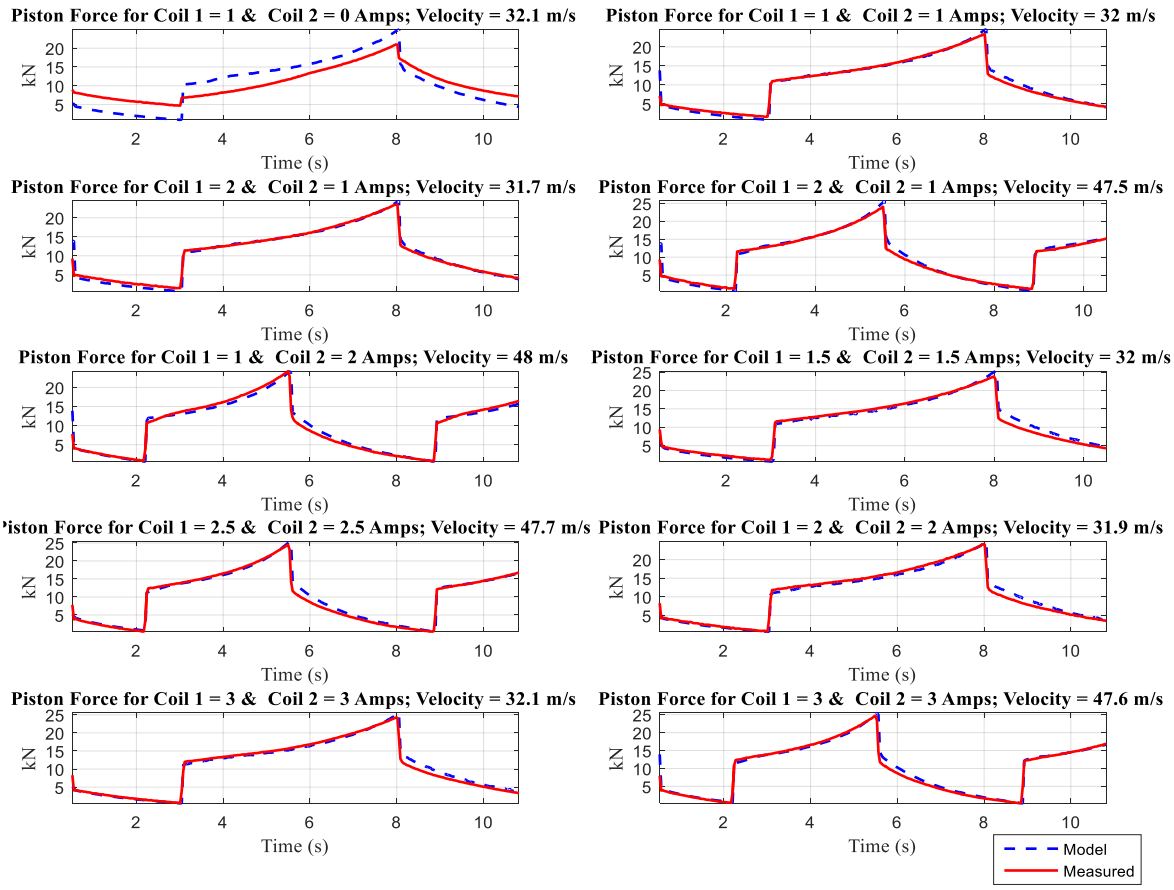

Figure 6. 7: MR4S4 Physics Based Model validation against experimental data

Although the model is not able to predict the output forces of the suspension system without error, it certainly provides a very good approximation of the output characteristics. Figure 6.7 provides confidence that the MR4S$_4$'s physics based model can capture the full system's output characteristics by anticipating the internal physical conditions. The same correlation is observed in Figure 6.8 for the model's output forces in the displacement domain in comparison with measured forces.

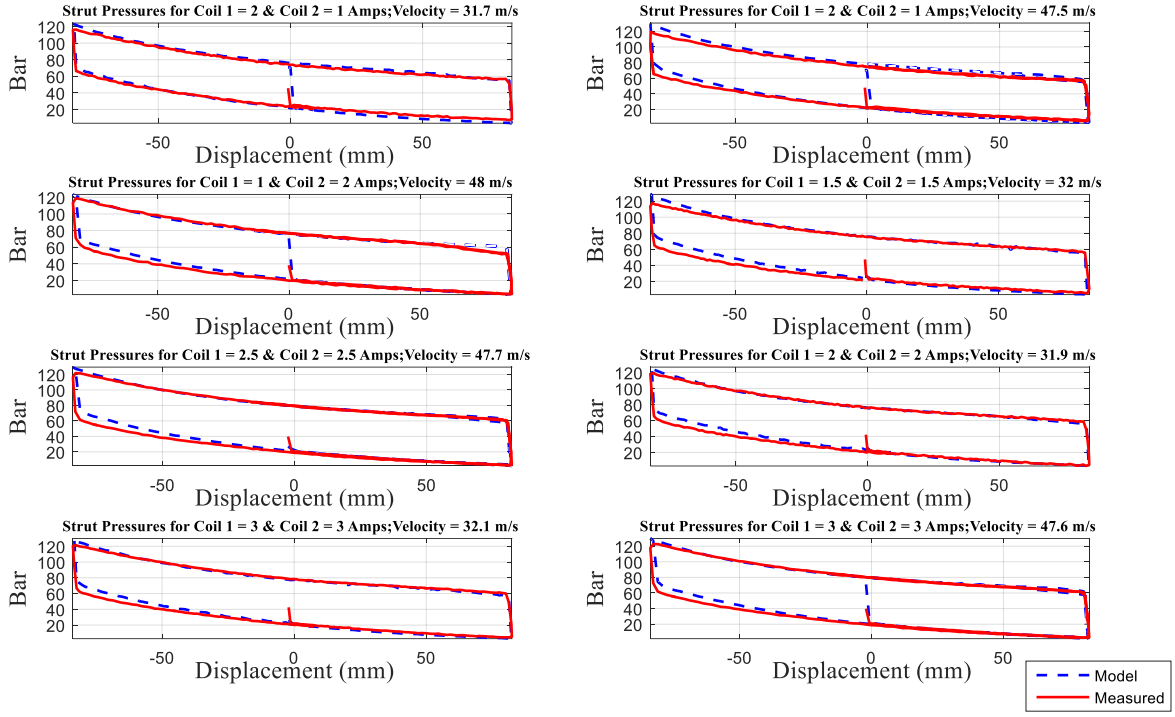

Figure 6. 8: MR4S4 Physics Based Model Validation against experimental data

From the validation study above it was found that the physics based model is able to capture and predict the full system's characteristics to a large extent. This work provides the required assurance that the model can now be used to predict the effective full system characteristics of the new $MR4S_4$ if the damper sub-model is updated to the current MR valve's characteristics. The full system characteristics could thus successfully be evaluated without the need for further experimental work on the full system.

6.4. Sub-model Analysis and Interpretation

After the implementation of the new MR valve damping model, the physics based model was run through a series of triangular displacement inputs while the coil states were controlled to obtain multiple suspension stiffnesses and damping characteristics. During this process the output strut force, accumulator pressures and damping pressure drops were monitored to ensure that feasible solutions were obtained. The following suspension setting were tested by appropriate coil control:

Table 6. 1: Simulated Suspension Settings

Suspension Settings and Applied Control				Coil States			
No.	**Suspension Setup**	**Effective Air Volume**	**Damping**	**Large Accumulator Damper Coil**	**Large Accumulator Blocking Coil**	**Small Accumulator Damper Coil**	**Small Accumulator Blocking Coil**
1	Soft Suspension 0% Damping	Large and Small Accumulator	Frictional Only	0%	0%	0%	0%
2	Soft Suspension 30% Damping	Large and Small Accumulator	30%	30%	0%	30%	0%
3	Soft Suspension 70% Damping	Large and Small Accumulator	70%	70%	0%	70%	0%
4	Soft Suspension 100% Damping	Large and Small Accumulator	100%	100%	0%	100%	0%
5	Medium Suspension 0% Damping	Large Accumulator	Frictional Only	0%	0%	100%	100%
6	Medium Suspension 30% Damping	Large Accumulator	30%	30%	0%	100%	100%
7	Medium Suspension 70% Damping	Large Accumulator	70%	70%	0%	100%	100%
8	Medium Suspension 100% Damping	Large Accumulator	100%	100%	0%	100%	100%
9	Hard Suspension 0% Damping	Small Accumulator	Frictional Only	100%	100%	0%	0%
10	Hard Suspension 30% Damping	Small Accumulator	30%	100%	100%	30%	0%
11	Hard Suspension 70% Damping	Small Accumulator	70%	100%	100%	70%	0%
12	Hard Suspension 100% Damping	Small Accumulator	100%	100%	100%	100%	0%
13	Both Large Coils	Large and Small Accumulator	-	0%	100%	0%	100%
14	Suspension Lock	Large and Small Accumulator	100%	100%	100%	100%	100%

The soft suspension is achieved through allowing flow to both the large and small accumulator while simultaneously controlling the small coils within the MR valve on both of these paths to set the level of damping. On the other hand, the medium suspension is achieved by blocking off the small accumulator through fully energising the small and large coil on the flow path to the small accumulator while the level of damping is controlled by the controlled application of current to the small coil on the opposite path. The hard suspension setting is achieved through the inverse operation of the medium suspension while suspension locking is simply energising both flow paths' MR valves fully.

To demonstrate how the MR4S$_4$ model can appropriately predict the changing physical conditions within the suspension system during operation, the system's accumulator pressures are plotted for the soft (1), medium (5), hard (9) and locked (14) suspension settings during a triangular displacement input to the suspension strut.

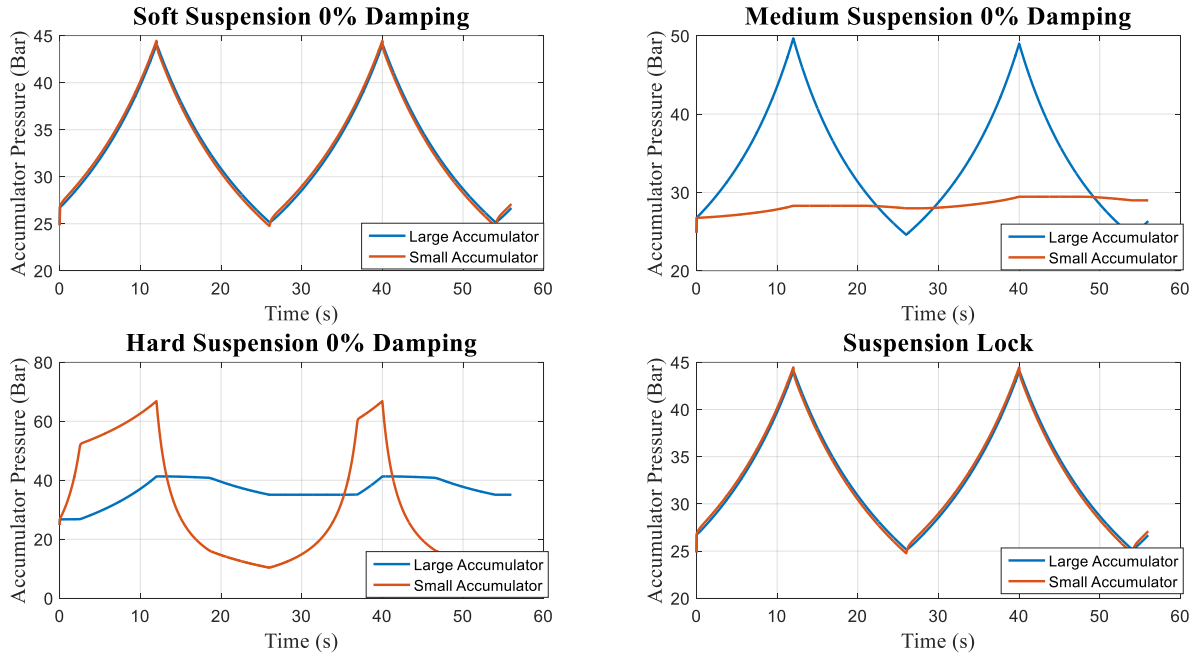

Figure 6. 9: Accumulator pressure changes during simulation of various suspension settings.

As Figure 6.9 illustrates, when the soft suspension setting is selected both the large and small accumulators follow an identical compression and extension cycle and are in pressure equilibrium with each other as they share the suspension forces – but not the displaced volumes. To the contrary, for the medium and hard suspension settings, the accumulator pressures of the respective soft and large accumulators are held almost constant by the MR valve which has been activated to block flow. This flow switching allows the suspension to change its characteristic stiffness as it changes the effective accumulator volume. It is noticeable that there is a point at which the MR valve leaks and fluid is allowed through, thus changing the effected accumulator pressure, an effect which is particularly prominent in the case of the hard suspension. This leakage occurs at a point when the pressure difference across the MR valve becomes larger than the MR valve can block with the applied MR effect. Once

this leakage has occurred, the leaked fluid is trapped within the respective accumulator, changing the characteristics of the system after that. This effect is illustrated in Figure 6.10 where there is a discrete change in the output force curve of the hard suspension, bottom left subplot, at 25 mm of compression. This is the point where the pressure in the system overcomes the blocking pressure of the MR valve and fluid leaks to the large accumulator, lowering the gradient of the compression. This leaked fluid is then trapped during extension and not allowed out of the large accumulator thus changing the force-displacement curve during the second and third compression cycles where it resultantly follows a different curve. This is what creates the three observable independent curves in Figure 6.10's hard suspension force-displacement plot. Finally, the suspension lock setting shows an identical spring rate gradient to the soft suspension because this setting has, in effect, the same accumulator volume available to it even though the output force is drastically increased by the dampers.

The $MR4S_4$ predicted output force versus displacement is plotted in Figure 6.10 along with the ideal gas compression curve for the respective 'effective' accumulator volumes achieved due to flow switching.

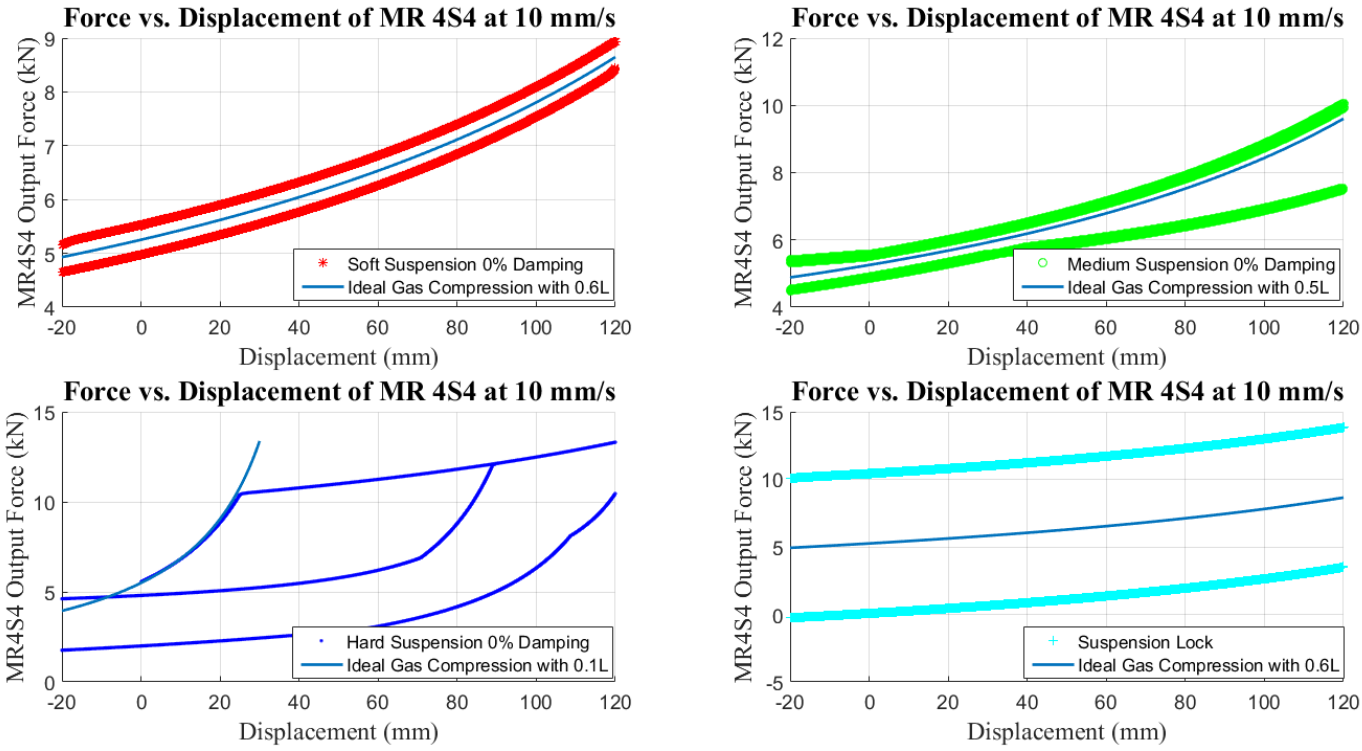

Figure 6. 10: Force vs. displacement characteristics achievable with the MR4S4

Looking at the above results it is clear that the $MR4S_4$ is able to effectively switch its spring characteristic through the use of the newly designed MR valves. The spring rate of the system follows the ideal gas compression curves for each of the settings at least until the MR valve is overcome and the effective accumulator volume changes, thus changing the stiffness characteristics.

These results are in line with what would be expected of the system and as such they provide valuable assurance that the $MR4S_4$ physics based model is able to accurately predict the characteristics of the complex system. Additionally, because the damping MR valve model is extensively based on

experimental results, one has reasonable assurance that the predicted characteristics from the model will closely match those of a real system. For this reason this physics based model of the MR4S$_4$ could now be used as a tool to evaluate and extract the full system's force-displacement and force velocity characteristics across a range of suspension settings achievable through coil control. It is also possible to evaluate the contribution such a suspension system could have on the dynamics of a vehicle, with reasonable assurance, before incurring the cost of physical manufacturing and testing.

6.5. Complete MR4S$_4$ Characteristics Extracted from the Physics Based Model

Due to the interaction of the two MR valves and two independent accumulators, the output characteristics of the MR4S$_4$ is non-linear and highly complex and depends on the operational conditions of all four of the contributing elements at every point in time. For this reason, extracting a 'look-up' table of characteristics is not possible as it would have to be multi-dimensional. This effect, for example, is illustrated by the change in spring rate when the system is 'actuated' at different velocities. However, in an attempt to suggest some of the achievable damping and spring characteristic curves, simulations across various input velocities, and with various coil current conditions, were investigated.

6.5.1. Full MR4S$_4$ System Force vs. Displacement Characteristics

What makes the MR4S$_4$ fundamentally different in comparison with the original 4S$_4$ system is its use of an MR valve to achieve flow blocking instead of a mechanical flow valve. This has the fundamental effect on the system's quasi-static characteristics as the MR4S$_4$ cannot achieve flow blocking at very low flowrates due to the valves leaking. Leaking valves cause a characteristic change if given sufficient time. One could argue that this is simply a numerical effect created by forcing the MR valve model through zero, as was discussed in Section 6.2, as a real MR valve could possibly block flow completely. Grobler also noted significant leakage effects during his very slow spring rate characterisation tests. The model predicted the following velocity dependence of the MR4S$_4$ spring rate or stiffness for the soft, medium and hard setting.

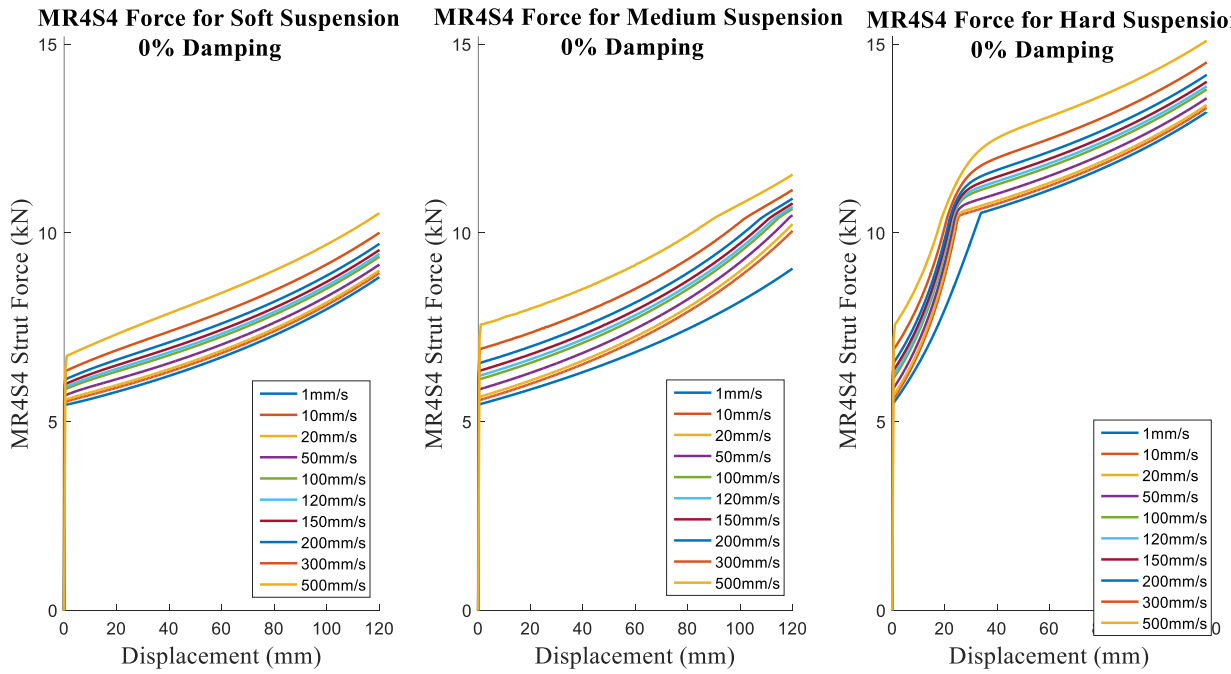

Figure 6. 11: The effect of velocity on MR4S4 Spring Rate Switching

There is a clear increase in the strut force for higher velocities which is expected due to the fact that MR dampers are in series with the accumulators. The removal or subtraction of the damping force would provide an unrealistic spring force curve as the MR4S$_4$ would never be able to function, and achieve the spring rate switching, without the addition of the dampers. Thus analysing the effective spring rate without taking into account the velocity and damping effects would be non sensical. Figure 6.12 highlights the achievable spring force through flow switching achieved by the MR4S$_4$ system at 10 mm/s.

As illustrated in Figure 6.12, the achieved spring force curves are almost identical to the ideal gas upon which their accumulator pressures and volumes are modelled, although they are offset by the damping effect which increases the output force as expected.

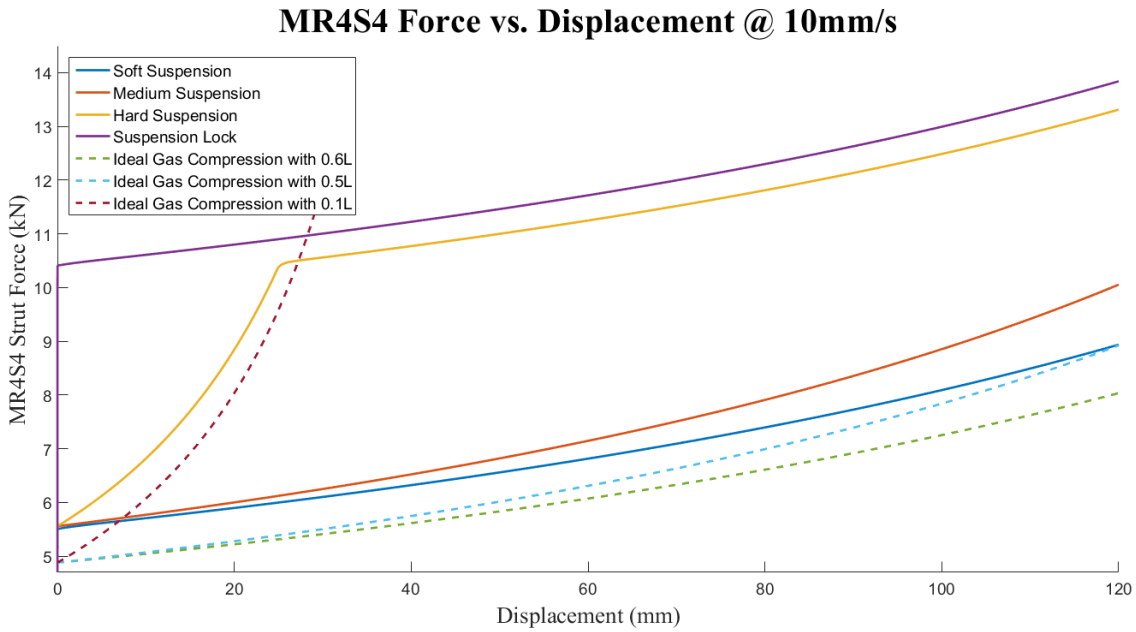

Figure 6. 12: Achieved Spring Rates by MR valve coil current control

6.5.2. Full MR4S$_4$ System Force Velocity Characteristics

Running the MR4S$_4$ model through a series of triangular inputs at various velocities, the damping characteristics of the system were extracted through a simulation based study. Here a range of suspension settings were investigated and the obtained characteristics plotted for comparison.

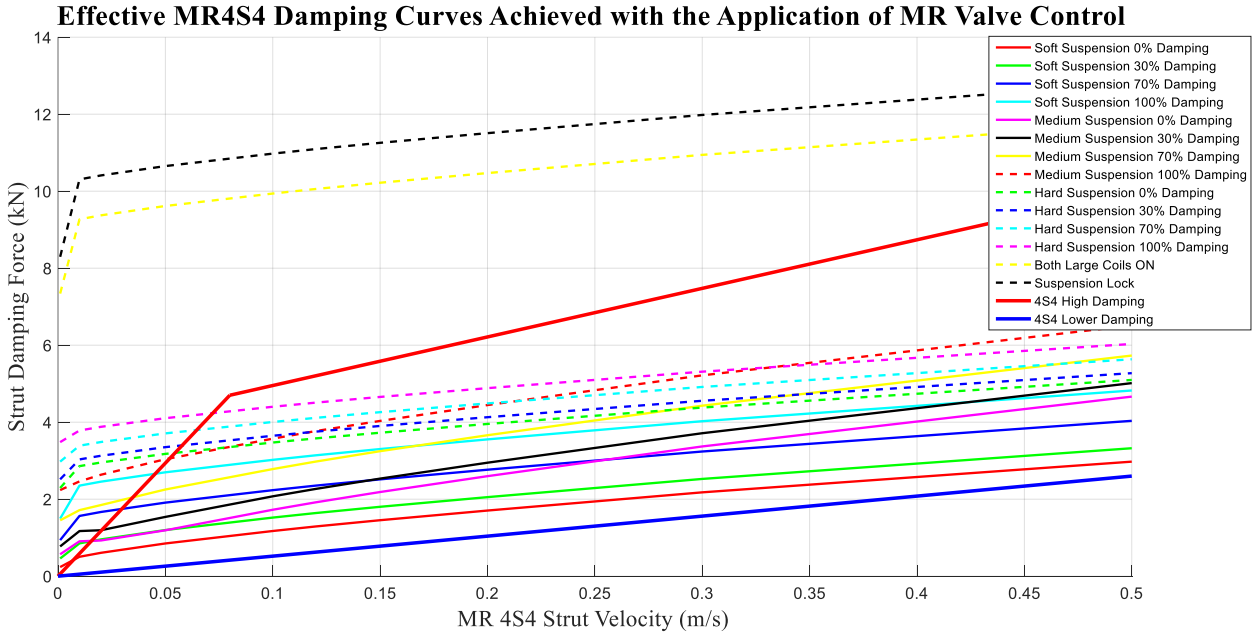

Figure 6. 13: MR4S4 damping characteristics achieved

Figure 6.13 illustrates that the MR4S$_4$ system, as a whole, is able to achieve a wide range of damping characteristics by simply changing the current conditions of the four respective coils of the MR valves. The figure plots the characteristics of several suspension settings. Of major importance is the fact that continuous characteristics could be obtained all the way to the suspension lock characteristic since the above investigation ignored any variability in the large coil current, switching it at either full current or zero current.

6.6. Accuracy of the Physics Based Model Iterative Solution

After obtaining the expected full system characteristics from simulation based tests of the physics based model, one could question their validity in predicting the actual characteristics of the $MR4S_4$ system. The physics based model requires considerable computational effort in comparison with a simplified look-up table or mathematical model. The model's accuracy is not only determined by the accuracy of the accumulator and damper sub-models, but also by the numerical solution obtained by the iterative solver in an attempt to define the physical conditions within the system.

In general, when sampling at 1000-2000Hz, the model returned the acceptable equilibrium error as shown in Figure 6.14 during the characterisation tests in Section 6.4 and 6.5. Note that this error is defined as the difference in equilibrium pressure of each of the respective flow paths obtained by the iterative solver, as defined by equation 18.

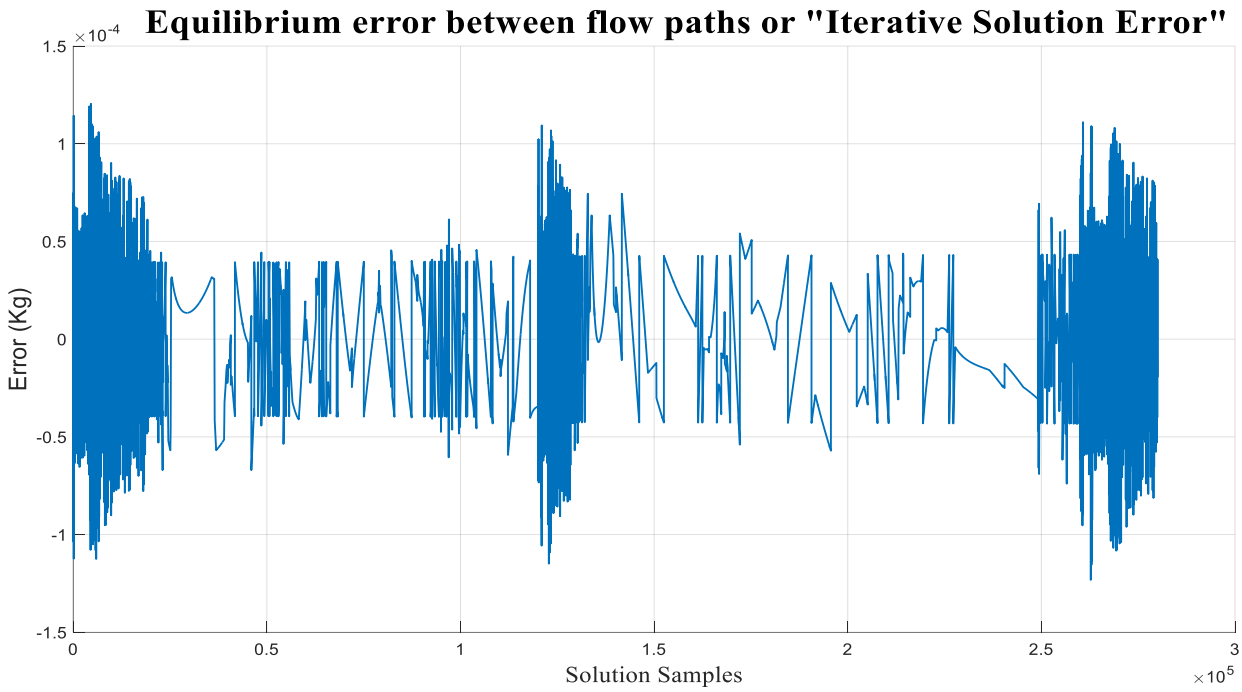

Figure 6. 14: Iterative Solution Error for a 10mm/s input test

As is illustrated by Figure 6.14 the error of the solution obtained during the characterisation tests, plotted in kilograms, is insignificant. However, the accuracy of the physics based model is detrimentally affected by large input velocity spikes, such as step displacement input, where it becomes problematic for the iterative solver to solve the non-linear highly complex system at the instance of a sharp input.

The last area for concern relating to the accuracy of the model is due to the fact that the damping element was forced through zero in order to obtain a numerically solvable system. The consequences of this adjustment to the model is difficult to anticipate because it is still unknown whether the MR valve will actually block flow at very low flowrates. It was decided that the amount of the time the model actually spent within this very low flowrate region would be investigated in order to determine if the effect could be detrimental to the solutions obtained. A normal distribution of the flowrate in both paths were drawn where the area, which fell within the +-0.005 L/s affected model region, was integrated to find a

percentage of the iterations spent within it. It was found that during a quarter-car simulation, discussed in the section 7.2, the model's flowrates were within the effected region for 1.29% percent of the iterations as is illustrated on the normal distribution below.

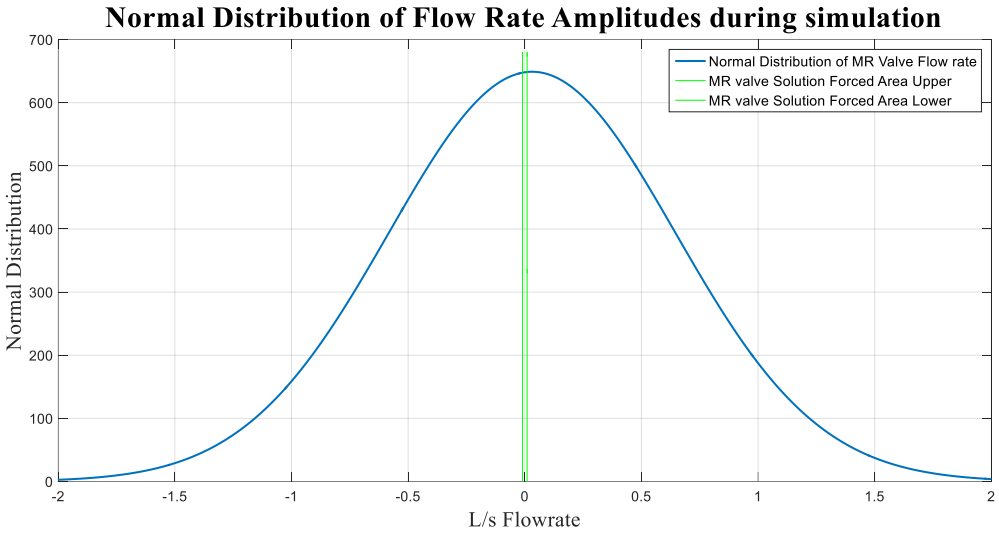

Figure 6. 15: Normalised distribution of MR valve flow rate during a Belgian paving simulation

This observation suggests that the effect of reducing the MR valve damping characteristics at low velocities should not have a significant impact on the simulation results over road inputs such as the Belgian paving, as very little of the time is spent with flow that falls within this flow regime.

Conclusion

This chapter discussed the development of the MR4S$_4$'s physics based model which is able to capture the output characteristics of the suspension system. Using this model the expected full MR4S$_4$ system spring and damping characteristics were extracted through simulation based investigations. It was significant to note that the MR4S$_4$ is capable of achieving various spring characteristics by controlling of the MR valves. This modelling and characterisation process has proved that the MR4S$_4$ as a full system now provides a suspension platform which can achieve both variable stiffness and damping characteristics thus opening new avenues of research. This suspension characteristic variability could be of use in improving or solving an off-road vehicle's ride comfort versus handling compromise. To investigate the possible impact of the MR4S$_4$ system on a vehicle's dynamics, this model will be implemented in a quarter-car based simulation study and the dynamic responses of representative vehicle analysed. Chapter 7 describes this quarter-car based study conducted to determine how the MR4S$_4$'s characteristics could be of benefit to a vehicle.

CHAPTER 7

QUARTER-CAR SIMULATIONS

Introduction

This chapter aims to investigate the dynamic response of the MR4S$_4$, as it operates in a quarter-car simulation. The simulations are performed to evaluate the potential vehicle dynamics related benefits of such MR suspension technology. The MR4S$_4$ characteristics are extracted from the physics based model developed in Chapter 6 which is able to capture the complex physical conditions within the suspension system. The dynamic responses of the quarter-car vehicle is investigated over several road inputs for its performance in both the frequency and time domain. It is known that the MR valve requires at least 50-100ms in order to effectively change its damping characteristics, and as such the effect of this delay on a skyhook control algorithm will be investigated. This investigation should indicate whether continuous active skyhook control could provide feasible improvements in ride comfort of a vehicle and as such support further development of the suspension technology.

7.1. Quarter-Car Setup

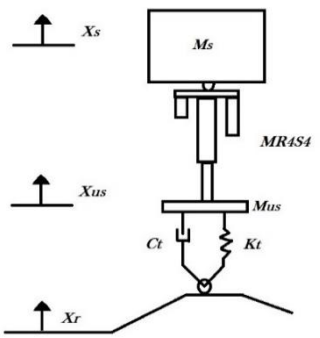

A quarter-car model was developed and simulated in Matlab. The relative displacement and velocity between the vehicle unsprung mass (Mus) and the sprung mass (Ms) was passed to the physics based model of the MR4S$_4$ as the dynamics of the system was solved. The output force of the MR4S$_4$ inherently contains a damping and spring force which differs from a conventional parallel spring and damper setup. In this study the sprung mass was set as 497 kg while the unsprung mass accounts for 115 kg. These weights were derived from the masses of the LandRover Defender upon which the MR4S$_4$ system is to be implemented. A point follower tyre model was used over the road input (Xr) with a tyre stiffness of 220 kN/m and a 100 Ns/m damping coefficient.

During the quarter-car simulations the same set of 14 suspension settings form Chapter 6 were used for each of the road profiles. This was done in order to evaluate if changing the MR4S$_4$ suspension characteristics through passive, and later active, coil control can have a positive effect on the responses of the vehicle and possibly improve ride comfort.

7.2. Passive MR4S$_4$ Suspension Control

A set of passive control tests were conducted whereby the quarter-car model was exposed to a step input, a measured Belgian paving road input, a sine sweep (or chirp input) as well as some repetitive road corrugations. For all of these tests the sprung mass dynamics were examined and the important observations noted.

7.2.1. Step Input Analysis

In order to observe whether the ride comfort of a vehicle could be improved through passive control of MR4S$_4$ characteristics a step input was used to excite the system and the sprung mass accelerations were observed. It was investigated whether by switching the MR4S$_4$ one could effectively change the natural frequency characteristics of a vehicle and that this effect would be demonstrated by a step input test. Thus the quarter-car model was excited by a 50mm step input while travelling at a velocity of 30km/h. The sprung and unsprung mass responses for the various suspension settings are illustrated in Figure 7.1.

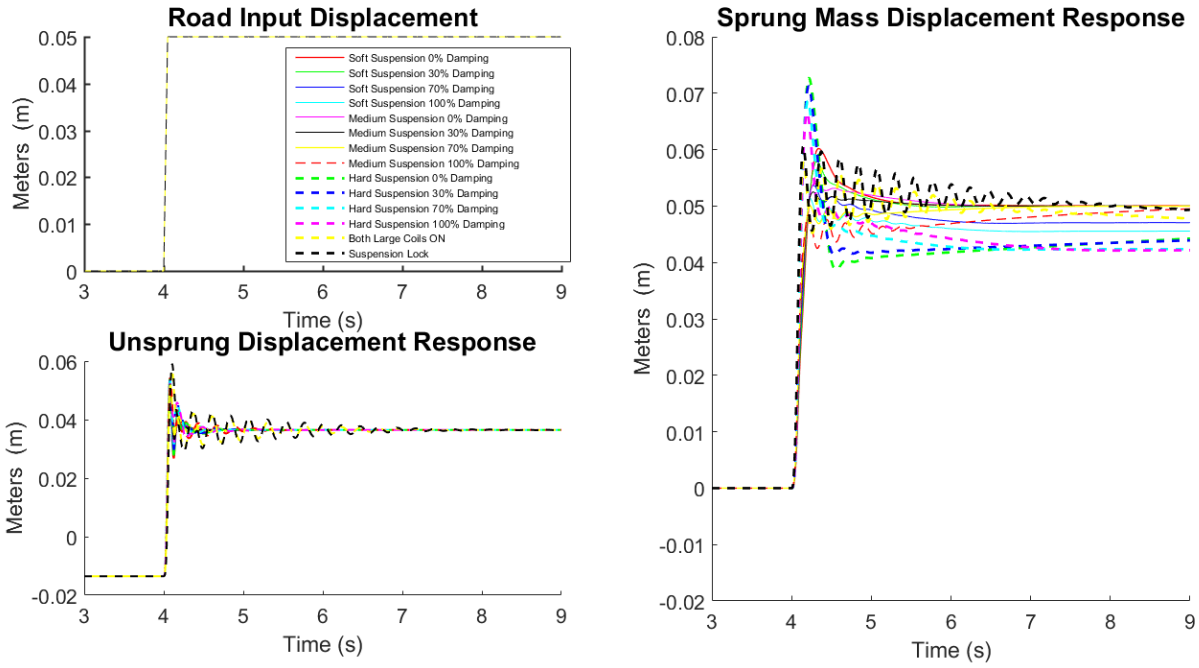

Figure 7. 1: Step Input Simulation Results

This quarter-car study suggests that the dynamics of the sprung and unsprung masses are certainly influenced by the MR4S$_4$ characteristic changes achieved through passive MR valve control through the various settings applied. It can be noted from Figure 7.1 that the passive control of the MR valves caused the suspension system to absorb and hold some of the displacement after the step input, as it takes a considerable time for the locked suspension to return to the neutral length. This happens because the compressed accumulators within the system are held by the MR valves when passively controlled, especially in the cases where the MR valves are energized creating high resistance for the suspension to move. However, given sufficient time the MR4S$_4$ does extend to its static equilibrium length.

To access the ride comfort influence of the suspension system on the vehicle body, the sprung mass acceleration is plotted in Figure 7.2 under the four most extreme suspension settings. The sprung mass acceleration for the soft, medium, hard and locked suspension settings (settings 1,5,9,14 in Table 6.1) are illustrated along with the sprung mass acceleration averages in Figure 7.2. Note that the average acceleration is calculated as the average of the absolute acceleration value of the sprung mass acceleration between the time of 3.4 to 4.4 seconds.

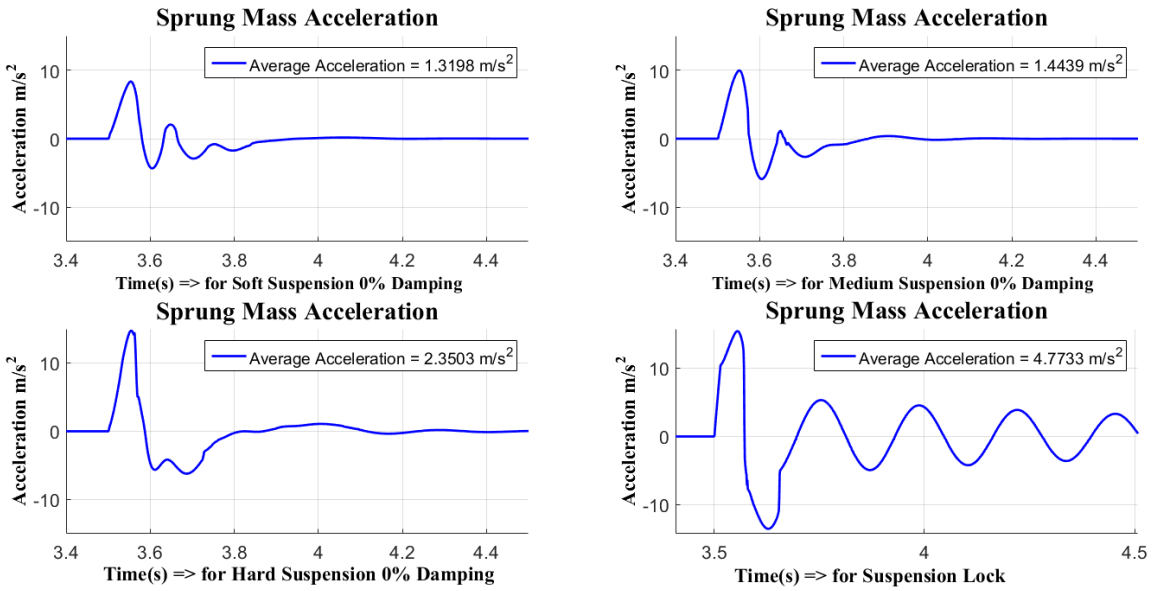

Figure 7. 2: Weighted and unweighted sprung mass acceleration

It is clear from the average values in Figure 7.2 that the soft suspension setting provides better ride comfort than the medium, hard or locked suspension as it reduces the average vehicle body accelerations as one would intuitively expect. This shows that the MR4S$_4$ suspension system is able to influence the dynamics of a vehicle through passively controlling the MR valve's damping and locking condition. Through the application of additional damping to the system with the use of the small coils on the respective suspension settings it was also noted that the ride comfort is affected. This is obviously to a much smaller degree than the cases plotted in Figure 7.2 as the effective damping added by the small coil is less than that of the larger coil. In these cases, it was observed that the suspension ride comfort also deteriorates with the application of additional damping by the small coil which is again expected as the application effectively stiffens the system.

Figure 7.3 depicts the frequency response for the various suspension settings as exited by the step input. As one would expect the soft suspension system has a lower natural frequency as compared to the hard suspension setting. However, an interesting observation is made in the medium suspension that the natural frequency is in fact higher than the frequency observed for the hard suspension. This demonstrates the significant influence the non-linearity present within this suspension system. In order to obtain the below results the simulation was run over the step input at a sampling frequency of a 1kHz.

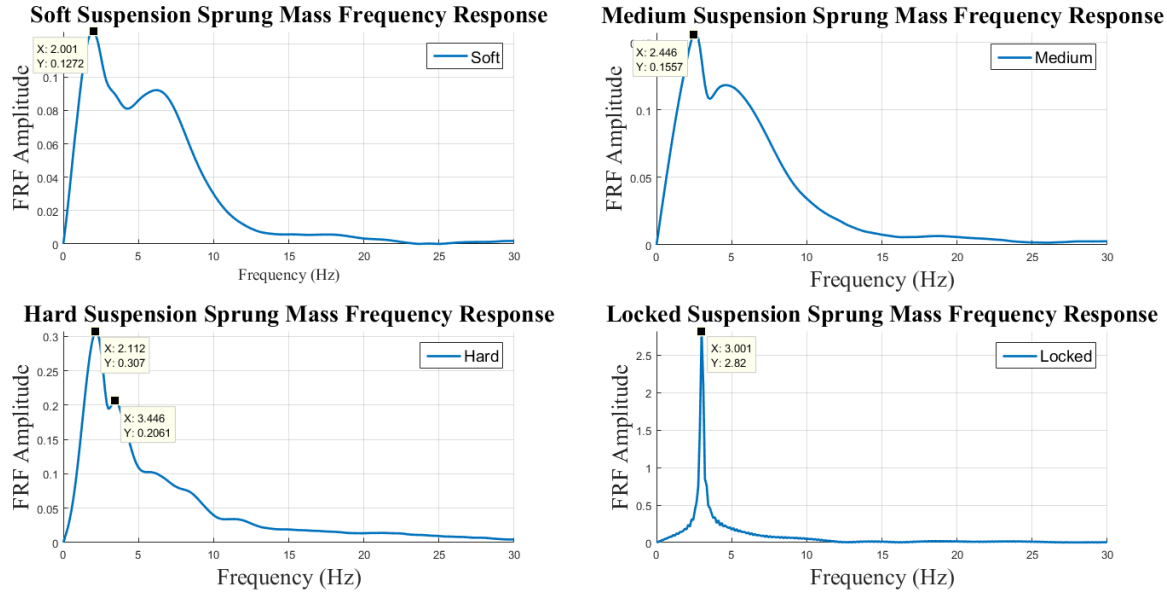

Figure 7. 3: Frequency response of sprung mass for several suspension settings.

For the locked suspension setting plotted in the bottom right subplot of Figure 7.3 the system is very rigid with little damping. The high stiffness clearly indicates the natural frequency of the combined sprung and unsprung mass as they vibrate on the tyre stiffness. The locked suspension dynamics was verified with the simple linear spring stiffness natural frequency equation based on the tire stiffness of 220 kN/m and a sprung and unsprung mass respectively 490 and 15kg.

$$\omega = \sqrt{\frac{K}{m}} = \sqrt{\frac{220\ kN/m}{(490+115)kg}} = 18.96\ rad/s\ or\ 3.01\ Hz.$$

The correlation between the above simple calculation and the obtained frequency response confirms that the suspension system is indeed locked as the sprung and unsprung mass effectively become a single mass with very little damping, only tire damping, causing a spike in the frequency response of the system as plotted. This result was expected because the MR4S$_4$ is able to change its stiffness characteristics through switching the MR valves as was proved in Chapter 6. This change in stiffness should lead to more observable natural frequency shifts between the various suspension settings. However, due to the high level of damping present in the system these natural frequency shifts are somewhat obscured although slight changes in the frequency domain are still observed in Figure 7.3.

Figure 7.4 makes it clear that increasing the amount of passive damping within the suspension increases the sprung mass acceleration. This effect is expected as the suspension system becomes more ‘rigid’ due to the inline dampers stiffening the flow of the fluid. The higher the damping and stiffness of the system, the worse the ride comfort will become over a step input as is highlighted by the average sprung mass acceleration (absolute) values in Figure 7.4.

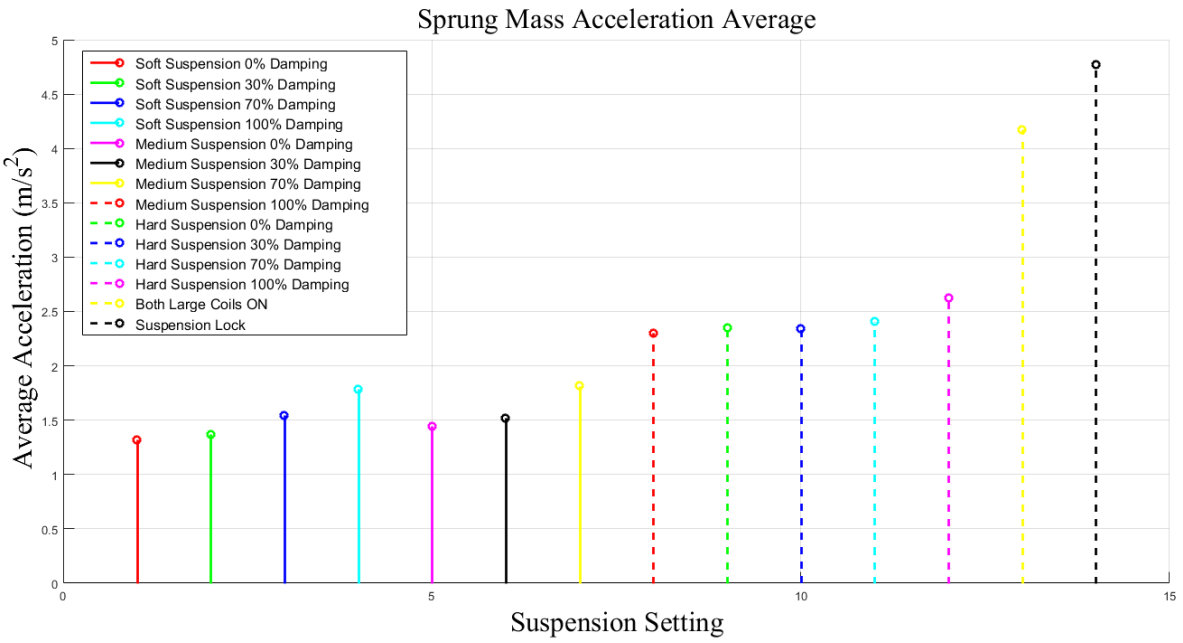

Figure 7. 4: Sprung mass acceleration over a step input.

7.2.2. Belgian Paving Input Analysis

The influence of a passively controlled MR4S$_4$ on the ride comfort of a vehicle over rough terrain was evaluated by running the quarter-car model across a Belgian Paving input. A Belgian paving input was selected because it provides a good road profile upon which to evaluate a vehicle's ride comfort. To improve the suitably of this road input it was decided that a measured Belgian paving profile would appropriately 'filtered' through a F-Tire model instead of deriving a representative road profile mathematically. The obtained profile served as the unsprung mass displacement signal as the tyre dynamics had already been accounted for by the tyre model and as such it was inputted to the quarter-car model directly to the unsprung mass. It is important to note that this method effectively removes the dynamics of the point follower tyre model and replaces it with more appropriate tyre dynamics. The resulting simulated sprung mass displacement over this road profile is plotted in Figure 7.5. for a vehicle travelling at 50km/h with the various suspension settings passively applied.

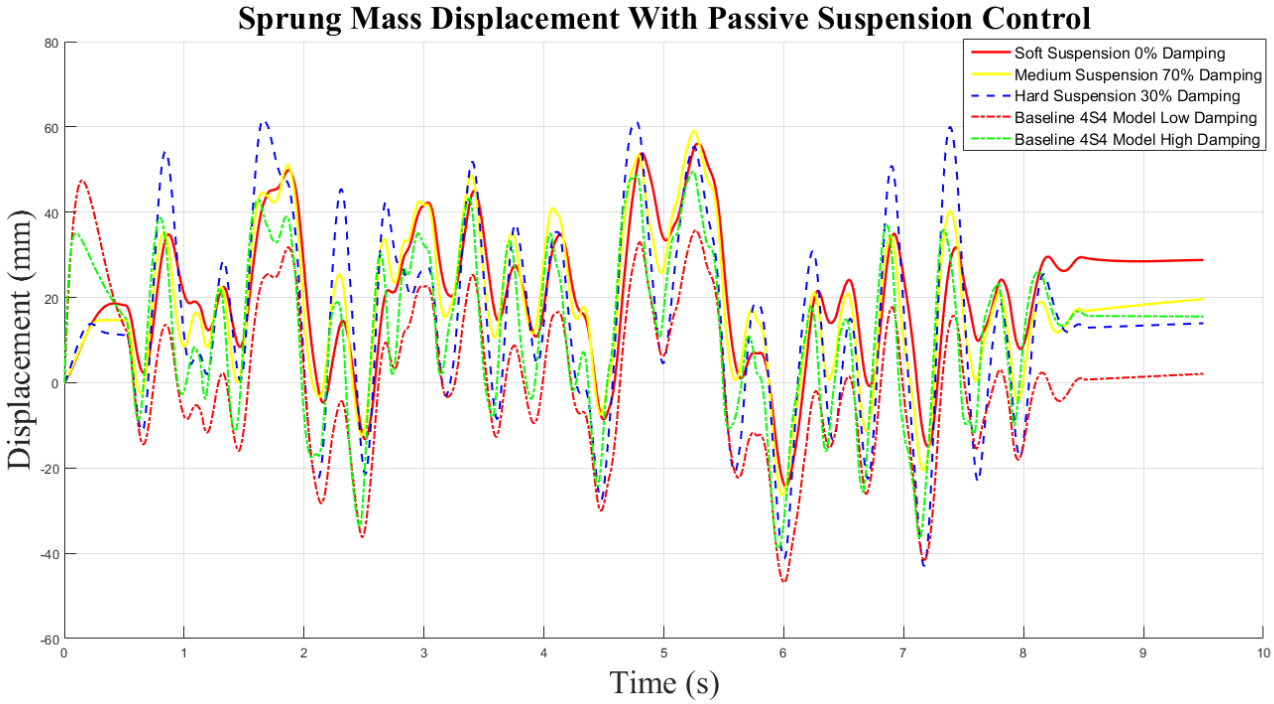

Figure 7. 5: Quarter-car simulated responses for the sprung mass

It is clear that the harder the suspension is set, the more of the road input is applied onto the sprung mass by the suspension system. In order to validate the obtained results, a set of baseline simulations were also conducted using the original $4S_4$ mathematical model developed by Els (2006). These baseline simulations were used to verify that the dynamics predicted by the $MR4S_4$ physics based model by providing validated results over this road profile. Figure 7.5 bring assurance that the $MR4S_4$ model is providing representative dynamics across all of its settings as the results are comparable to the baseline $4S_4$ models. A more quantitative representation of the ride comfort offered by each of the suspension settings across the Belgian paving road input is presented by the weighted acceleration RMS values in Figure 7.6. To obtain these weighted RMS values of the sprung mass acceleration was frequency weighted according to the BS6841 Standard (British Standards Institution 1987) which scales human discomfort based on the acceleration frequency to give a more deterministic measurement of ride comfort of a vehicle. Here it is observed that the softer the suspension and the lower the passive damping is, the better the ride comfort becomes as the sprung mass is allowed to oscillate freely over the road input. The obtained results are in accordance with what is expected since Els also found that ride comfort is optimal when there is as little as possible additional damping in the system.

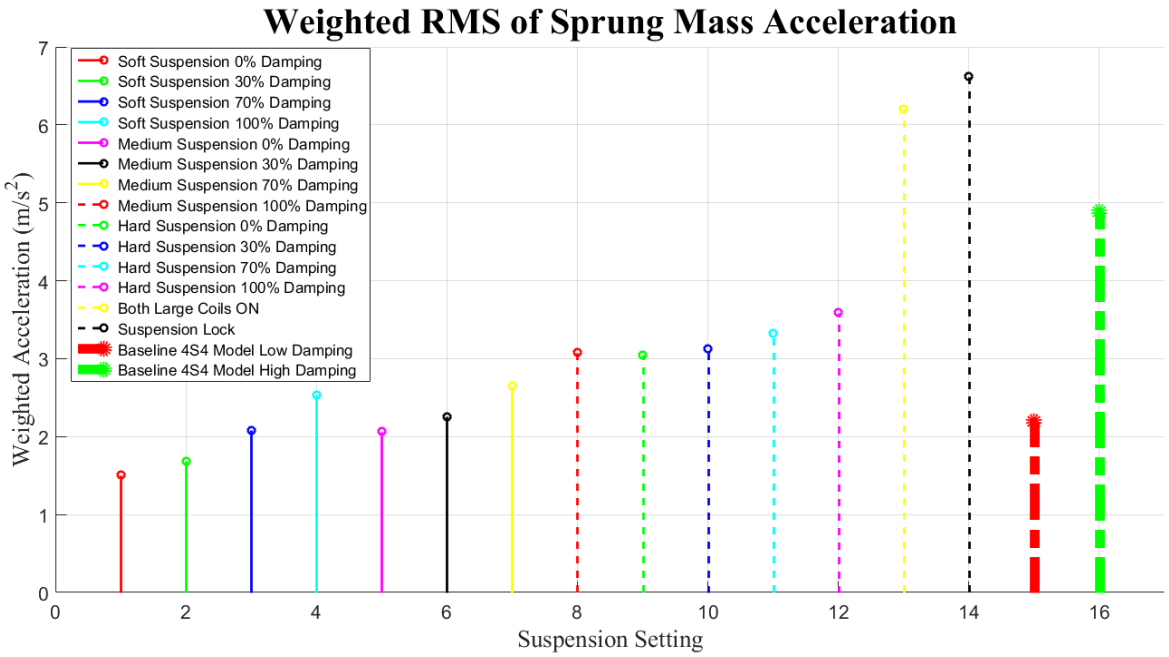

Figure 7. 6: Belgian paving sprung mass acceleration RMS with passive suspension control

The obtained MR4S$_4$ ride comfort results in Figure 8.6 were also validated by the baseline 4S$_4$ model (plotted with the thick lines) and provided a good comparison. The original 4S$_4$ model was run at its high and low damper settings while operating on its soft suspension. This was done to ensure that the obtained RMS values are appropriate and in doing so validating the output characteristics of the MR4S$_4$ model and the conclusions drawn from it. As Figure 7.6 suggests, the MR4S$_4$ actually provides a slightly improved ride comfort at its softest setup in comparison with the original 4S$_4$ system while it can also become more rigid making the ride comfort much worse than that of the original 4S$_4$ with its high damping setting. This investigation thus proves that the MR4S$_4$ is able to provide a vehicle with a very wide range of suspension settings through the simple passive control of low energy consuming coils in the MR valves.

7.2.3. Sine-Sweep Input Analysis

Due to the clear changes in the sprung mass dynamic responses observed when switching the MR4S$_4$ characteristics in the Sections 7.2.1 and 7.2.2, it was decided that the quarter-car model would be run through a sine-sweep input to investigate whether one can excite the shifted natural frequencies and in doing so visibly observe the changes in the vehicle's natural frequency due to passive suspension control. A sine based 'road' input was generated whose amplitude decreased with increasing frequency so as to obtain a constant acceleration road input. The sine-sweep was written such that the frequency shift would be reasonably slow at 10 seconds/Hz from 0Hz to 15Hz in order to obtain relative steady conditions during the excitation of the system at each frequency. The resulting acceleration frequency response is illustrated in Figure 7.7.

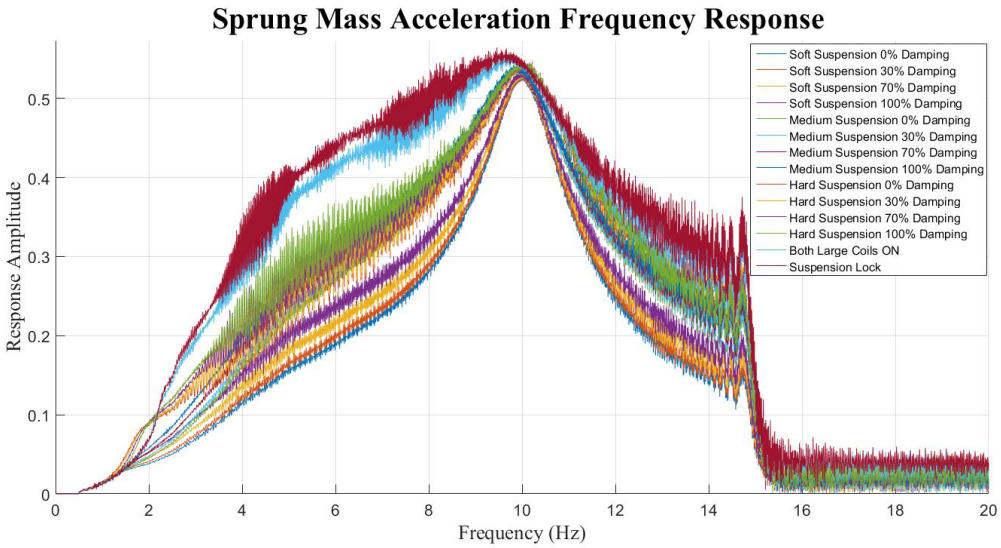

Figure 7. 7: Sine-Sweep Input Frequency Response Characteristics

This study shows that little change is observable in the frequency domain responses of the sprung mass for the various suspension settings tested. There is an observable shift for the 'suspension lock' and 'large coil on' settings due to the drastic stiffening of the system under these conditions. The obscurity of natural frequency shift in these results is perhaps an effect which can be explained by the non-linearity of the suspension stiffness. It could also be that during the higher frequencies the road input amplitude, to keep the acceleration constant, became too small to develop sufficient suspension travel. Simply put, a high frequency input would note excite stiffer suspension regions as it would be oscillating the suspension under very little suspension travel and thus not activate much of the non-linear stiffer spring components. The observed acceleration RMS values again indicated that the addition of damping to the suspension system increased the accelerations and decreased the ride comfort of the sprung mass as it travels over the sine-sweep.

7.3. Active Skyhook MR4S$_4$ Suspension Control

Following the passive implementation in Section 7.2, it was of interest to investigate whether the ride comfort of a vehicle could be improved with the implementation of a Skyhook active control of the semi-active MR4S$_4$ suspension system. The Skyhook control logic's main objective is to minimize the vehicle's body movement and in turn improve ride comfort. The controller attempts this through active control of the MR valve's small coil current. Note that during this investigation only the small coil current conditions were changed by the controller as the small coil was developed to provide rapid characteristic changes. Inherent system delays were also later added to the control system to observe whether these delays will negatively impact the control systems' ability to improve the quarter-car vehicle dynamics.

7.3.1. Skyhook Control

In order to understand the application of an active skyhook controller a brief introduction into this control strategy is described in this section. Skyhook is a comfort oriented active control strategy developed by Crosby and Karnopp. Skyhook control attempts to limit vertical motion of the vehicle body by applying an ideal semi-active damper between the sprung mass and fixed vertical height above the sprung mass as indicated below. (Strydom 2013)

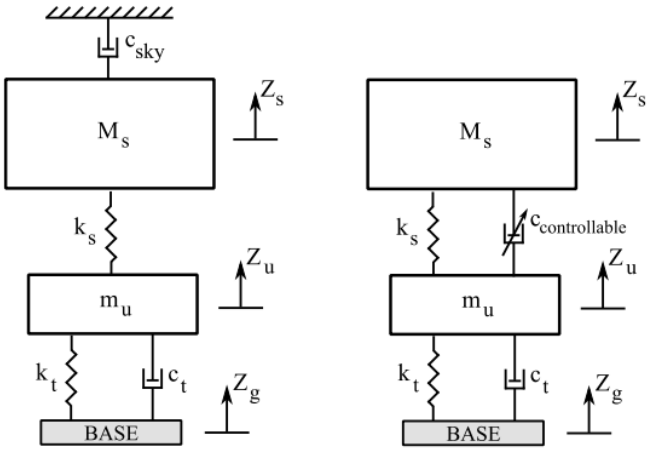

Figure 7. 8: Ideal skyhook control configuration (Left), Real skyhook implementation on a quarter-car configuration (Right) (Strydom, 2013)

In a quarter-car model this is achieved through control of a semi-active controllable damper, as is depicted on the right of Figure 7.8. The control of the damping characteristics (c_{sky}) of a semi-active or active damper is based on the measured velocities of the sprung (Z_s) and unsprung (Z_u) masses.

Skyhook control is implemented through the logic defined in the following equations. When the sprung and unsprung masses are moving away from one another and the sprung mass is moving upwards, the damping coefficient will be set as a function of the ideal skyhook damping coefficient:

$$\dot{Z}_s \dot{Z_{su}} > 0 : F_{damper} = c_{sky} \dot{Z}_s \qquad (2.22)$$

Where $c_{sky} = 2\zeta\sqrt{k_s M_s}$ or simply a control gain $c_{sky} = c_{gain}$

Whereas if the sprung mass is moving downwards but the two masses are still separating, then the control system switches of the damper according to:

$$\dot{Z}_s \dot{Z_{su}} < 0 : F_{damper} = 0 \qquad (23)$$

Skyhook control is relatively simple to implement in simulation based studies as the sprung and unsprung mass velocities are readily available, however, practical implementation proves more challenging as these values are not as easily measurable.

7.3.2. Skyhook Control over a displacement step input

Active skyhook control of the MR4S$_4$ was implemented during the simulations as the quarter car travelled over the same step input as was passively tested in Figure 7.1. Figure 7.9's sprung mass displacement plot shows the investigation across a variety of controller gains which were tested to observe the effect thereof. As expected, the system becomes more overdamped as the controller gain is increased and the Skyhook controller attempts to keep the sprung mass steady. The observed responses are illustrated in Figure 7.10. Note that the absolute acceleration RMS values are also indicated within the legend of the figure.

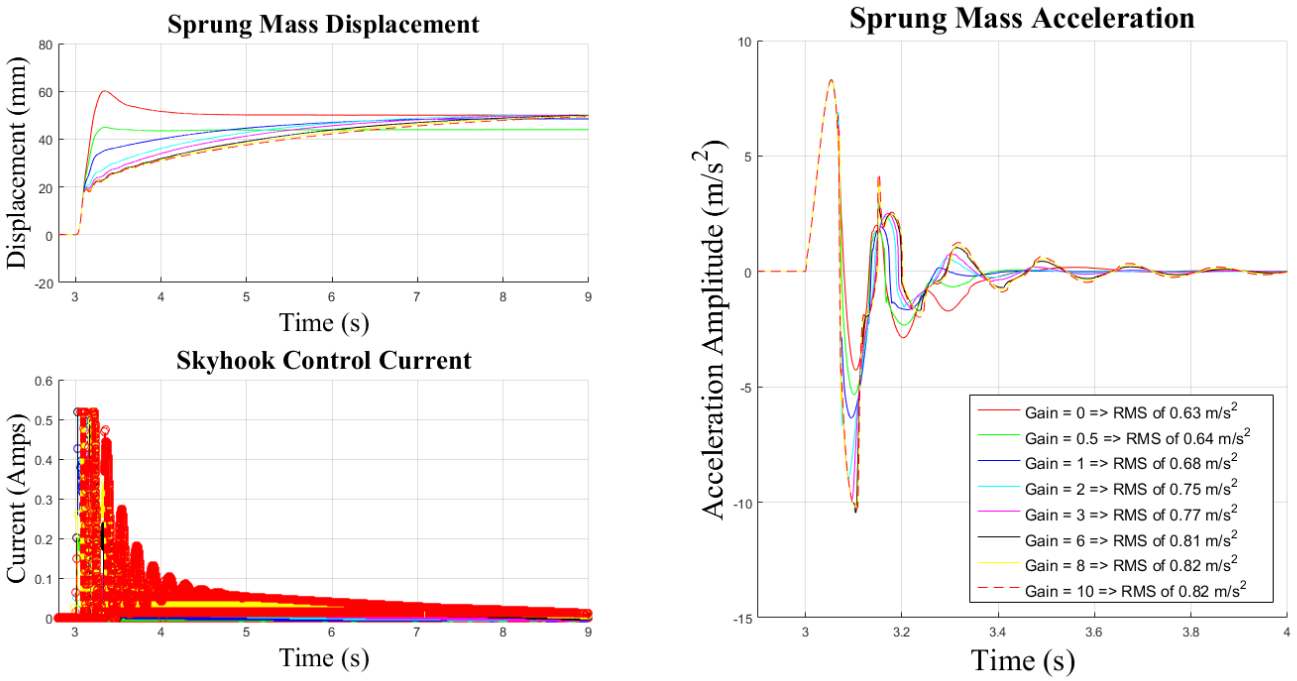

Figure 7. 9: Step input with Skyhook Gain investigation

Interestingly, the absolute acceleration RMS values increase as one increases the controller gain suggesting a deterioration in ride comfort. This is contrary to the expected results from an active Skyhook control strategy. This observed effect is explained by the fact that the dampers stiffen the system to keep the sprung mass from oscillating as the controller tries to keep the sprung mass's displacement as steady as possible. One can observe the controller's focus to reduce the sprung mass displacement in the displacement RMS as well as the displacement transmissibility in Figure 7.10. This is an effect which increases as the gain is increased decreasing the ride comfort as the Skyhook gain is increased. Figure 7.10's transmissibility plot (estimated by Matlab's *tfestimate.m* function) shows the presence of the body hop and wheel hop natural frequencies in the order of 1-2Hz and 7-8Hz although it also shows a drastically high transmissibility at 22Hz. The reason for the 22 Hz transmissibility is not known exactly but it is speculated that this is the frequency at which the controller switching is maximally influencing the dynamics of the sprung mass.

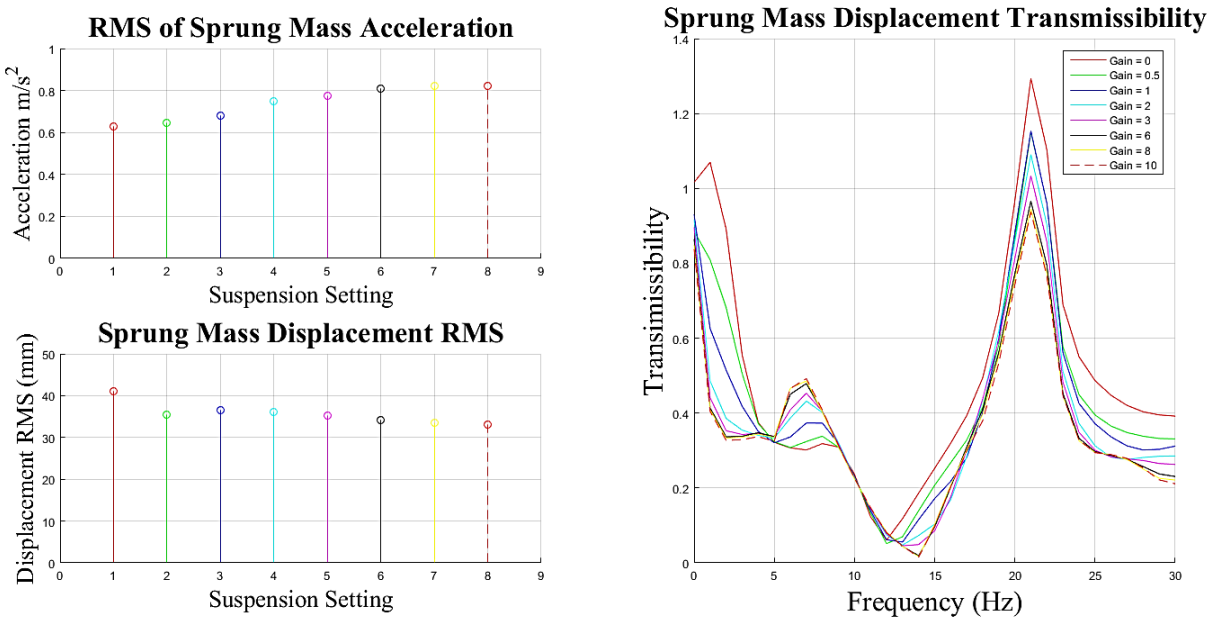

Figure 7. 10: Sprung mass response characteristics over a step input with several skyhook controller gains

One could argue that this deterioration of ride comfort is undesirable since the overall objective of active control would be to obtain better ride comfort. It is again anticipated that the MR valve damping characteristics are too drastic and are the cause of the deterioration in the ride comfort. To confirm whether the high level of damping is the reason for the reduction in ride comfort the same investigation was conducted with a damping model which was reduced to 10% of the actual characteristics. In this reduced damping investigation, it was observed that the ride comfort now does improve by increasing Skyhook control up to a gain of 2 where it saturates. Figure 7.11 provides the acceleration and displacement RMS values obtained in this investigation which support the anticipated hypothesis that the original system is too heavily damped for active control to improve ride comfort.

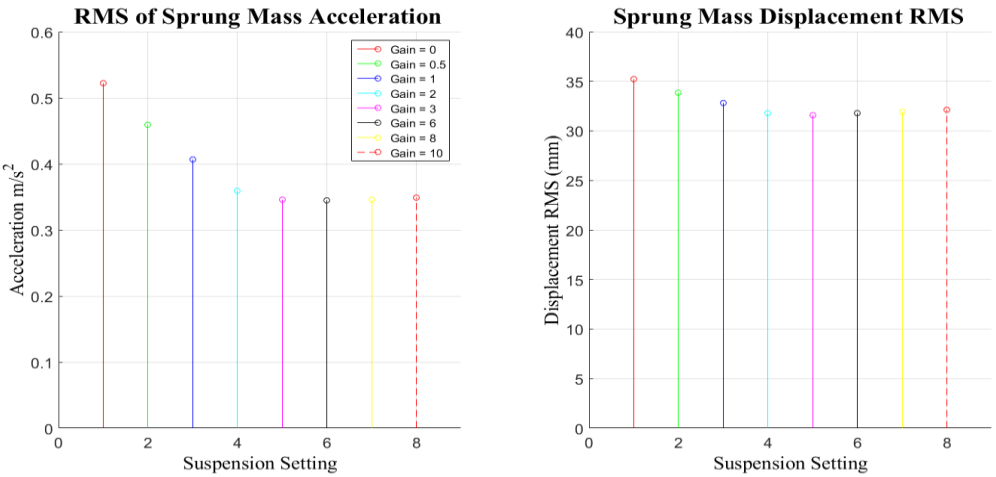

Figure 7. 11: Sprung mass acceleration and displacement RMS with 10% of the original damping and various Skyhook gains

This overly damped characteristic of the MR4S$_4$ is further illustrated by Figure 7.12 which shows the modelled force components of the MR4S$_4$ during the Belgian paving simulation in Section 7.2.2. Here one can observe that the original damping element often makes a very large contribution to the system's output force in comparison with the spring components from the accumulators. The damping force is

very erratic over the Belgian paving causing very large dynamic changes in the output force, and in turn explaining the deterioration of ride comfort as the controller gain is increased.

The second subplot in the same figure, Figure 7.12, shows a much lower and less erratic damping contribution obtained from a simulation where the damper has been reduced to 10% of the original characteristic over the same road input. Note that the plotted 'Effective Damping' component is the absolute damping pressure drop across the MR valves.

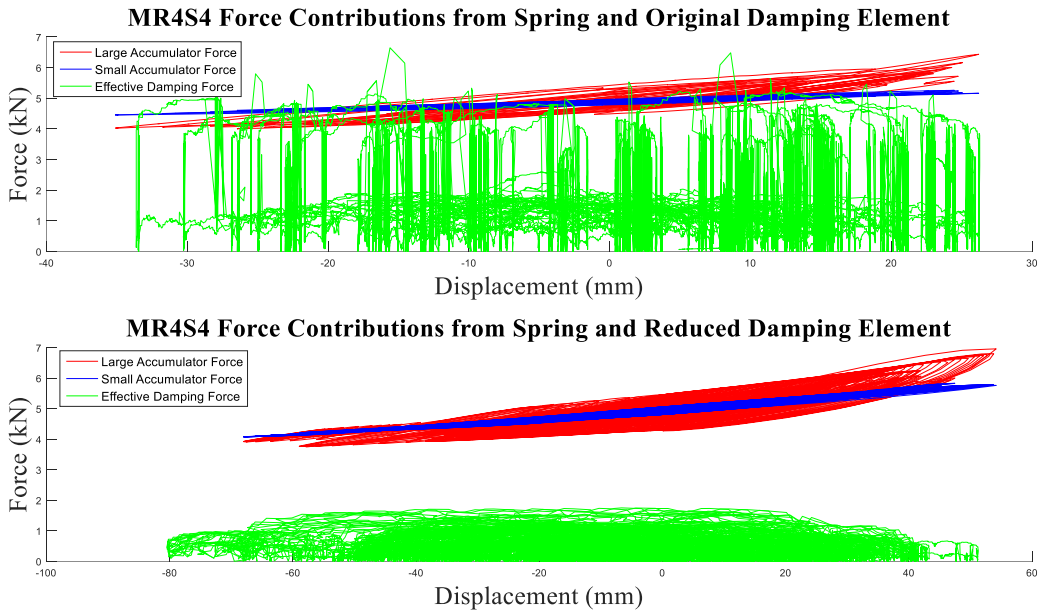

Figure 7. 12: Comparison of Damping Element contribution to the MR4S4 output Force.

This brings one to the conclusion that if the objective is to achieve better ride comfort through active control of the suspension characteristics, the MR valve damping characteristics needs to be drastically reduced to make this feasible. The use of the current designed MR valves with Skyhook control simply deteriorates the ride comfort as there is already too much passive damping present in the system.

7.3.3. Skyhook Controller over a step input with control delay

Since Section 7.3.1 is based on the ideal case where there is no delay in the control of the system it is slightly unrealistic to consider its results in isolation. To perceive how the vehicle dynamics would be affected by a more realistic control of the $MR4S_4$ which incorporates some control delay, a first order control delay was built into the Skyhook controller and the same analysis conducted over the step input as was performed in Section 7.2.1.

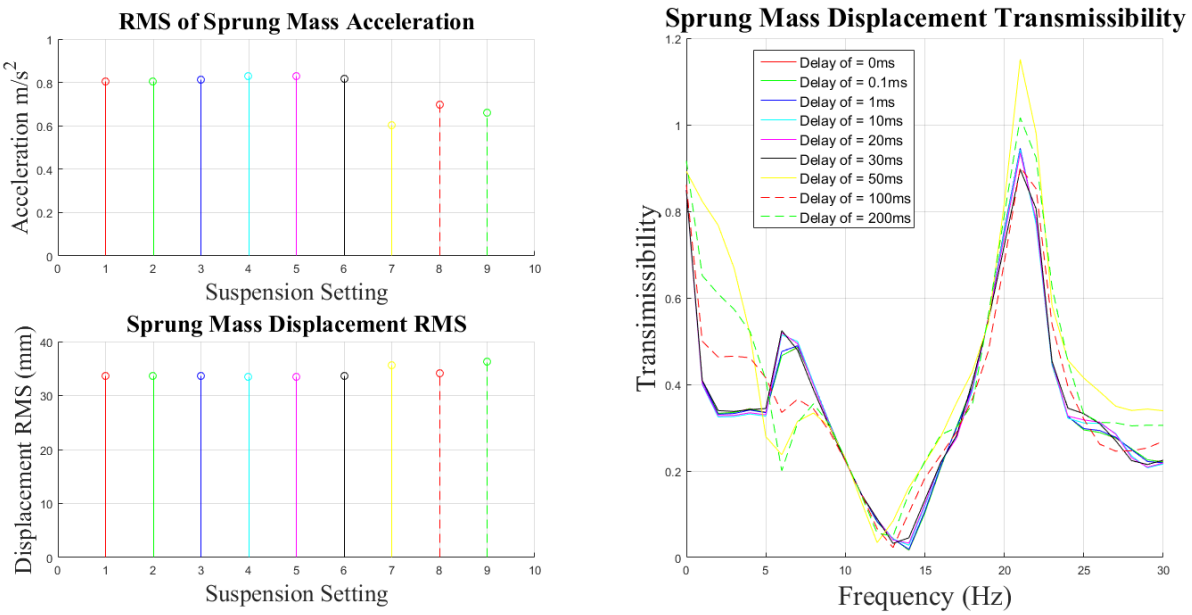

Figure 7. 13: Step input sprung mass response characteristics with Skyhook control delays

Figure 7.13 very interestingly suggests that a controller delay of anything less than 30ms has minimal effect on the obtained dynamics, whereas incorporating a 50ms or larger delay actually improves ride comfort. This conclusion can again be attributed to the over damped effects of the $MR4S_4$. If the controller 'misses' a sudden high velocity input, due to the control delay of over 30ms, it does not switch the coils in time to create an over-stiff system. This has the unexpected knock-on effect that the overall ride comfort of the vehicle actually improves, an observation which is highly contradictory to the expected results and which is attributed to an over stiff semi-active damper.

7.3.4. Skyhook Controller over Belgian Paving with no control delay

To determine how the dynamics of a vehicle will be affected as it travels over an unpredictable and rough road such as the Belgian paving with the application of an ideal skyhook controlled $MR4S_4$, an investigation was launched which excites the quarter-car model over this road with various Skyhook controller gains. This yielded similar results to those observed in Section 7.3.2 where the application of the controller actually worsened the ride comfort due to the considerable damping forces added by the controller to stiffen the system. Figure 7.14 shows the sprung mass displacement reducing in amplitude as the controller gain is increased while it also shows that the sprung mass acceleration increases with numerous additional spikes for the higher controller gains, showing that the stiffness added to the suspension system by the active control is transfering much more of the road input to the vehicle body.

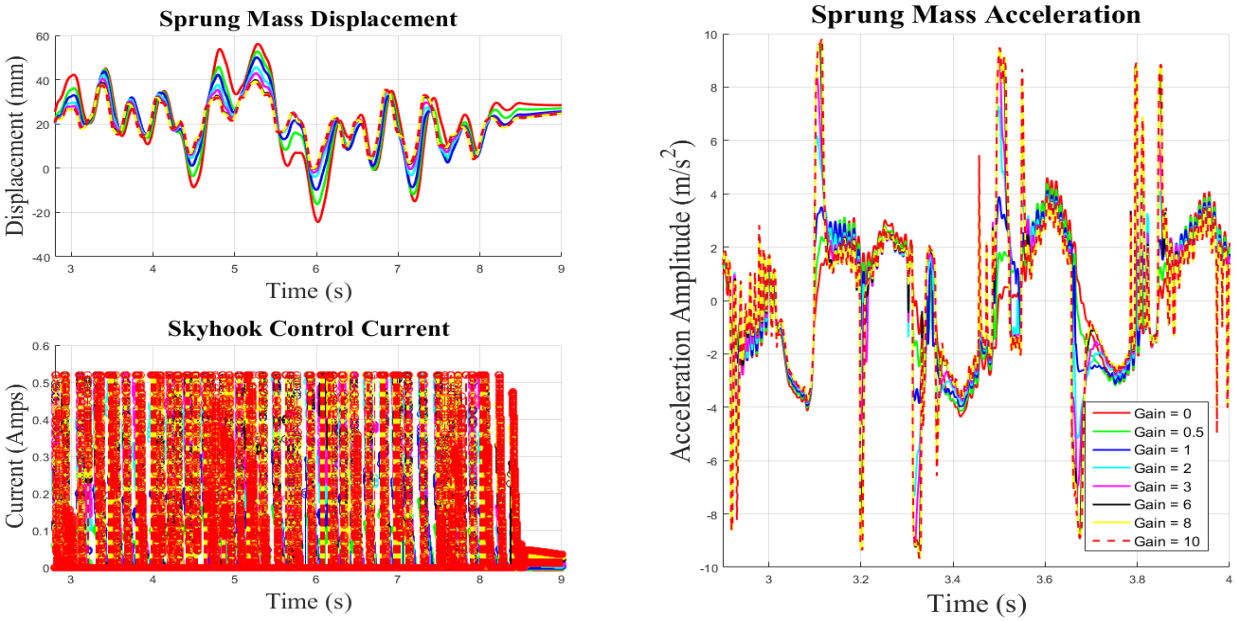

Figure 7. 14: Belgian paving simulation with active Skyhook control results

It is observable that the Skyhook control reduces the displacement response and holds the sprung mass as steady as possible as is set out to by the control algorithm, but in doing so it stiffens the system to such a degree that the acceleration experienced by the sprung mass increases significantly. Thus, the ride comfort worsens as the control gain is increased. Illustrated in the transmissibility plot of Figure 7.15, that for road inputs which happen at greater than 3Hz, the application of the Skyhook control actually increases the displacement transmissibility, worsening ride comfort, whereas it does manage to reduce the transmissibility at lower frequencies.

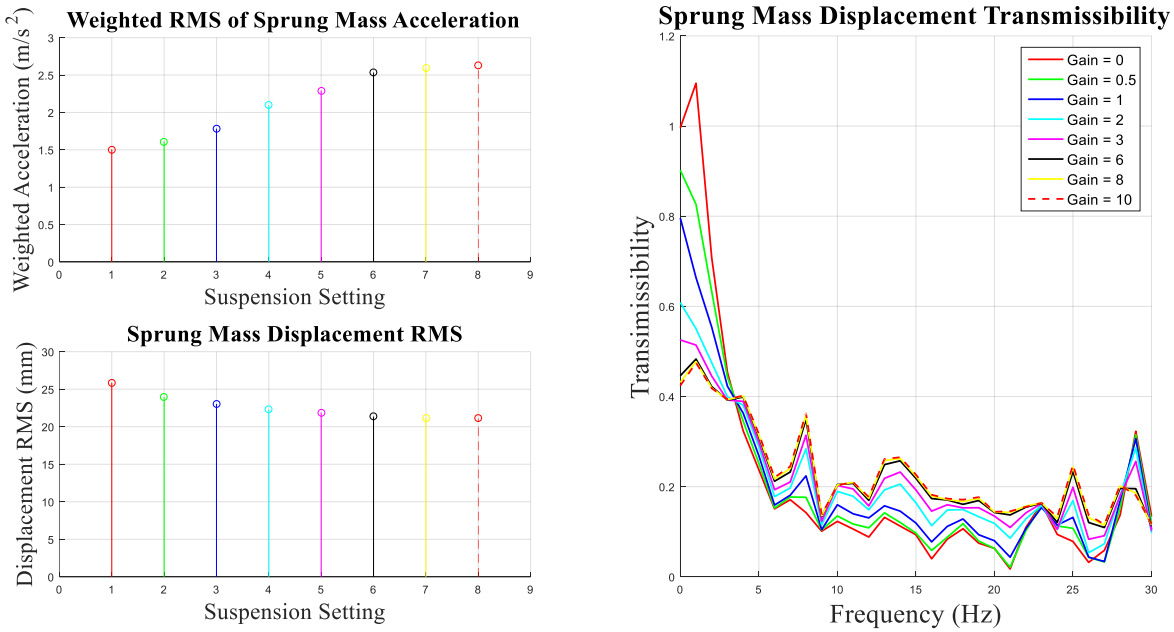

Figure 7. 15: Belgian paving sprung mass response characteristics with Skyhook control applied

Again the Belgian paving analysis at various controller gains was conducted with a factor of 10 lower damping characteristic and the result compared with the original results in Figure 7.16. Figure 7.16 confirms that the MR dampers are negatively impacting the ride comfort characteristics of the vehicle as it travels over the rough terrain. The figure shows that increasing the active controller gain reduces

the ride comfort in the original MR valve characteristic while improved ride comfort is to be obtained when more gain is added if the damping characteristic has been significantly lowered.

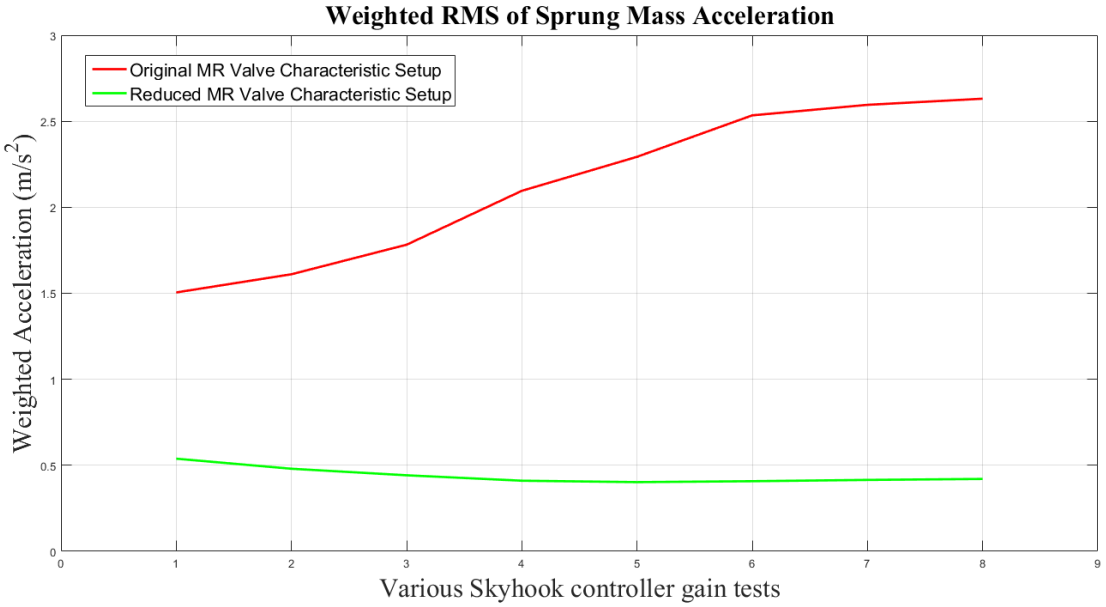

Figure 7. 16: Comparison between weighted RMS values over Belgian paving with low and highly damped MR valve characteristics

Figure 7.16 proves that although the MR4S$_4$ is able to successfully switch characteristics through the control of the MR valves, inherently the original system exhibits a too large damping characteristic which is detrimental to the ride comfort of a vehicle. If the MR valve is decreased by a factor of 10, one can use an active Skyhook control strategy to improve the ride comfort, however if the damping characteristic is not lowered skyhook control adds to the discomfort of a vehicle. This is somewhat counter-intuitive to what is expected since active control usually provides better ride comfort than a passive control strategy. This contradictory observation is due to the very large and non-linear change in damping characteristics of the MR valve when current is applied, the dynamics are greatly influenced by only a small current change in the MR valve as Figure 5.9 illustrates. One thus needs to spend considerable effort to optimise the controller for achieving a much finer current control, a depth of control implementation which has not been done during this investigation. Alternatively, one needs to decrease the damping characteristic so it does not change as erratically, in order for active suspension control to improve ride comfort.

7.3.5. Skyhook controller over Belgian paving with control delay

By subjecting the Skyhook controller to a control delay during the Belgian paving simulation the resultant RMS values suggest that the dynamics of the quarter-car is reasonably insensitive to control delays when the road input is very dynamic and unpredictable. There are noticeable time shifts in the displacement responses of the vehicle masses, however the RMS values suggest that a control delay is not detrimental to the suspension's performance and hardly influences the ride comfort over very rough terrains, as is illustrated by the RMS values in Figure 7.17.

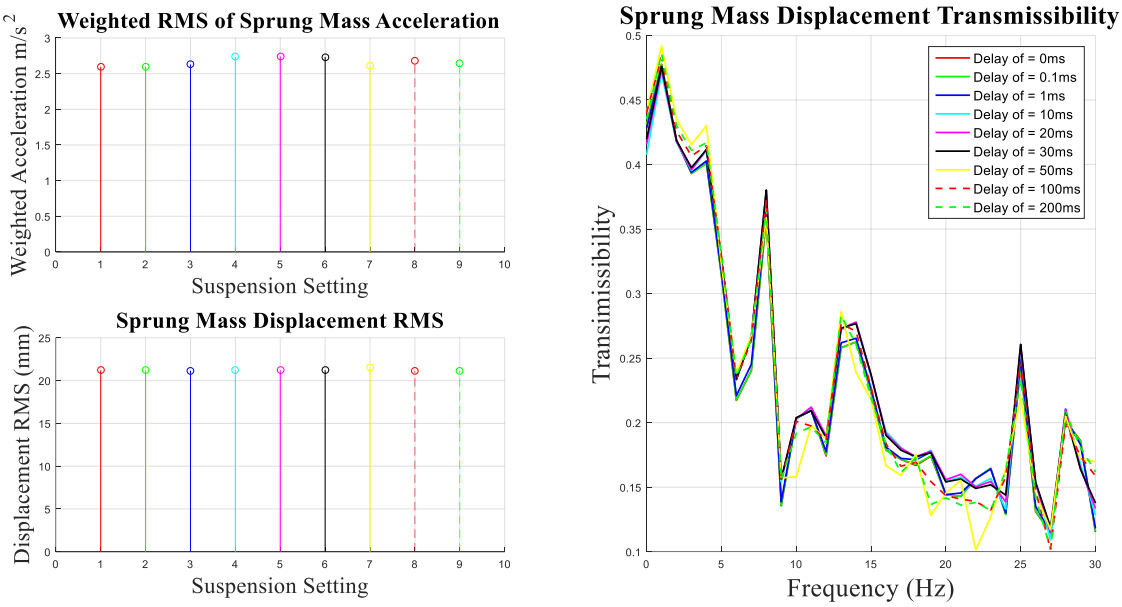

Figure 7. 17: Belgian paving sprung mass response characteristics with Skyhook control and delays applied

The best ride comfort is obtained by driving over the Belgian paving road input with no additional MR induced damping added, as was passively observed to lead to a RMS value of 1.5. As soon as active Skyhook control is placed over the damping elements, the ride comfort is reduced with the acceleration RMS is lifted to 2.5. Figure 7.17, does suggest that, should an active control strategy such as Skyhook be used to try and improve the ride comfort of a vehicle, it appears that the controller would not be detrimentally affected by delays. To confirm this the damping characteristic of the MR valve was again reduced and the analysis re-run. In this case it was observed that the RMS value of the sprung mass acceleration remained around 0.5 and was not greatly affected by any delays, again showing that reduced damping characteristics improve ride comfort over rough roads.

7.4. Simulation Computational Requirements

As a last point to this chapter the computational requirements of the quarter-car investigation will be briefly discussed. Due to the iterative nature of the MR4S$_4$ physics based modelling approach, the quarter-car simulation based on ODE45 requires significant computational effort. The stiffer the MR4S$_4$'s characteristics become, the more difficult the numerical computation becomes to obtain a suitable solution, and as a result the higher the computational time required. An example of the typical solution time requirements across the various suspension settings are shown in Figure 7.18 for solutions obtained on an Intel i7- 4 GHz processor as the quarter-car model was run across a Belgian paving input.

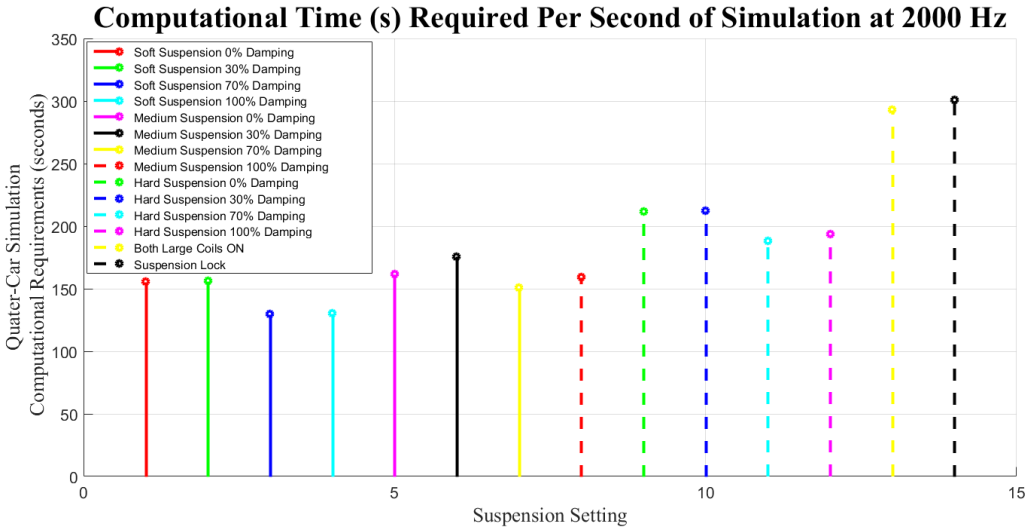

Figure 7. 18: Typical Computational Requirements on an Intel i7- 4 GHz Processor for the Belgian Paving simulation.

These values could increase drastically on 2.4GHz pc's and could reach values over a 1000 for the very stiff system. This large computational requirement makes the implementation of this model unrealistic on a multi-body dynamic simulation which incorporates the dynamics of a full vehicle and multiple suspension struts, and possibly limits its application to quarter-car studies.

Conclusion

This chapter investigated, through simulation based studies the potential vehicle ride comfort benefit of applying a semi-active suspension system, such as the MR4S$_4$ either through passive or active control strategies. The aim was to determine whether this suspension technology promises sufficient dynamic benefits to a vehicle to justify further investment into its development. A number of conclusions were drawn from the quarter-car based simulation studies.

The first of such conclusions is that a vehicle's responses could be successfully influenced by controlling the two MR valve conditions within the MR4S$_4$ to achieve suspension characteristic switching. The continuous control of the MR valves will enable this semi-active suspension to generate an almost continuous spectrum of characteristics.

It was observed from the step input simulations that one can effectively shift the natural frequencies of a vehicle by controlling the suspension settings in the MR4S$_4$, although this effect is obscured by the large amount of damping in the system. Additionally, it was proven through simulation studies that the ride comfort of a vehicle can be drastically influenced by even passively controlling the suspension settings, while one would expect its handling ability to also change.

In general, it was observed that the lower the damping is, the better the vehicle's ride comfort becomes as would be expected of a system which is already as highly damped as the MR4S$_4$. One the other hand, passively switching the suspension system to a stiffer and higher damped 'handling mode' through the use of the newly developed MR valves, one should be able to obtain better handling.

It was furthermore noted that if one wants to obtain better vehicle ride comfort through active Skyhook control, significant reduction in the damping characteristics of the MR valves are required. This is because the system is already very heavily damped and the addition of more damping causes the system to become too dynamically stiff leading instead to a reduction in ride comfort.

The study also indicated that active Skyhook control exhibits little sensitivity to the inherent delays one can expect of a physical implementation of the MR valve control. This was observed for both the Belgian paving and a step input. As such, the only area of concern is the over-stated damping characteristics which are detrimental to the controller's ability to improve ride comfort.

The simulation based investigations in Chapter 7 pointed out that in order to achieve ride comfort improvements through active and passive control of the $MR4S_4$ one possibly needs to consider searching for entirely new optimal characteristics for both the spring and damper elements within the system. The optimal characteristics upon which this prototype $MR4S_4$ was developed was based on optimal characteristics for the $4S_4$ suggested by M.J Thoresson (2009). However, in this study of the $MR4S_4$, a system whose characteristics mimic Thoresson's optimal characteristics closely, the MR based suspension application has been unable to improve the ride comfort of a vehicle, either actively or passively. This inability of the $MR4S_4$ to improve the ride comfort of a vehicle is explained by the extremely complex and non-linear interaction of the MR Valves and Pneumatic Accumulators within the $MR4S_4$ which combine to create a very stiff dynamic output characteristic deteriorating ride comfort. Thus, further research must include finding new optimal $MR4S_4$ suspension characteristics such that an $MR4S_4$ can be developed to improve both ride comfort and not simply handling characteristics.

CHAPTER 8

Study Conclusions

Introduction

This study set out to design, implement and validate a new and optimised MR valve for implementation into a Magneto-Rheological equipped Hydro-Pneumatic semi-active suspension system. The foremost objective was to improve the response time characteristics of the initial prototype system through utilising a new MR valve design methodology using finite element optimisation. Secondly, the development focused on ensuring that the MR valve had the ability to create sufficient resistance to fluid flow such that the working principle of the $4S_4$ could still be realised. This while also providing a desired continuous range of damping characteristics between the off-state and flow blocking. Lastly, by encompassing experimental work as well as simulation based investigations this study aimed to provide a recommendation regarding the feasibility and possible contribution that such an $MR4S_4$ suspension system could offer to the comfort of an off-road vehicle and thus comment on the systems' merit for further research and development.

8.1. Response Time Characteristic

In Chapter 4 it was observed that the new MR valve has an electrical response time which is significantly faster than that of the previous prototype developed by Grobler (2016). The newly designed and tested MR Valve can settle electrically to the 95% mark within 31ms for the unsaturated energisation of the small coil. Within this period the MR valve can achieve 40% of the maximum MR effect and generate more than 75% of its characteristic changes when also using the large coil in this time. It was, however, difficult to observe these rapid responses in the damping force characteristics generated during the experimental investigated in Chapter 5. Here it was believed that the responses are slowed by inherent MR fluid build-up delays and/or the responses are not built up fast enough due to experimental actuator effects. Through a displacement response analysis, it was observed that the MR valve requires 1-20 mm of suspension displacement to achieve 63% characteristic responses while a full 95% was reached in under 40mm for both coils. Although these responses can be drastically shorter at low valve fluid flowrates. With these response times mentioned, it is still possible to argue the obtained results could simply be the observable upper limit, limited by the hydraulic test equipment, and that faster responses are possible. Although the test platform was setup such to minimize the delay created by the equipment, it could arguably be playing a large role in obscuring the actual system force response characteristics, else there is still some unknown reason to explain for the discrepancy between the MR valve's magnetic field response time and the overall suspension output responses. It is known that MR fluid reacts within a few milliseconds to a changing magnetic field, however, inherently it is difficult to obtain testing equipment which can reliability provide insight into the response time area of

interest being less than 50 milliseconds. This is because the test platform must offer a high force, displacement and velocity capability while having extremely sharp and fine control over these aspects such to remove the possibility of the actuator is influencing the observed dynamics. Achieving reliable results in the sub 50 millisecond region is quite a challenge on a 2.5-ton actuator by itself. And for this reason the above response characteristic conclusions can only be confidently noted as the observable upper limit and could, in theory, still be faster.

8.2. MR Valve Characteristics

The MR valve damping pressure drop characteristic, as was experimentally observed in section 5.7, exhibits a highly desirable range and falls within the recommendations made by Els (2006). The off-state characteristic of the MR valve follows the recommended optimal low damping curve of the $4S_4$ very closely while the MR valve is able to obtain, through appropriate coil current control, most of the characteristics of the recommended high damping curve as well. Chapter 7, however, suggested that the MR valve's optimal set of characteristics could actually be significantly lower than what is currently expected if better ride comfort was to be obtained from the active and continuous control of the damping force across the MR valve. This required shift in optimal characteristics is explained by the MR fluids high dynamic viscosity which creates a very stiff damping characteristic, especially at low flow rates creating undesired secondary ride discomfort. The $MR4S_4$'s system characteristics are too greatly influenced by its damping characteristics and this should be minimized over rough terrains to achieve better overall ride comfort.

8.3. $MR4S_4$ System Characteristics

Chapter 6 illustrated, through the physics based modelling of the $MR4S_4$, that it is possible to achieve suspension stiffness adjustability or switching through active or passive control of the MR valves within the system while at the same time retaining continuous damping control. This could be instrumental in solving the ride versus handling compromise of off-road vehicles.

One cause for concern that should be noted, is the apparent overstated damping characteristics, particularly at low velocities, of the MR valve. If this was to be reduced to improve active ride comfort, as discussed in Chapter 7, it certainly would have a detrimental impact on the flow switching (blocking) ability of the system, and as a result one would start to lose the ability to achieve discrete spring states. Thus the $MR4S_4$'s future hinges on one's ability to find a solution to the complex compromise between the flow blocking and the 'off-state' low damping requirements of the MR valve within the semi-active suspension design.

8.4. MR4S$_4$ Recommendations

The application of this MR4S$_4$, with the newly developed MR valves implemented, will enable a vehicle to continuously control, either passively or actively, its suspension damping characteristics while also providing a platform for semi-active stiffness switching. This is an innovative capability as few semi-active suspensions are capable of controlling both the stiffness and damping characteristics while the MR4S$_4$ is able to achieve this through the control of two MR valves.

Currently it is believed that the MR4S$_4$ will provide an off-road vehicle with the ability to stiffen its suspension and in doing so improve its handling and stability significantly. This stiffening is possible in a response time which has been greatly optimised. Even though the system's response time characteristics have possibly been saturated, it has done so at a point where the changes in the characteristics happen fast enough to positively influence the dynamics of a vehicle under both passive and active control, especially if one considers the spatial response characteristics as discussed.

Furthermore, it is believed that the MR4S$_4$, as developed and tested within this research might not yet be sufficiently optimised to enable ride comfort improvements through semi-active control. The system requires further development and characteristic adjustment to ensure that this technology will provide a ride comfort contribution instead of the contrary. This said, the MR4S$_4$ will certainly be able to provide improved dynamic handling and stability for a vehicle through low energy consuming semi-active suspension control, which in itself might already justify its continual development. Very few systems provide one with the opportunity for continuous characteristic control across such wide ranges, and those that do, often consume significantly higher amounts of energy. As a result, this technology should certainly receive further developmental commitment even though its responsiveness cannot be further improved.

Areas of Further Research

1) Optimise MR4S$_4$ characteristics to obtain ride comfort improvements

This study highlighted, in Chapter 7, that a new set of optimal spring and damping, characteristics are applicable to the MR4S$_4$ which have changed from the original 4S$_4$ characteristics due to the inherently applied low velocity damping effects imposed by the MR valves. It was observed that the MR4S$_4$ has a negative impact on ride comfort, when actively and passively controlled, due to the non-linearity and overdamped nature of the coupled system. For this reason, it is advised that the developed MR4S$_4$ physics based model be used as a tool in quarter-car simulation studies to investigate the effect of changing accumulator volumes and pressures as well as the reduction in the MR valve damping characteristics. Such a study could provide meaningful answers as to how the system could be used to obtain both improved handling as well as ride comfort for a vehicle. Alternatively, the MR4S$_4$ needs a complete conceptual re-design to find a solution to the dynamic stiffness problem of the system, thus removing the low velocity damping problem. Only in this way, can the optimised characteristics defined

by Theron and Els (2007) become applicable again to this system. One possible such conceptual re-design is discussed in point (2) below.

2) Alternative MR4S$_4$ concept

During the course of this study it was noted that the flow blocking requirement of the MR valve creates a detrimental knock-on effect of over damping the system. The flow blocking requirement also has the effect of prolonging the response properties of the MR valve as it requires a much larger coil to generate sufficient magnetic strength to achieve lockup. For these reasons a concept was developed, which is also based on MR fluid technology, but one that separates the MR blocking ability from the MR damping ability, allowing faster and lower damping characteristic control as well as spring characteristic switching.

In this concept a single MR valve damper is used before the flow splits into the respective flow paths. Additionally, a much stronger MR valve focused only on flow blocking must be applied to the large accumulator flow path while no MR valve is applied to the small accumulator path. Particularly important to note is that the flow blocking valve must receive a completely new conceptual design. It is believed that implementing a valve with sufficient area, as to not generate undesired damping effects, while achieving thorough flow blocking is possible through a completely new geometrical and functional design of this valve. The implementation of a MR blocking valve similar to the valve developed by Meeser is believed to provide stronger flow blocking abilities while minimizing passive influences due to its geometry as depicted in Figure 8.1. This setup will enable both suspension stiffness switching while simultaneous and continuous damping characteristic control can be achieved through a less invasive continuous damper which does not have a flow blocking requirement to adhere to.

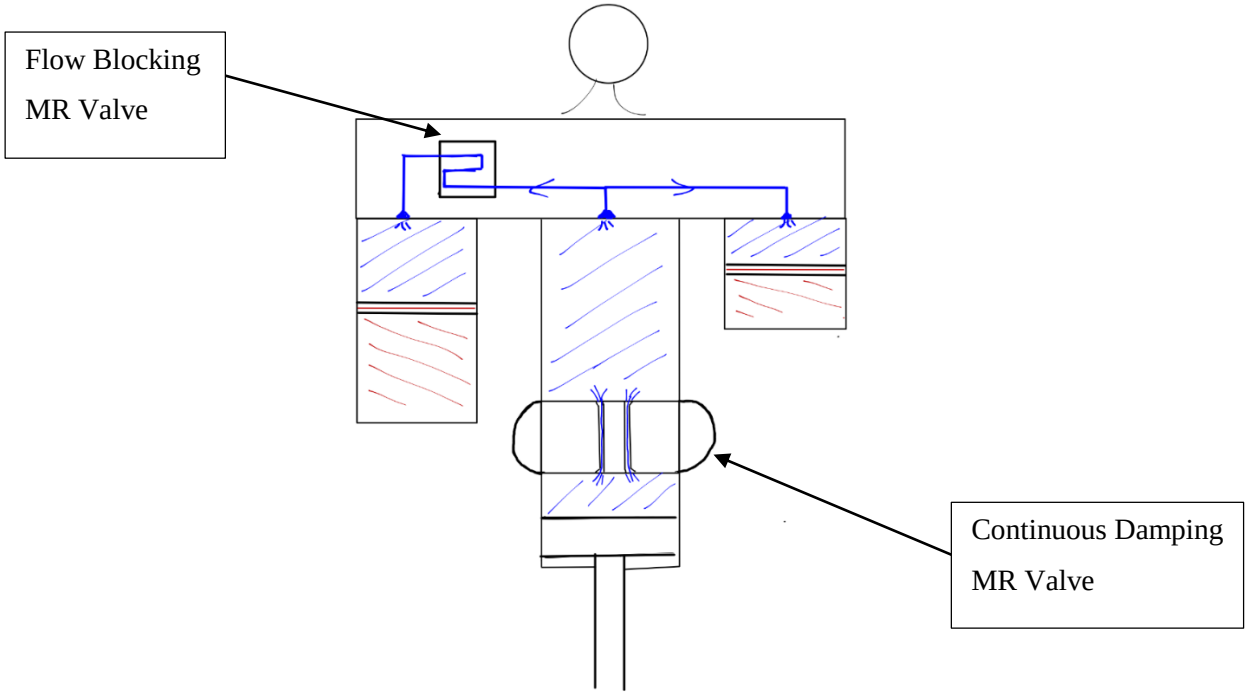

Figure 8. 1: Schematic representation of alternative MR4S4 concept

3) Implementation of accumulator bladder/floating piston to remove friction piston

An initial design was developed that replaces the floating piston, separating the MR fluid and the compressed air within the accumulator, with a rolling diaphragm or accumulator bladder. This implementation shows promise as it removes floating piston friction which creates additional damping in the system. This design was never physically manufactured as it was decided that the original floating piston design would be used during the course of this study to ensure timely completion thereof. However, the removal of the friction effects must certainly be incorporated in future work. The proposed design applies BFA 90 80 90 Rolling Diaphragm beneath the MR valve and the implementation of this design is recommended in future research initiatives.

Figure 8. 2: Implementation of Rolling Diaphragms to eliminate accumulator friction effects

4) Application of the MR4S$_4$ Control Module.

Lastly, during the course of this thesis a current control box/module which can be used to energise the coils on the MR4S$_4$ was developed. It was known that controlling the MR valve coils by energising through a current driver would help improve their electrical responsiveness as compared to a constant voltage drive use in the experimental work. Unfortunately, the current driver control module had not yet been finalised and assembled before the experimental work was scheduled and so the use thereof was never implemented. The repetition of the experimental work was not possible due to limitations on the availability of test equipment when the module was completed. This control module has the capability of controlling the two independent MR valves - each one with its two independent coils. During the process the module can provide a continuously controllable current to the small coils, while also switching the large coils in parallel with their respective small coils. The control module uses two independent current drivers to power the MR valve coils through the application of a 12-24V supply. The control module takes in 2 continuous voltage control signals, with which the supply current is controlled, as well as two digital voltage inputs to switch the respective large coils on and off. In addition to this, the MR4S$_4$ control module outputs an amplified signal of the coil current provided by the current drivers to the appropriate coils and provides an output reading of the applied coil voltages. Thus interfacing the control module with a PC-104 computer one could very easily control the magnetic

conditions within the MR valves. The required circuitry and PCB layout was designed and the circuit board manufactured. It is suggested that the manufacturing and implementation of the control module be finalised and the required programming written such that the control module can be implemented onto a full $MR4S_4$.

Figure 8. 3: MR4S4 Valve Control Module

References

A. F. Jahromi, A. Zabihollah. 2010. “Linear Quadratic Regulator and Fuzzy controller Application in Full-car Model of Suspension System with Magnetorheological Shock Absorber.” *Mechatronics and Embedded Systems and Applications (MESA)* 523-528.

A. Grunwald, A.G. Olabi. 2008. “Design of magneto-rheological (MR) valve.” *Sensors and Actuators A : Physical* 211-223.

British Standards Institution. 1987. “Measurement and evaluation of human exposure to whole-body mechanical vibration and repeated shock.” *BS6841.*

Butz, T, and O. Von Stryk. 2002. “Modelling and Simulation of Electro- and Magnetorheological Fluid Dampers.” *Journal of Applied Mathematics and Mechanics.*

Carlson, J. D. 2005. “MR Fluids and Devices in the Real World.” *International Journal of Modern Physics B* 3-9.

David Meeker, Ph.D. 2014. 14 04. http://www.femm.info/wiki/HomePage.

Els, Pieter Schalk. 2006. *The Ride Comfort vs. Handling Compromise for Off-Road Vehicles* . Pretoria: University of Pretoria.

F. Gordaninejad, S.P. Kelso. 2000. “Fail-Safe Magneto-Rheological Fluid Dampers for Off-Highway, High Payload Vehicles.” *Journal of Intelligent Material Systems and Structures, Vol 11* 395-406.

G. Priyandoko, M. Mailah, H. Jamaluddin. 2009. “Vehicle active suspensions systems using skyhook adaptive neuro active force control.” *Mechanical Systems and Signal Processing Vol 23* (Mehanical Systems) 855-868.

Gillespie, T. D. 1992. *Fundamentals of Vehicle Dynamics.* Warrendale: Society of Automotive Engineers, Inc.

Gravatt, John W. 2003. *Magneto-Rheological Dampers for Super-sport Motorcycle Application.* Blacksburg: Virginia Polytechnic Institute and State University.

Grobler, Jacob Frederick. 2016. *Multi-State Hydro-Pneumatic Suspension System Through the Use of Magneto-Rheological (MR) Valves.* Pretoria: University of Pretoria.

GS Heymans, JF Grobler, PS Els. 2016. “Physics Based Modelling of a Magneto-Rheological Equipped Hydro-Pneumatic Semi-Active Suspension System.” *ASME 2016 International Design Engineering Technical Conferences (IDETC 2016-59922).* North Carolina: ASME.

H. Lee, K Sung, S Choi, M.K Park, M.K Park. 2011. “Performance Evaluation of a Quarter-vehicle MR Suspension System with Different Tire Pressure.” *International Journal of Precision Engineering and Manufacturing, Vol. 12* 203-210.

H. Metered, P. Bonello, S.O. Oyadiji. 2010. “The experimental identification of magnetorheological dampers and evaluation of their controllers.” *Mechanical Systems and Signal Processing* 976-994.

J. Yao, J. Chang, D. Li, X. Yang. 2016. “The Dynamics analysis of a ferrofluid shock absorber.” *Journal of Magnetism and Magnetic Materials* 28-33.

Lord Corporation. 2011. *MRF-132DG Magneto-Rheological Fluid Technical Data.* Cary: LORD.

M.J Thoresson, P.E Uys, P.S Els, J.A Snyman. 2009. “Efficient optimisation of a vehicle suspension system, using a gradient-based approximation method.” *Mathamatical and Computer Modelling* 1437–1447.

M.R Jolly, J.W. Bender, J.D Carlson. 1999. “Properties and Applications of Commercial Magnetorheological Fluids.” *Intelligent Material Systems and Structures* 5.

Meeser, Riaan F. 2014. *Magneto-Rheological (MR) Damper Design for Off-Road Vehicle Suspensions with Flow Blocking Ability.* Pretoria: University of Pretoria.

Phillips, R. W. 1969. *Engineering Applications of Fluids with a Variable Yield Stress, Ph.D Thesis.* Michigan: University of Microfilms.

R..S. Prabakar, C. Sujatha, S. Narayanan. 2009. “Optimal semi-acive preview control response of a half car vehicle model with magnetorheological damper.” *Journal of Sound and Vibration* 400-420.

Rosół, B. Sapiński and M. 2008. “Autonomous control system for a 3 DOF pitch-plane suspension model with MR shock absorbers.” *Computers and Structures, Vol. 86* 379-385.

Strydom, A. 2013. *Controllable Suspension Design using Magnetorheological Fluid (Masters' Thesis).* Pretoria: Univeristy of Pretoria.

Tao, R. 2013. “Microstructures and Physics of Super-Strong Magnetorheological Fluids.” In *RSC Smart Materials*, by Norman Wereley, 211-214. Philadelphia: RSC Publishing.

Theron, N.J., and P.S. Els. 2007. “Modelling of a semi-active hydropneumatic spring-damper unit.” *International Journal of Vehicle Design* 501-521.

Ulaby, F.T., E. Michielssen, and U. Ravaioli. 2010. *Fundamentals of Applied Electromagnetics.* Prentice Hall.